POLITECNICO DI TORINO

Corso di Laurea Magistrale
in Ingegneria Aerospaziale

Tesi di Laurea Magistrale

Numerical modeling of servomechanisms: comparison between different development environments

Relatori:
Prof. Paolo Maggiore
Prof. Matteo Davide Lorenzo Dalla Vedova
Ing. Gaetano Quattrocchi

Candidato:
Francesco Nudo

Dicembre 2020

Dedicated to my beloved family

who has supported me in everything

and to all people, like me, who have

overcome successfully, like me, their difficulties

in this so strange 2020 because of the COVID-19.

Contents

-Abstract-

The main objective of this thesis is the numerical modeling of mechanical systems and electro-servomechanisms in two different development environments, Simscape and Simulink, with their comparison. The backlash phenomenon in mechanical transmission is also analysed with Simscape. During the first three chapters the theory of servomechanisms and EMAs is shown, in the fourth chapter the reference Simulink models are discussed while in chapters 5 and 6 the Simscape modeling is developed. Final results and considerations are exposed in the final chapter.

1) Introduction

1.1) Overview

The main theme of this thesis is to create a simple model on Simscape environment of a typical mechanical transmission with backlash phenomena in an Electro Mechanical Actuator (EMA) for aircraft flight controls developed on Matlab-Simulink.
Electro Mechanical Actuators are basically composed by an electric Brushless DC motor paired with a mechanical transmission line linked to the moving surface; as it is shown on the following figure:

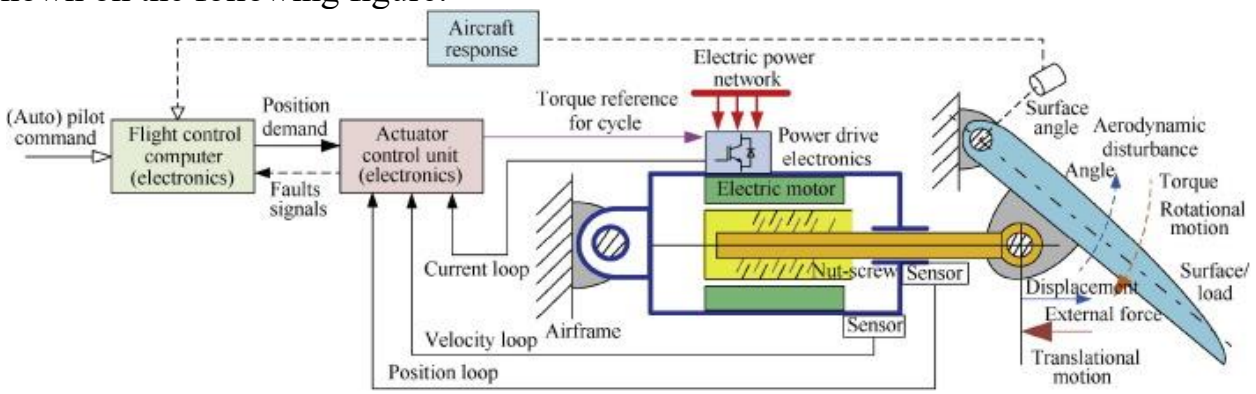

Figure 1: EMA system

Simscape enables to rapidly create models of physical systems within the Simulink environment and it's possible build physical component models based on physical connections directly integrate with block diagrams.
Assembling a scheme of the system the equations for the network of physical components are derived automatically and models are easy to understand and interpret because each model matches the physical structure of the system.
Regarding EMAs concept ensures to lower:

- the total weight because of electrical systems are generally much lighter than, for example, hydraulics due to the absence of hydraulic fluid used on Electro Hydraulic Actuators EHA;
- complexity of on-board systems;
- operational costs and environmental impact of the aviation transportation segment.

Moreover Electromechanical Actuators are becoming increasingly attractive in the field of more electric aircraft because of their outstanding benefits, which include reduced fuel burn and maintenance cost, enhanced system flexibility, and improved management of fault detection and isolation.
However, electromechanical actuation raises specific issues when being used for safety-critical aerospace applications like flight controls: huge reflected inertia to load, jamming-type failure, and increase of backlash with service due to wear and local dissipation of heat losses for thermal balance fuel consumption; EMAs are mostly used to operate Secondary Flight Controls and other utilities like landing gear retraction or cargo bay opening despite they are the best solution to actuate Primary Flight Controls too.

Although the advantages of EMAs are mostly used to operate Secondary Flight Controls, due to:

- lower reliability requirements needed (the higher reliability needed for Primary Flight Control is impeding their full implementation);
- as "recent" technology it isn't their fault mode are still not entirely known.

1.2) Flight Controls

Thanks to Flight Controls pilot controls the direction, trajectory and attitude of an aircraft in flight; so the orientation of body axis relative to an external reference system, are controlled by creating local modifications of the aerodynamical forces through the variation of the position of moving surfaces and these modifications produce unbalanced aerodynamic torques that changes the overall aerodynamic forces and so the aircraft attitude. Given an air foil with a moving surface like on Figure 2, immersed inside an airflow at the speed V∞, when the air foil changes his attitude angle α, the moving surface trends to line up to the direction of the flow, varying of a deflection angle δ. Therefore it's necessary to maintain a neutral position of the moving surface to apply a correct hinge moment: so applying strength, the pilot generates this moment by acting on the commands connected to the flight controls.
This hinge moment can be calculated with the formula

$$M_c = \frac{1}{2} C_{Mc}\, \rho {V_\infty}^2 Sc$$

Where S is the area of moving surface, c is the chord, ρ is the density of air and C_{Mc} is the coefficient of the hinge moment estimated as:

$$C_{Mc} = b_0 + b_1\alpha + b_2\delta$$

Where respectively: b_0 is the form's factor of the profile, b_1 is the incidence's factor and b_2 is the deflection's factor.
Moreover first two factors can be represented with the following way:

$$C_{M0} = b_0 - b_1 \frac{i}{1+F}$$

$$C_{M\alpha} = b_1 \left(1 - \frac{d\varepsilon}{d\alpha}\right)$$

Where: $\left(1 - \frac{d\varepsilon}{d\alpha}\right)$ is the down-wash factor, i is the aerodynamic fitting and F is a assigned parameter.

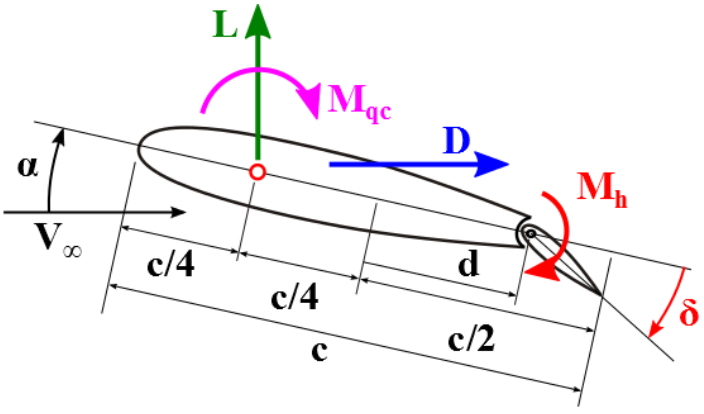

Figure 2: Hinge moment

Flight control systems are subdivided into what are referred to as Primary and Secondary Flight Controls. Primary Flight Controls are required to safely control an aircraft during flight and consist of ailerons, elevators (or, in some installations, stabilator) and rudder.
Secondary flight controls are intended to improve the aircraft performance characteristics or to relieve excessive control loading, and consist of high lift devices such as slats and flaps as well as flight spoilers and trim systems.
Movement of any of the primary flight controls causes the aircraft to rotate around the axis of rotation associated with the control surface. The ailerons control motion around the longitudinal axis (roll), the elevator controls rotation around the lateral axis (pitch) and the rudder controls movement around the vertical axis (yaw).
The most basic flight control systems are mechanical and, although they date back to the earliest aircraft types, are in use in the majority of light, general aviation aircraft. In this design, a collection of mechanical components such as cables, pulleys, rods and chains transmit the movement of the flight deck controls to the appropriate control surfaces. In larger and faster aircraft, the aerodynamic forces become too great for the pilot to overcome without assistance so hydraulic systems are often incorporated to move the flight control surface. In some newer aircraft models, the quest for reduced weight, improved reliability, damage tolerance, more effective control of the aircraft and the associated fuel savings has led designers to replace most of the mechanical components with computers and fibre optics to produce control systems which are referred to as Fly-By-Wire (FBW).
Therefore FBW is the generally accepted term for those flight control systems which use computers to process the flight control inputs made by the pilot or autopilot, and send corresponding electrical signals to the flight control surface actuators. This arrangement replaces mechanical linkage and means that the pilot inputs do not directly move the control surfaces. Instead, inputs are read by a computer that in turn determines how to move the control surfaces to best achieve what the pilot wants in accordance with which of the available Flight Control laws is active.

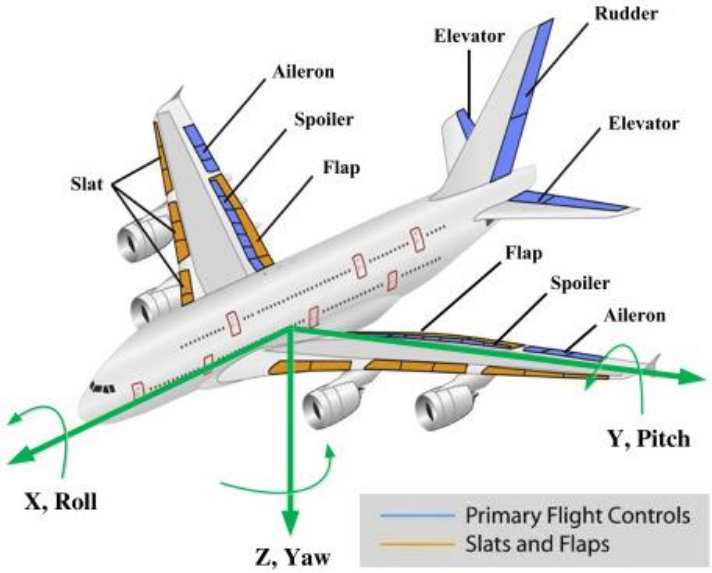

Figure 3: Primary and Secondary Flight Controls

1.3) Actuation System

On aircrafts to actuate control surfaces, usually several servomechanisms are exploited. These systems generally receive the input commands from the cockpit (as position, speed, force, torque, temperature, pressure or electrical magnitude), compare them with the actual situation of the system like output and accurately they follow the given command.

Flight controls, on modern aircraft, are usually operated in hydraulic or electric way:

- for Primary controls hydraulic actuation is used, with linear cylinder-piston motors or linear motors;
- the Secondary controls can be actuate using hydraulic or electric rotary motors.

During last decades, because of the development of reliable electric motors (with a high power/weight ratio) and the consolidation of innovative technologies, secondary electromechanical controls have established in the field of small powers (typically < 7 kW) and they begin to be uses also for the implementation of primary commands, especially for UAVs and small aircrafts.

In this way it will can be possible completely substitute hydraulic power with the electric one, which for now is starting to apply in actuators of EHA (Electro-Hydraulic Actuator). It is important to keep in mind that actuators requirements are robustness, reliability and safety.

In these servomechanisms the output signal of an actuator is compared to the command sent to the system. Based on the difference between these two signals, an input is sent to the controller, which has the goal of varying the input and output signal of the actuator. The difference between the input supplied to the system and the output of the actuator defines the performance of the entire system.

Common servomechanisms used in aircraft's environment which will be describe in detail on paragraphs below are:

- Hydromechanical actuation
- Electrohydraulic actuation
- Electro-hydrostatic actuation (EHA)
- Electromechanical actuation (EMA)

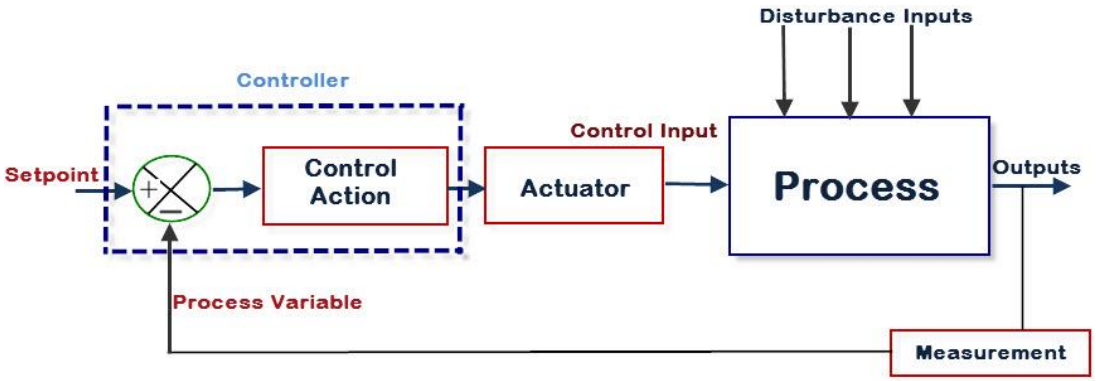

Figure 4: actuation system's control blocks scheme

1.3.1) Hydromechanical actuation system

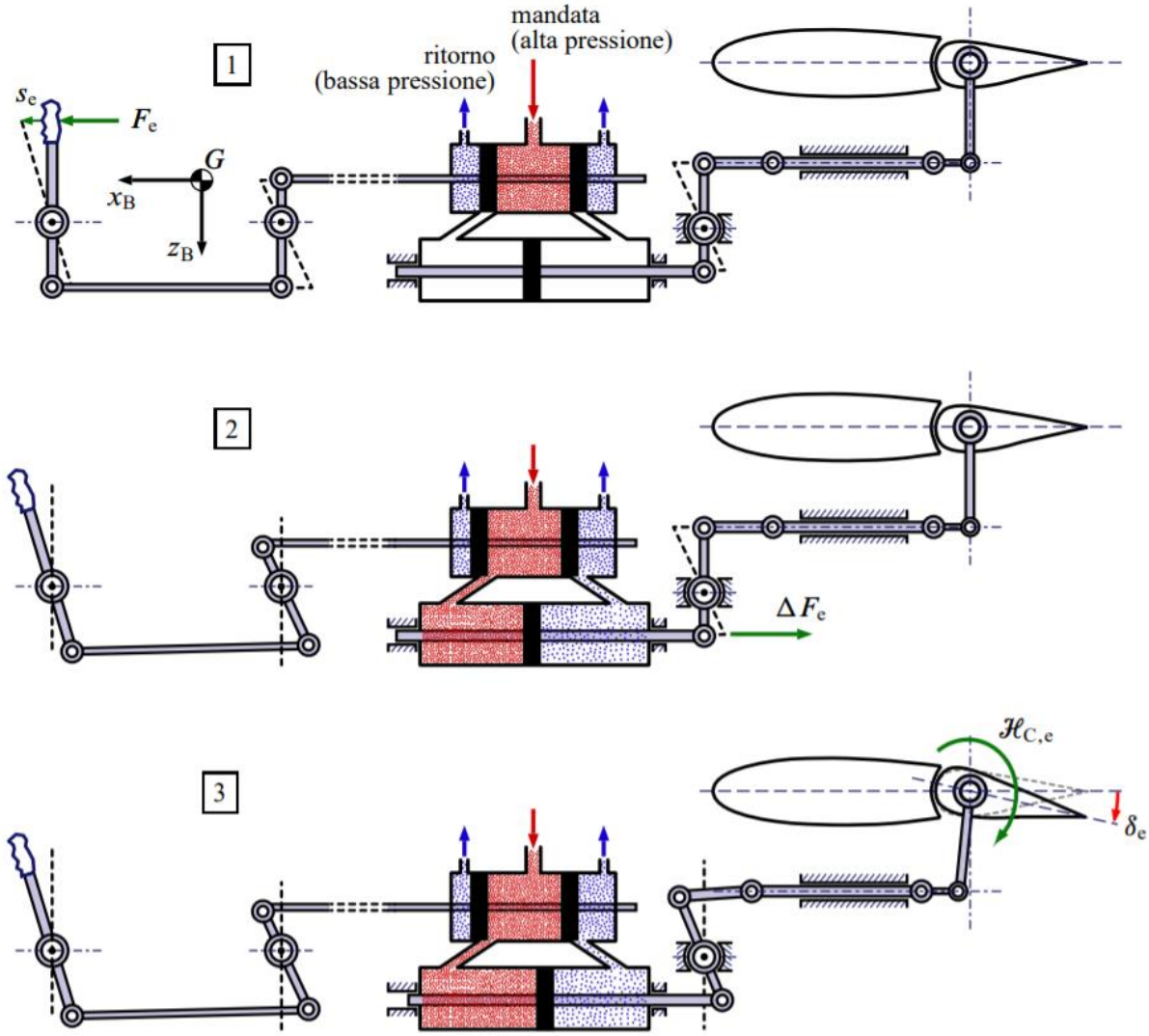

Figure 5: Hydromechanical actuation system's operations

In Hydromechanical actuators the input signal is given by the pilot and applied through a connection to the spool of a servo-valve. This is supplied as pressurized hydraulic fluid flow from aircraft hydraulic circuit at p_{mand}. The variation of node $x_i(t)$ position rotate the three-centre a-b leverage around the instantaneous centre of rotation located at the end of the cylinder jack (point T) opening the valve and producing a flow rate $Q_1(t)$. Finally, position of the jack y(t) is estimated and mechanically subtracted, through the three-centre lever, from the input signal. In this way, when the surface gets to commanded position, the servo-valve will automatically close itself.
The three-centre lever consists to a mechanical proportional controller because it multiplies the position error by a factor dependent by the lever's geometry. It's necessary on these servomechanisms puts inside pipes filters to maintain the fluid clean.

This solution is reversible: changing the direction of the input, so the direction of the spool motion, actuator's shaft will move towards the other side. If the shaft has to sustain a greater aerodynamic load, the valve's spool opens a duct and supplies the needed pressurized flow to support it.

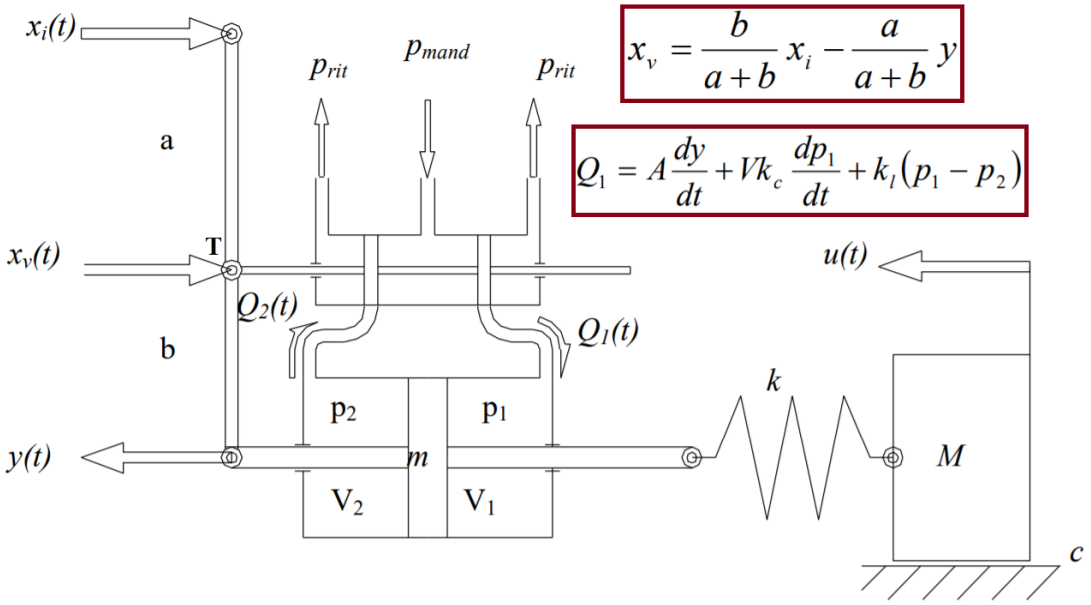

Figure 6: Hydromechanical actuation system scheme

1.3.2) Electrohydraulic actuation

Electrohydraulic servomechanisms is the most used actuation system on modern civil and military aircraft where mechanical feedback is replaced by a fly-by-wire control system.

Here, trough pressurized fluid, power hydraulic is provided by Flight Control Computer signal of fly-by-wire architecture and not directly by pilot action.

The component that regulates hydraulic oil is the servo valve, which, in its simplest form laminates the fluid.

The most commonly adopted servo valves are:

- two stage "flapper-nozzle" servo valves (Figure 7);
- three stage "jet pipe" servo valves (Figure 8);
- "direct drive" valves DDV (Figure 9).

In flapper-nozzle servo valve there is an electrical component, called torque motor, which transmits the command instead of a mechanical lever.

Electric torque motor moving the flapper, which is the first stage hydraulic valve and in this way the amount of fluid that flows from the ducts, so also the pressure, changes.

Pressure regulated by the flapper acts on the spool of the second stage valve, distributing pressure to the actuator jack.

The spool position is returned to the flapper mechanically through the feedback spring, while the piston position is measured by a Linear Variable Differential Transducer (LVDT) and transmitted to the control electronics.

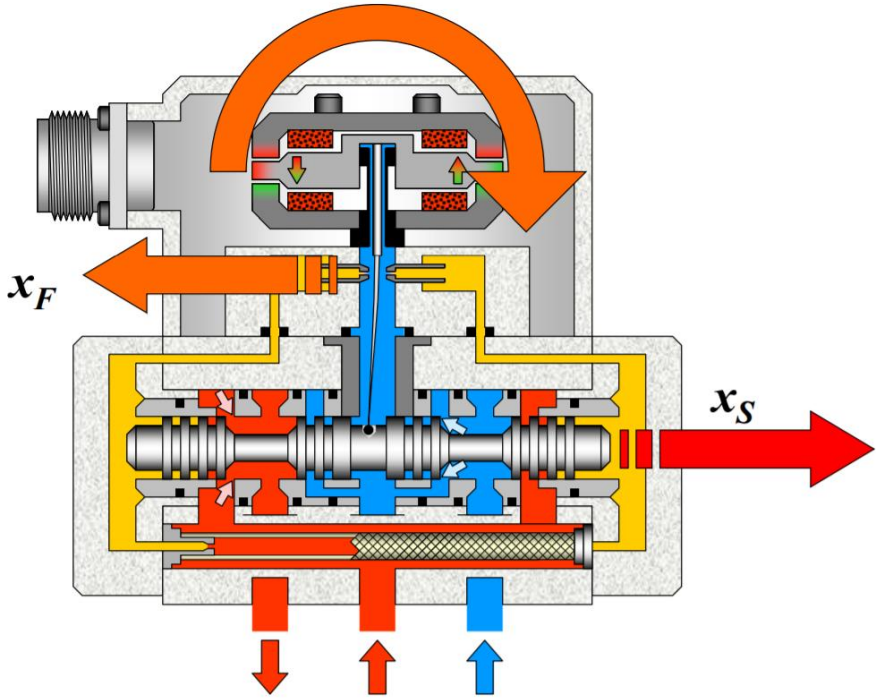

Figure 7: Flapper-nozzle servo valve

Compared to flapper-nozzle, in jet pipe servo valve a torque motor of a bigger entity directs a suitable flow of oil into two opposite chambers, capable of causing the spool to move due to the received overpressure. In this case, an oil flow is not deviated, but the efflux channel called jet pipe is appropriately oriented.

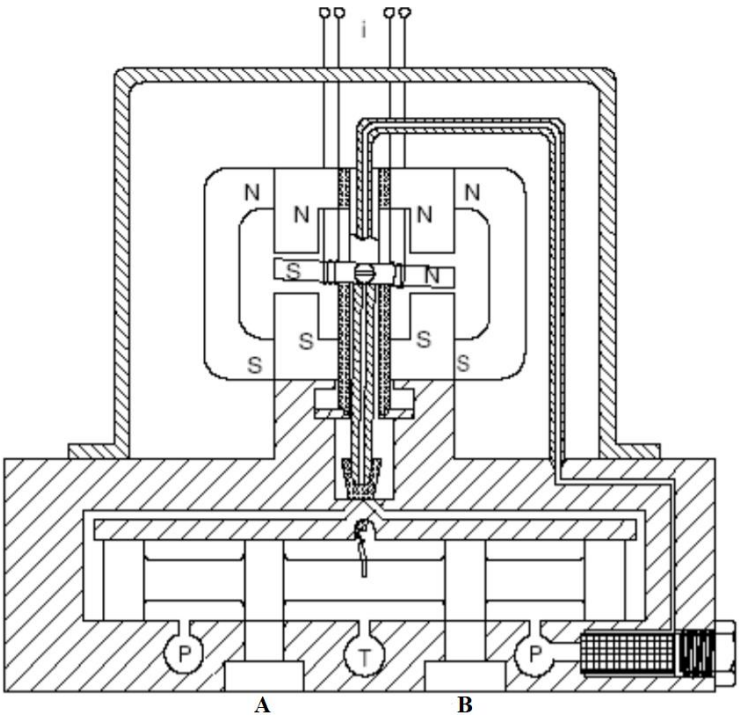

Figure 8: Jet pipe servo valve

Also in this electrohydraulic system there is not a direct feedback between the control valve and the actuator: the absolute position of the piston is surveyed by a Linear Variable Differential Transducer (LVDT) and sent to the control electronics.

Respect to flapper nozzles:

- jet pipe valve has better performance;
- jet pipe valve uses high-speed jet of orifice to change pressure into kinetic energy that is obtained in two receiver holes, then to control this energy for spool action;
- jet pipe mouth is big, so debris or dirty particles cause small harm.

Finally there are Direct Drive Valves (DDV) which allow to eliminate the system based on torque motor or jet, since the spool is moved directly by a dedicated electric motor and they are the last frontier in the field of servo valves.

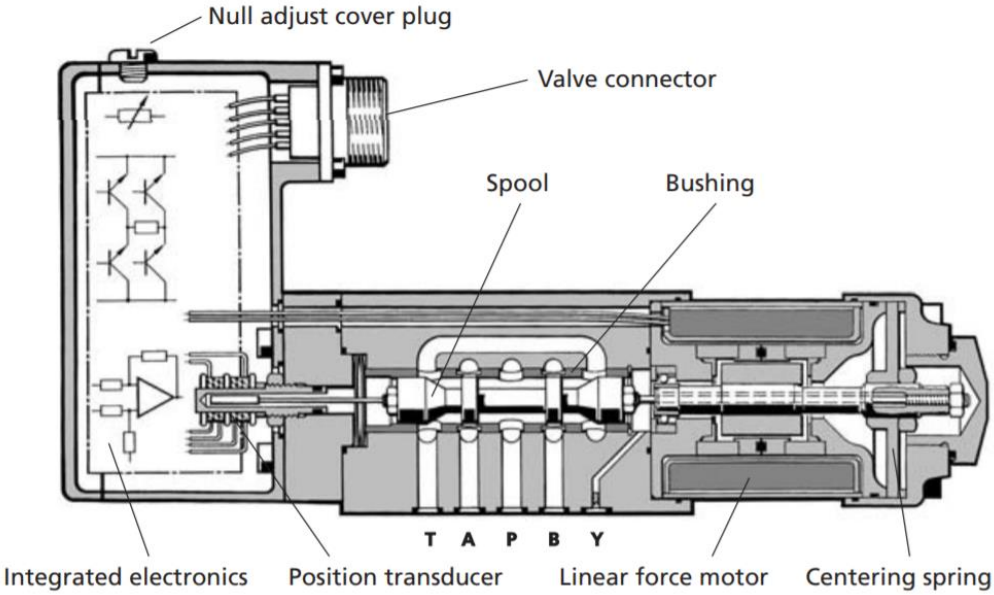

Figure 9: Direct Drive Valve

1.3.3) Electro-hydrostatic actuation (EHA)

With the aim to simplify, lighten and compact the hydraulics of modern aircraft, whose dimensions and performances tend to increase more and more, the electro hydrostatic actuators have been introduced.

In this case, the hydraulic system of the aircraft is reduced to a minimum and is no longer widespread within the entire aircraft.

The advantage of this type of system is that it keeps the pressurized hydraulic fluid only in a limit area near the actuator and it eliminates the hydraulic signal transmission replacing it with an electric signal with advantages in terms of overall weight of the Flight Control system.

So EHA are a power-by-wire type of motors that execute the movement of the control surfaces exploiting a localized hydraulic power obtained by the electrical power.

Thanks to the electro-hydrostatic actuators, it is possible to make the action on the controls even more prompt and dynamic, preserving the artificial sensitivity returned to the pilot. EHA also ensures structural simplicity and high efficiency.

This system is composed by a servomotor variable speed (usually a Brushless DC) controlled by electronics drives, a bi-directional pump with variable speed and a linear or rotary actuator.

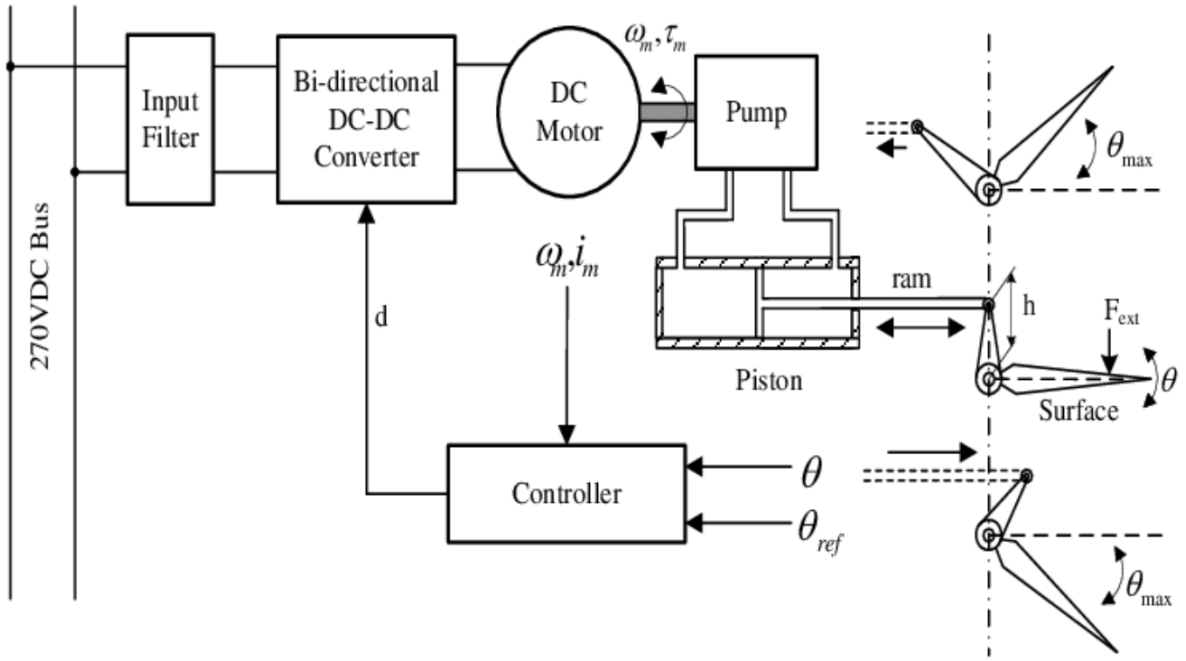

Figure 10: EHA's structure

The electric machine transforms electrical power into mechanical power, and the axial piston pump generates the controlled pressure which is used by the actuator to control the surface movement.

The fluid in the circuit is stored in a proper reservoir, composed by a low-pressure tank and two check valves able to maintain the minimum pressure required by the system. Close to reservoir there is a bypass valve electronically controlled and two relief valves arranged for safety of the system. The pressurized oil in the circuit it's not provided by the on-board main hydraulic system, but the pump takes the needed fluid from the tank. For this type of actuator too, the feedback ring needs a position sensor placed on the shaft. This is not the best structure if the aim is to decrease aircraft's weight, but it's very effective to reduce the critical issue related to a centralized hydraulic system. Furthermore, it allows maintenance and fuel cost savings while it assures the same precision and reliability of a traditional hydraulic system.

Pilot's input and FCS input travel on the electrical cable of the fly-by-wire architecture, which is again lighter in term of weight with respect to an hydraulically driven signal transmission system. Another advantage other

than reduced weight is the absence of friction losses or delays due to the flexibility typical of reversible mechanical control lines.

The command given by the pilot is than compared to a feedback signal measured by a Linear Voltage Differential Transducer LVDT or a Rotary Voltage Differential Transducer RVDT. The feedback signal of motor angular velocity is used to determine the exact amount of power needed. The error signal is then amplified and, filtered from noises, is used to control the actuation group.

1.3.4) Electromechanical actuation (EMA)

Nowadays, in civil transport, while EHAs are widely used by Airbuses mainly like A380/ A350) EMAs (electromechanical actuators), instead, are more used by Boeing like B787, both for first and secondary control systems. Electromechanical actuation moves aircraft design toward a "More Electric Aircraft" philosophy with great level of safety, efficiency, cost saving and a strong reduction of pollution.

This type of actuator allows:

- to reduce weights and dimensions of the appropriate redundancy systems required in any aerospace system thanks to the greater safety achieved by electrical and electronic components;
- to improve the response of the aircraft to the commands given by the pilot or the flight control computer.

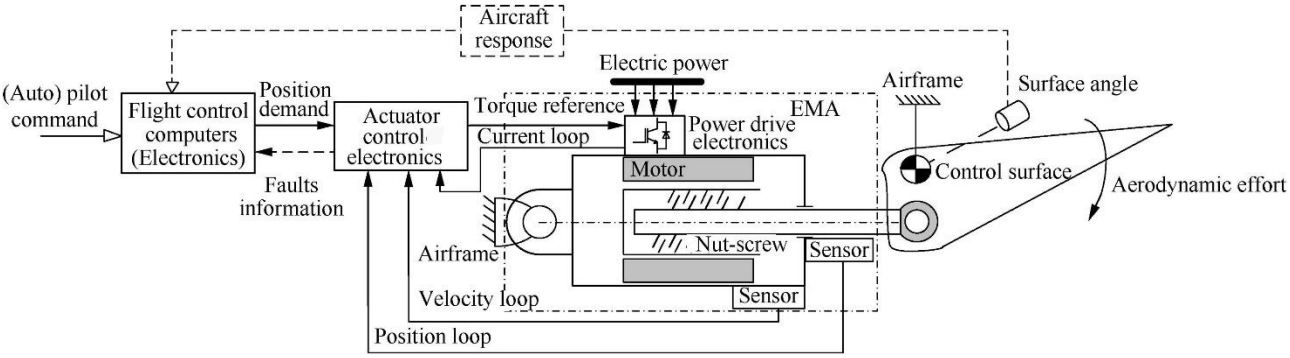

Figure 11: EMA's system

In EMAs the control electronics of the command acts, through power and control signals, on an electric motor, connected in closed loop to the control unit itself.

The motor is then connected via a reduction gear to a screw-nut or ball screw system actuator which is connected to the flight control surface by an appropriate mechanical connection.

This system excludes the possibility of leakages: those issues are often difficult to detect and hard to fix due the complexity and the scarce accessibility of the fluid circuit of EHA.

The movement signal of the actuator is constantly monitored by appropriate sensors, whose feedback is sent to the on-board computer of the aircraft.

The use of EMA new technology is confined to non-critical aircraft operations: secondary flight controls, landing gear retraction, cargo bay doors opening.

Small-medium UAVs (Unmanned Aerial Vehicles), are the only aircraft on which EMAs are being already used for primary flight controls, where the use of an onboard hydraulic system would be impracticable.

EMA system is commonly composed by the following components:

- ACE: the Actuator Control Electronics is the main controller of the system and executes all calculations needed to maintain the error closest to zero; in this device arrive all the feedbacks collected by the sensors. Once calculated angular deflection of the mobile surface instant by instant through position and speed loops, ACE sends the reference position to the Power Drive Electronics (PDE);
- PDE: Power Drive Electronics is usually composed by a three-phases inverter H-bridge and its goal is to provide the correct power flow to electric motor in order to reach the reference position;
- BLDC motor (Figure 12): it's a Brushless motor powered by DC direct current which transforms electrical input into mechanical rotational output for the reducer's gears. In this type of motors the permanent magnets are positioned on the rotor and are made with special materials that allow to have a very low rotor inertia, which allows to have an extremely precise control both in speed and in acceleration.
- a gears transmission to reduce motor angular speed transmitted and to increase the torque followed by roller or ball screw;
- roller screw or ball screw: a device which is able to transform rotary motion into a translational motion. Ball screw or roller screw, in addition to producing linear displacement, are preferred to a lead screw for their better efficiency and higher specific maximum load;
- a position transducer, usually an LVDT, to measure the user motion and transmit it to the controller.

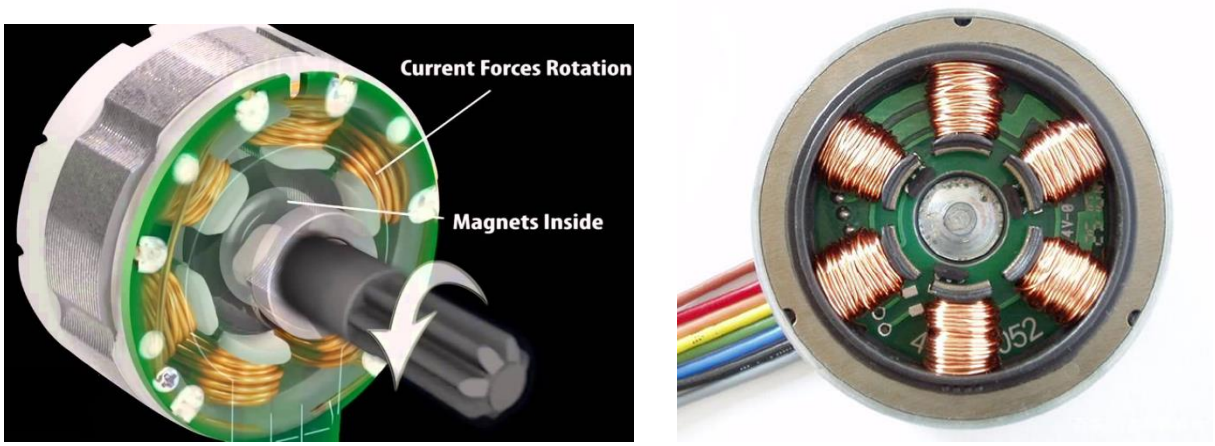

Figure 12: BLDC motor's operation and structure

The rotary to linear motion conversion (Figure 13) is performed by a ball screw or a roller screw which are shown on Figure 14 and Figure 15.

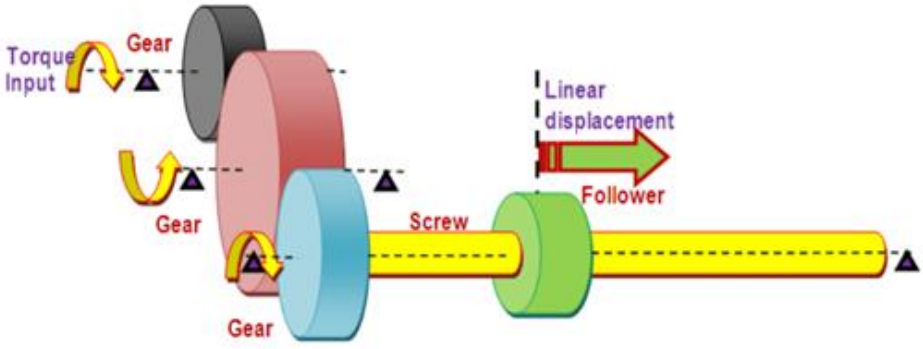

Figure 13: rotary-linear motion transformation

These devices are usually composed by a high precision screw and the transmission of motion is performed by a rolling component like spheres inside the nut circuit in the ball screw and satellite rollers in a roller screw.

Geometrically, it can be assert that are used spheres for the ball screw and shaped cylinders for the roller screw located between the rotating shaft and a nut.

Compared to other rotary-to-linear transmission devices such as lead screw; ball screw and roller screw have the following advantages: they grant an increased efficiency due to absence of dry friction in favour of rolling resistance. The type of friction forces involved in the motion transmission directly implies a lower wear of mechanical parts, due to lower stress acting on the components.

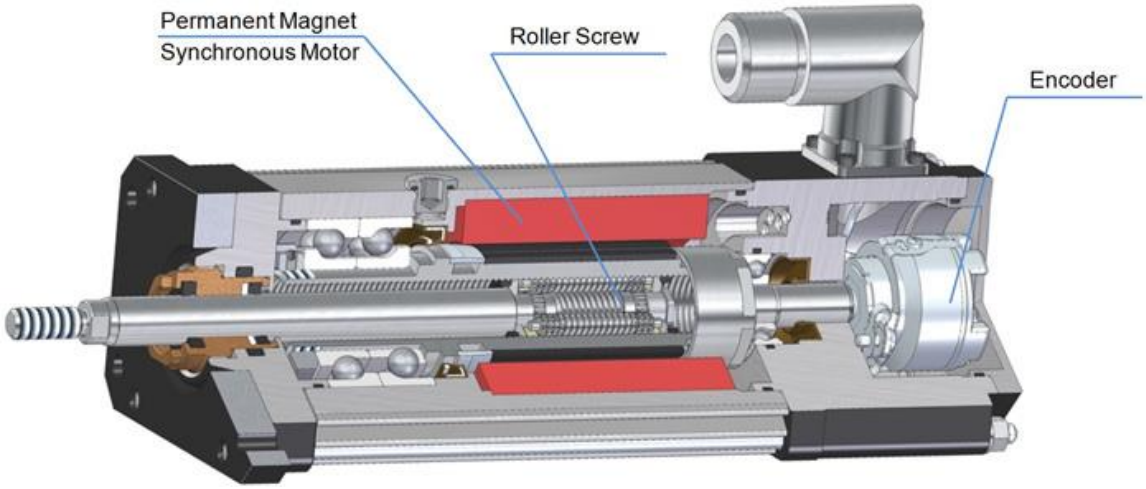

Figure 14: Roller screw actuator

The disadvantages of having an electric motor driven transmission is their difficulty to keep a fixed position with external load applied (i.e. delivering high torque in a near to near to zero velocity which would lead to a short-circuit). A motor in this situation tries

to deliver a torque powering always the same phases, resulting in winding's overheating and insulating material's melting.

So, after the application of a greater load, if the motor's speed is near to zero and the torque is high, all the current given to stator is dissipated by joule effect.

With an irreversible transmission these problems can be overcame but, in case of actuator failure, a reserve actuator can not move the connected surface. Therefore, a system for disconnecting the screw from the motor-reducer assembly would be required, but in this way there might be an increase of weight, cost and complexity.

A solution to the problem might be the use of a new type of stepper motor (maybe hybrid), that are able to output a controlled torque at zero speed.

It's important keep in mind that stepper motor is different from the brushless motor, used in the EMAs, because the stator windings are not all powered at the same time, but in a cyclic way so that the magnetic fields generated by them determine a rotation of the rotor obtaining a precise positioning of the same.

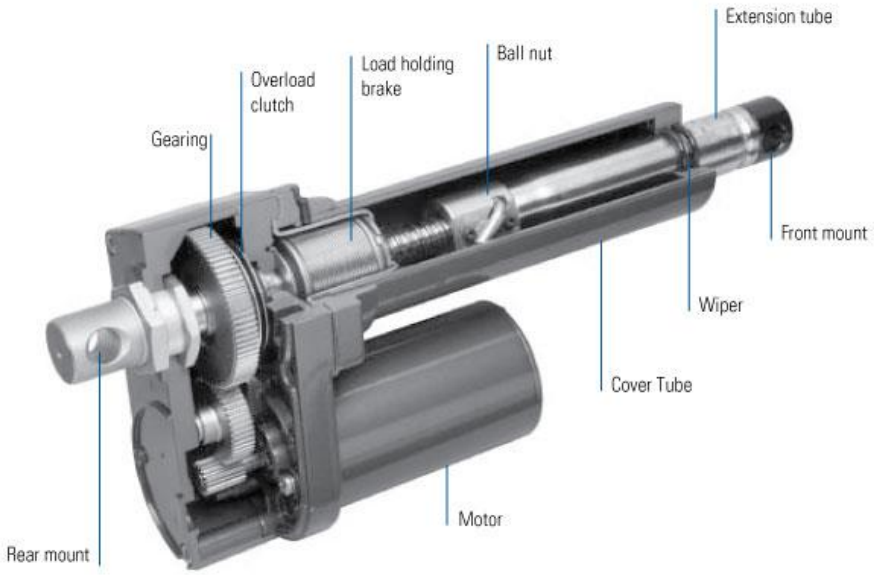

Figure 15: Ball screw actuator

2) Brushless DC motor

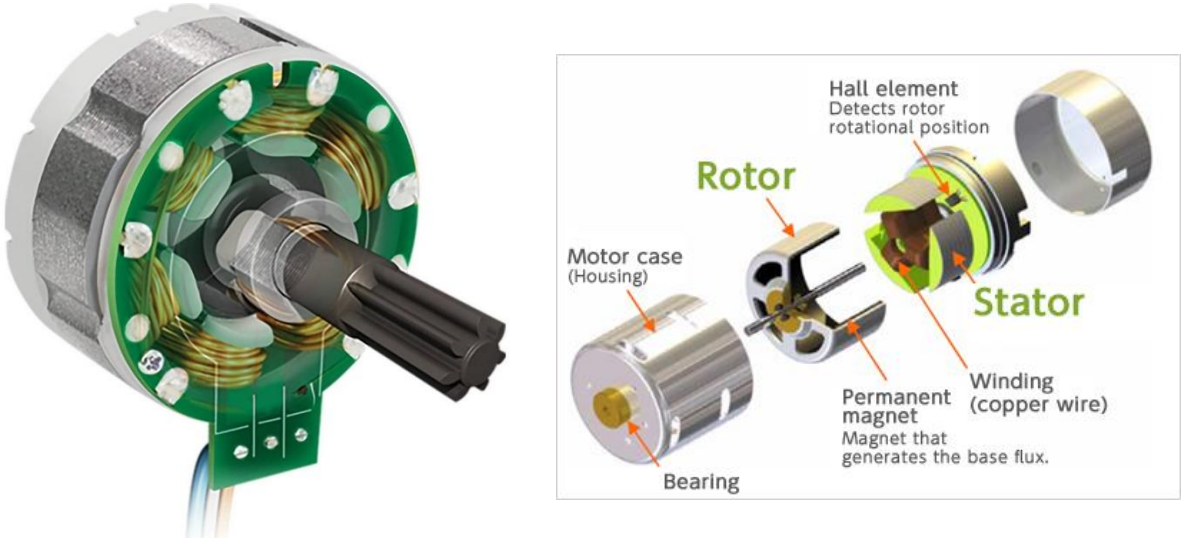

Figure 16: Brushless DC motor

As the name implies, BLDC motors do not use brushes for commutation; instead they are electronically commutated. BLDC motors have many advantages compared to brushed DC motors and induction motors.

A few of these are:

• Better speed versus torque characteristics;

• High dynamic response;

• High efficiency;

• Long operating life;

• Noiseless operation;

• Higher speed ranges.

In addition, the ratio of torque delivered to the size of the motor is higher, making it useful in applications where space and weight are critical factors.

BLDC motors are a type of synchronous motor. This means the magnetic field generated by the stator and the magnetic field generated by the rotor rotate at the same frequency. BLDC motors do not experience the "slip" that is normally seen in induction motors.

BLDC motors come in single-phase, 2-phase and 3-phase configurations. Corresponding to its type, the stator has the same number of windings of the respective number of phases. Out of these, 3-phase motors are the most popular and widely used. This thesis focuses on 3-phase motors.

BLDC motors have other advantages compared to brushed DC motors and induction motors like rugged construction and the absence of sparks caused by absence of brushes that is essential when the motor operates in environments saturated with volatile organic compounds such as fuels.

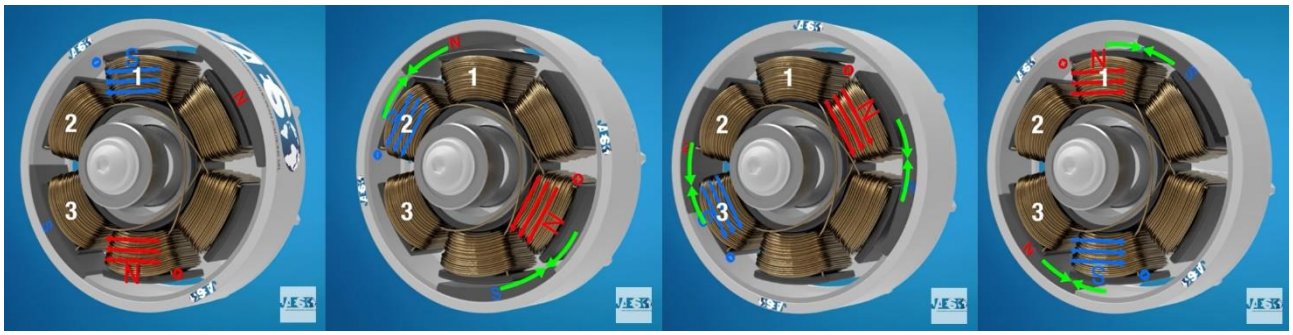

Figure 17: Brushless DC motor 3-phase configurations

2.1) Rotor

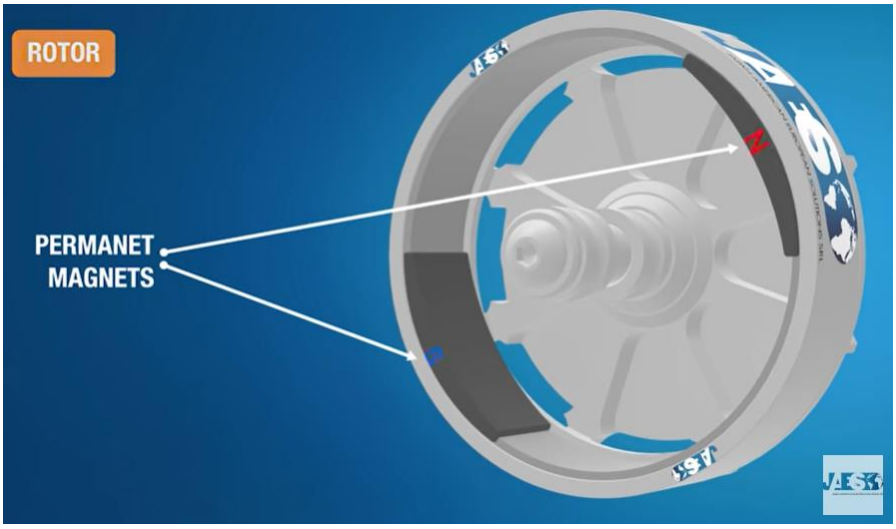

Figure 18: Rotor's configuration

The rotor is made of permanent magnet and can vary from two to eight pole pairs with alternate North (N) and South (S) poles.

Based on the required magnetic field density in the rotor, the proper magnetic material is chosen to make the rotor. Ferrite magnets are traditionally used to make permanent magnets. As the technology advances, rare earth alloy magnets are gaining popularity. The ferrite magnets are less expensive but they have the disadvantage of low flux density for a given volume. In contrast, the alloy material has high magnetic density per volume and enables the rotor to compress further for the same torque. Also, these alloy magnets improve the size-to-weight ratio and give higher torque for the same size motor using ferrite magnets. Neodymium (Nd), Samarium Cobalt (SmCo) and the

alloy of Neodymium, Ferrite and Boron (NdFeB) are some examples of rare earth alloy magnets. Continuous research is going on to improve the flux density to compress the rotor further.

Figure 19 shows cross sections of different arrangements of magnets in a rotor.

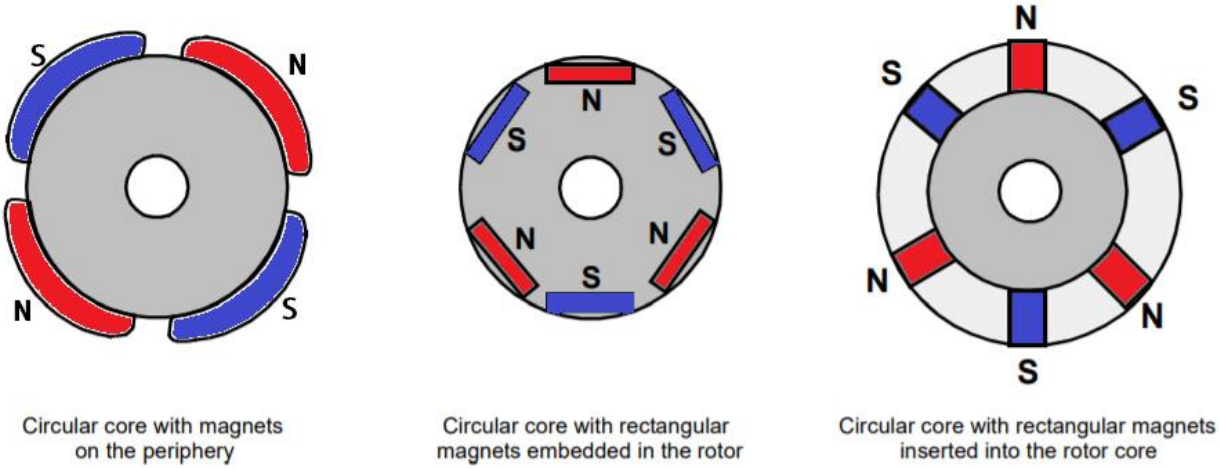

Figure 19: Rotor magnet cross sections

A higher number of magnets (i.e. an high number of magnetic poles) reduces the ripple of torque value, thus giving a "smoother" torque, but sets a maximum speed limit due to the limit of the switching frequency in the control electronics.

2.2) Stator

The stator of a BLDC motor consists of stacked steel laminations with windings placed in the slots that are axially cut along the inner periphery (as shown in Figure 20).

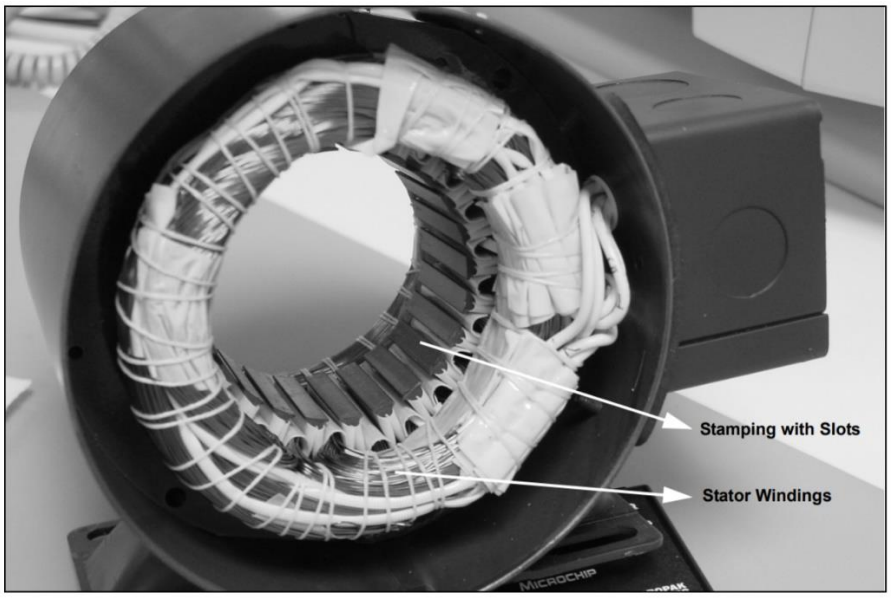

Figure 20: Stator of a BLDC motor

Traditionally, the stator resembles that of an induction AC motor; however, the windings are distributed in a different manner. Most BLDC motors have three stator windings connected in star fashion. Each of these windings are constructed with numerous coils placed in the slots and interconnected to form a winding.

Each of these windings are distributed over the stator periphery to form an even numbers of poles.

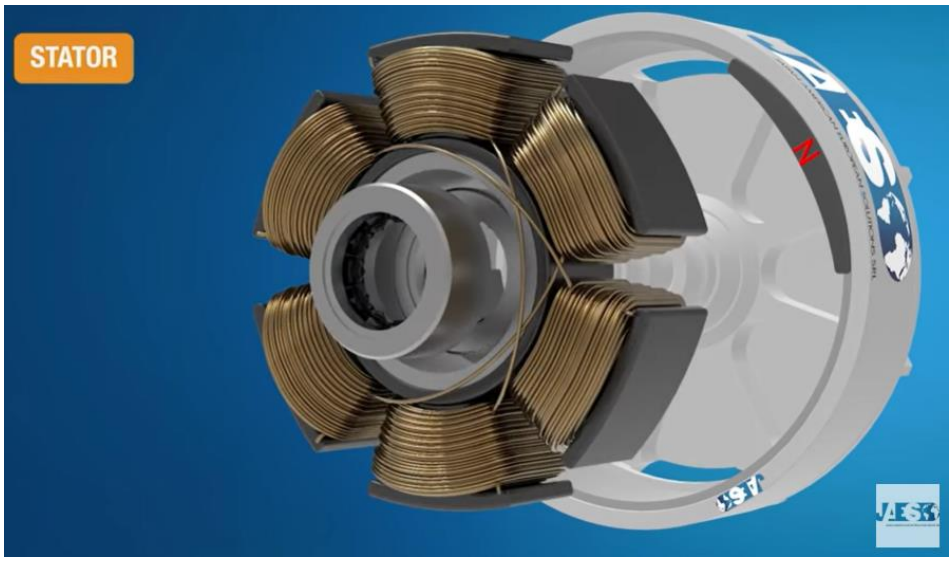

Figure 21: Stator's configuration

There are two types of stator windings variants: trapezoidal and sinusoidal motors. This differentiation is made on the basis of the interconnection of coils in the stator windings to give the different types of back Electromotive Force (EMF). Back EMF will be described in detail in 2.3 paragraph.

As their names indicate, the trapezoidal motor gives a back EMF in trapezoidal fashion and the sinusoidal motor's back EMF is sinusoidal, as shown in Figure 22.

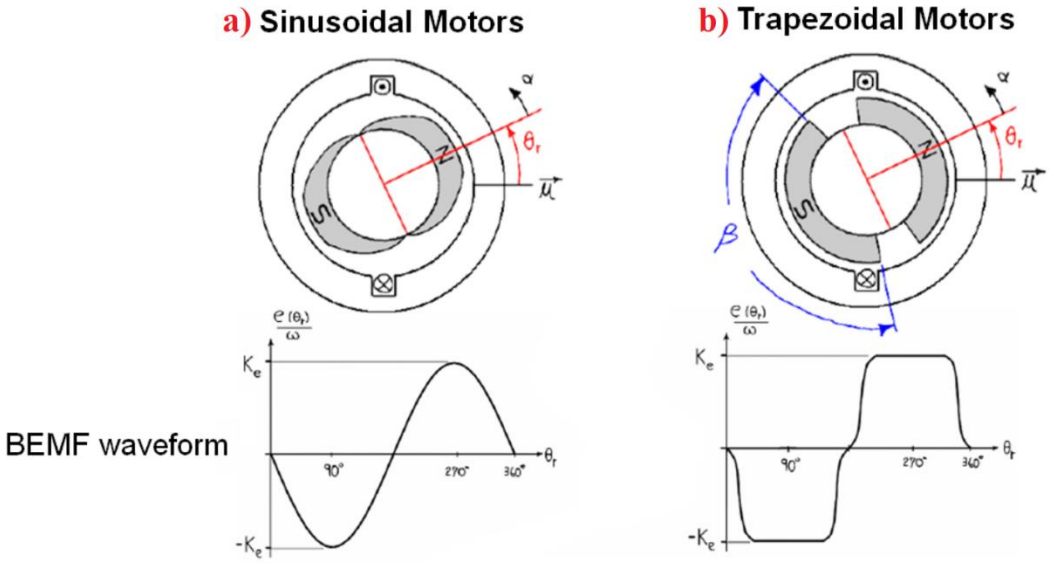

Figure 22: Sinusoidal VS Trapezoidal configuration

In addition to the back EMF, the phase current also has trapezoidal and sinusoidal variations in the respective types of motor. This makes the torque output by a sinusoidal motor smoother than that of a trapezoidal motor.

However, this comes with an extra cost, as the sinusoidal motors take extra winding interconnections because of the coils distribution on the stator periphery, thereby increasing the copper intake by the stator windings. Depending upon the control power supply capability, the motor with the correct voltage rating of the stator can be chosen.

Phase windings in a stator could be arranged in two different ways, star pattern (Y) or delta pattern (Δ): the main difference between these two configurations is the phase voltage.

In fact, in delta configuration the phase voltage is equal to the line voltage, in star configuration is equal to 1 √3 of the line voltage. Hence, it's clear that when the same voltage is applied, the delta pattern sees a higher current flow thus the torque (directly proportional to the current) is higher.

However, in delta pattern all the windings must be always powered and the commutation order is different; for this reason, this last solution is used only in special applications.

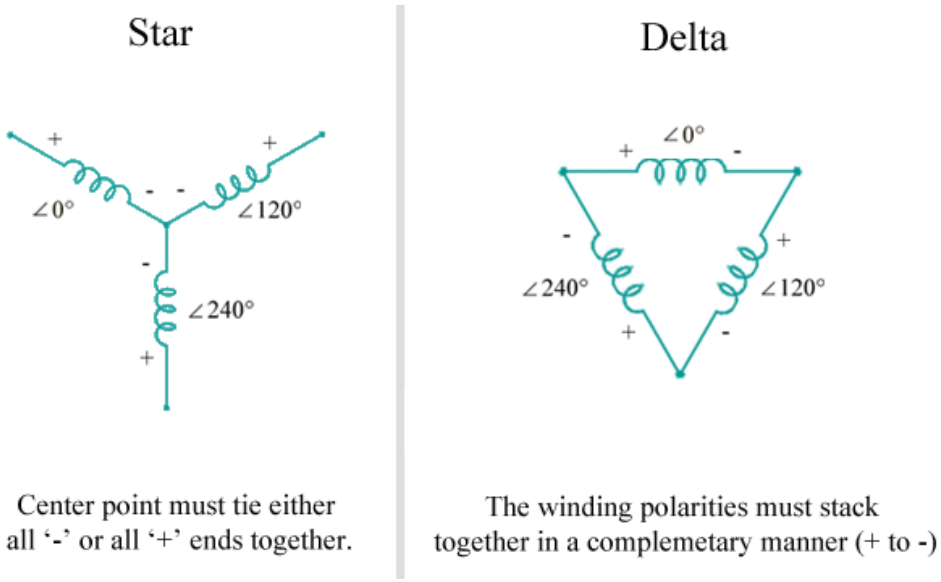

Figure 23: star and delta configurations

2.3) Back EMF

When a BLDC motor rotates, each winding generates a voltage known as back Electromotive Force or back EMF, which opposes the main voltage supplied to the windings according to Lenz's Law. The polarity of this back EMF is in opposite direction of the energized voltage. Back EMF depends mainly on three factors:

- Angular velocity of the rotor;
- Magnetic field generated by rotor magnets;
- The number of turns in the stator windings.

Back EMF may be expressed through the following law:

$$Back\ EMF = (E) \propto NlrB\omega$$

where:

- N is the number of winding turns per phase;
- l is the length of the rotor;
- r is the internal radius of the rotor;
- B is the rotor magnetic field density;
- ω is the motor's angular velocity.

Once the motor is designed, the rotor magnetic field and the number of turns in the stator windings remain constant. The only factor that governs back EMF is the angular velocity or speed of the rotor and as the speed increases, back EMF also increases.

The potential difference across a winding can be calculated by subtracting the back EMF value from the supply voltage. The motors are designed with a back EMF constant in such a way that when the motor is running at the rated speed, the potential difference between the back EMF and the supply voltage will be sufficient for the motor to draw the rated current and deliver the rated torque.

If the motor is driven beyond the rated speed, back EMF may increase substantially, thus decreasing the potential difference across the winding, reducing the current drawn which results in a drooping torque curve as it's visible in the following graph.

The last point on the speed curve would be when the supply voltage is equal to the sum of the back EMF and the losses in the motor, where the current and torque are equal to zero.

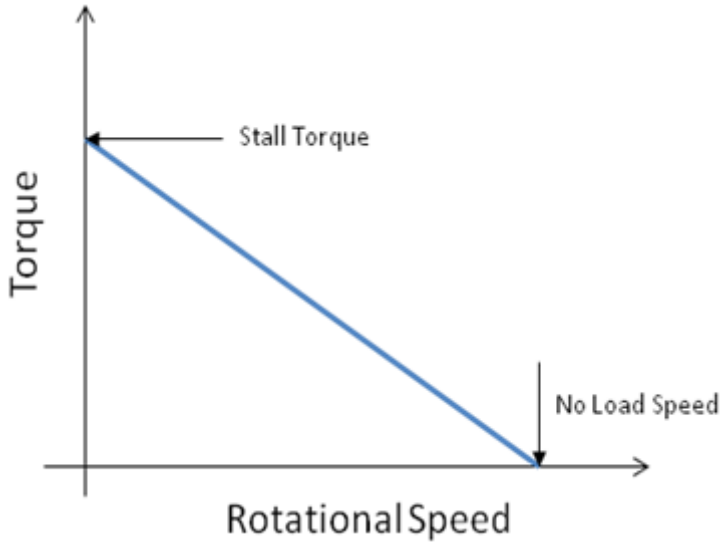

Figure 24: Drooping torque

3) Theory of Operation

Each commutation sequence works with one of the windings energized to positive power (current enters into the winding), the second winding negative (current exits the winding) and the third winding in a non-energized condition. Torque is produced because of the interaction between the magnetic field generated by the stator coils and the permanent magnets. Ideally, the peak torque occurs when these two fields are at 90° to each other and falls off as the fields move together. In order to keep the motor running, the magnetic field produced by the windings shift position because the rotor moves to catch up with the stator field; without ever reaching it completely because the next commutation begins shortly before. The "Six-Step Commutation" defines the sequence of energizing the windings.

3.1) Hall sensors

Unlike a brushed DC motor, the commutation of a BLDC motor is controlled electronically. To rotate the BLDC motor, the stator windings should be energized in a sequence. It is important to know the rotor position in order to understand which winding will be energized following the energizing sequence. Rotor position is sensed using Hall effect sensors embedded into the stator.

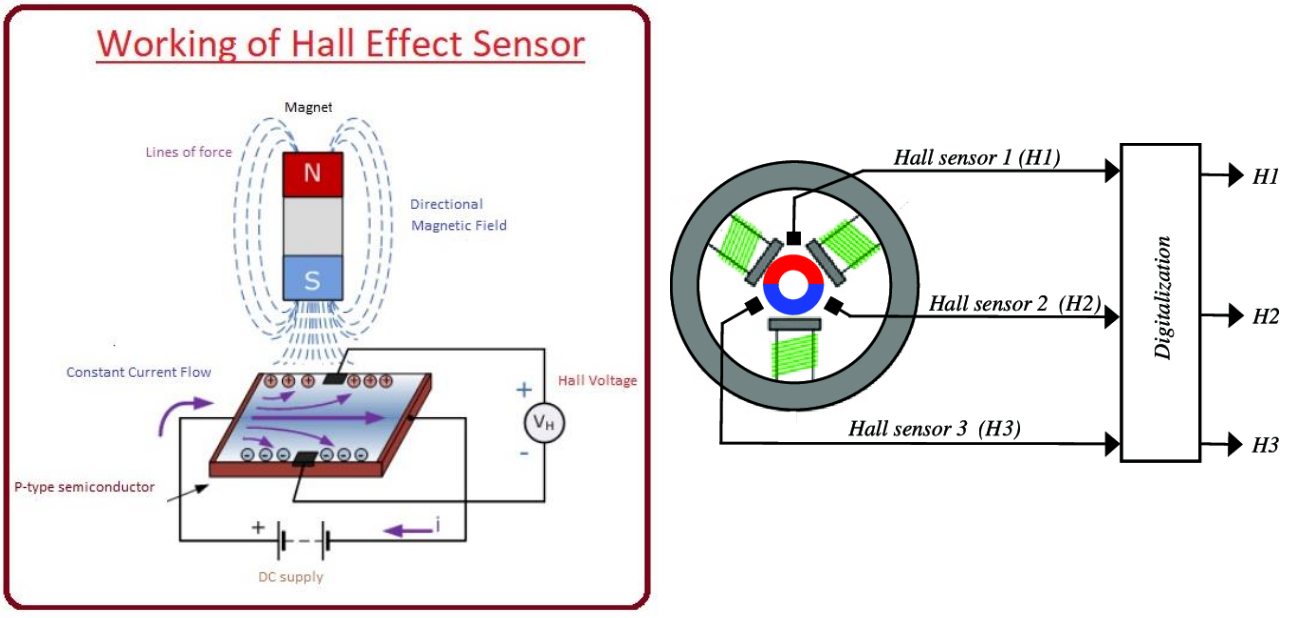

Figure 25: Hall sensor

Firstly, it's necessary to explain Hall Effect Theory in few words. If an electric current carrying conductor is kept in a magnetic field, the magnetic field exerts a transverse force on the moving charge carriers which tends to push them to one side of the conductor. This is most evident in a thin flat conductor. A build-up of charge at the sides of the conductors will balance this magnetic influence, producing a measurable

voltage between the two sides of the conductor. The presence of this measurable transverse voltage is called the Hall effect.

Most BLDC motors have three Hall sensors embedded into the stator on the non-driving end of the motor. Whenever the rotor magnetic poles pass near the Hall sensors, they give a high or low signal, indicating the N or S pole is passing near the sensors. Based on the combination of these three Hall sensor signals, the exact sequence of commutation can be determined.

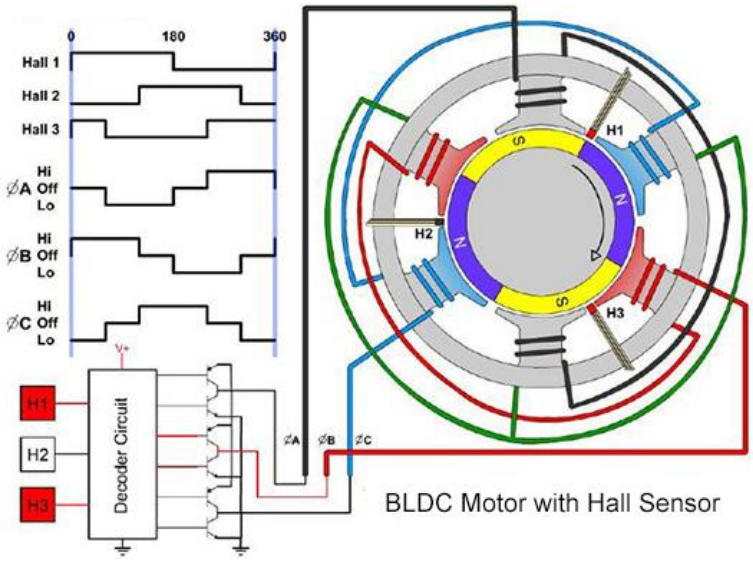

Figure 26: Hall sensor's arrangement

Figure below shows a transverse section of a BLDC motor with a rotor that has alternate N and S permanent magnets. Hall sensors are embedded into the stationary part of the motor. Embedding the Hall sensors into the stator is a complex process because any misalignment in these Hall sensors, with respect to the rotor magnets, will generate an error in determination of the rotor position. To simplify the process of mounting the Hall sensors onto the stator, some motors may have the Hall sensor magnets on the rotor, in addition to the main rotor magnets. These are a scaled down replica version of the rotor. Therefore, whenever the rotor rotates, the Hall sensor magnets give the same effect as the main magnets.

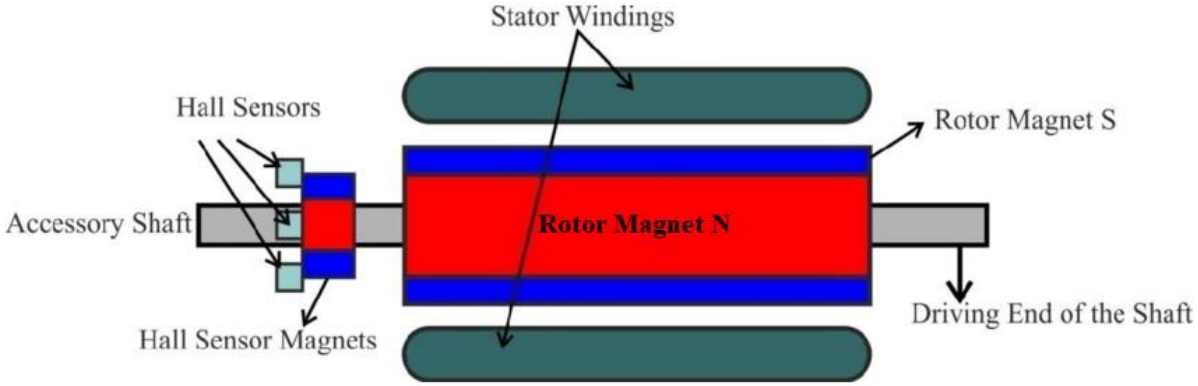

Figure 27: BLDC motor transverse section

3.2) Torque/speed characteristics

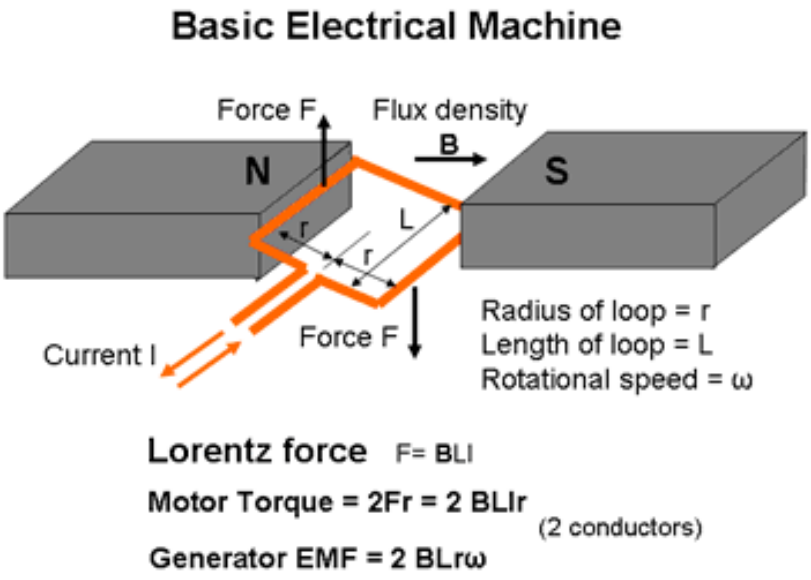

Figure 28: Lorentz force and motor Torque

Torque of a BLDC motor is generated by the interaction between rotor permanent magnets and stator windings. Generically, for a coil in which the current pass through and immersed in a magnetic field (Figure 26), the Lorentz law says that:

$$F = N\, i\, \vec{B}\, x\, l$$

Where $\vec{B}$ is the magnetic induction vector (expressed in Wb/m^2), i is the current, l is the length of the coil and N is the number of windings in the coil.

Knowing that the motor torque could be expressed as:

$$T = F \cdot r$$

where r is the radius of loop of the coil, substituting the expression of the Lorentz law when the angle between magnetic induction and the direction of the coil is 90°, it obtain:

$$T = iBlr = i\frac{\phi}{S} lr$$

where $\phi = B \cdot S \cdot cos\theta$ is the intensity of the magnetic flux (expressed in Wb and θ is the angular position of the coil) and S is the area interested by the magnetic flux. The rotation of the motor modifies ϕ which crosses each coil in stator windings according to Faraday's law which happens when the magnetic field flux across the surface bounded by an electrical circuit is variable over time. So a counterelectromotive force is applied at each phase because the law requires that an induced electromotive force is generated in the circuit equal to the opposite of the temporal variation of the flow. To find the expression of the torque is required to combine the previous expressions, finding:

$$T = k_c i$$

where k_c is the torque constant.

The total torque could be calculated adding the contributions given by the three phases of the motor.

This value is maximum when the magnetic field generated by the permanent magnet of the rotor and by the stator are perpendicular: so the control logic tries to maintain the phases closest to π/2.

Using the expressions listed above, the torque could be simply expressed as a function of speed. Knowing that a BLDC motor could be modelled with:

$$Vm = Ri + k_c\omega$$

isolating the current and remembering the previous equations, the torque is:

$$T = k_c i = \frac{V_m k_c}{R} - \frac{k_c^2}{R}\omega$$

In the same way, it could also express the output power of the motor as:

$$Pout = T\omega = \frac{Vmk_c}{R}\omega - \frac{k_c^2}{R}\omega$$

It's important to underline the speed dependency from the torque and the power: the former is a linear function, the latter is a parabola.

These two relations can be represented in the graph on Figure 29.

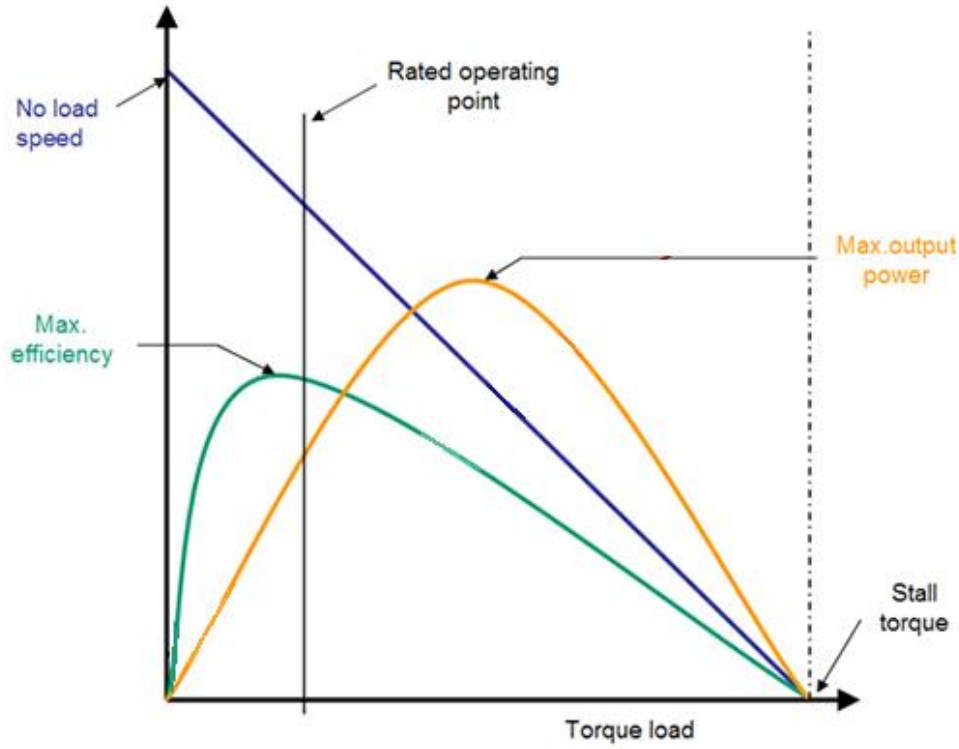

Figure 29: Power's graph

It can be noticed from the graph that torque is maximum with the rotor stopped and decreases linearly with speed, while maximum power corresponds to half the maximum no-load angular velocity.

Efficiency η is defined as the ratio between output power and input power:

$$\eta = \frac{Pout}{Pin} \text{ being } Pin = Vi$$

It results:

$$\eta = \frac{k_c\,\omega}{V}$$

In the above derivation losses due to friction and viscous effects have been neglected, since they are usually small compared to Joule effect losses.

There are two torque parameters used to define a BLDC motor, peak torque and rated torque. During continuous operations, the motor can be loaded up to rated torque.

This requirement comes for brief period, especially when the motor starts from stand still and during acceleration. During this period, extra torque is required to overcome the inertia of load and the rotor itself.

The motor can deliver a higher torque up to maximum peak torque, as long as it follows the speed torque curve.

Figure 30 shows the torque-speed characteristics of a BLDC motor. There are two torque parameters used to define a BLDC motor, peak torque (T_P) and rated torque (T_R):

- TR is the torque available on the shaft for the given speed range which depends on the physical and functional characteristics of the motor.
- The peak, or maximum torque required for the application, can be calculated by summing the load torque (TL), torque due to inertia (TJ) and the torque required to overcome the friction (TF). TP is the maximum torque that motor can deliver for a short duration of time. This torque may not be available for all the speed ranges.

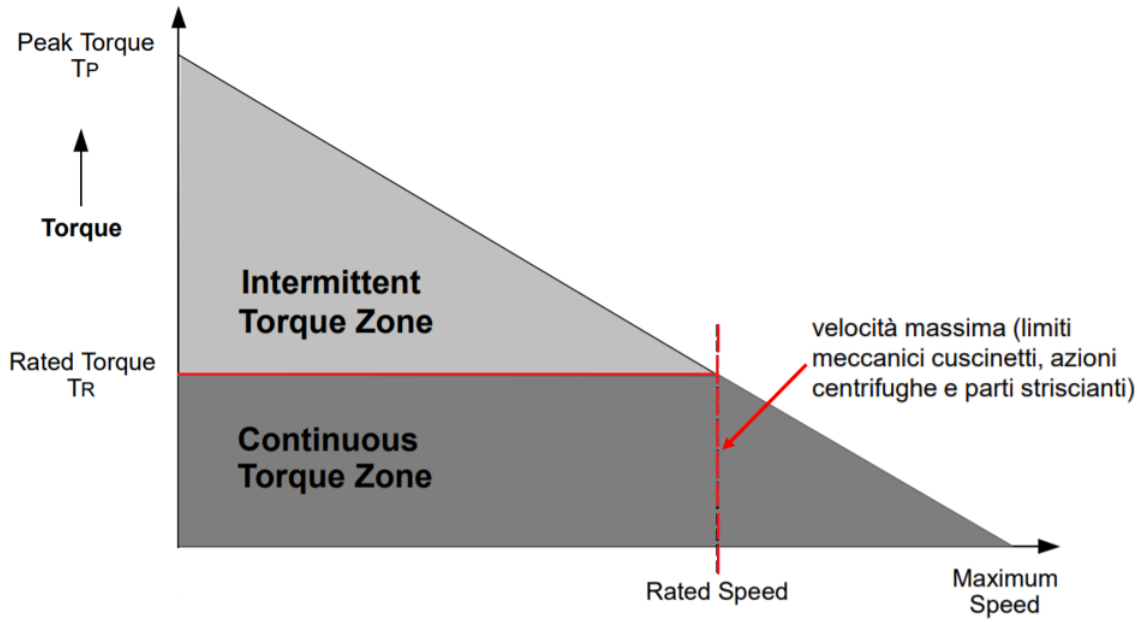

Figure 30: Torque vs Speed Characteristics of BLDC Motor

During continuous operations, the motor can be loaded up to the rated torque.

As discussed earlier, in a BLDC motor, the torque remains constant for a speed range up to the rated speed. The motor can be run up to the maximum speed, which can be up to 150% of the rated speed, but the torque starts dropping.

The stall torque represents the point on the graph at which the torque is maximum, but the shaft is not rotating. The no load speed, ω_n, is the maximum output speed of the motor (when no torque is applied to the output shaft).

If the phase resistance is small, as it should be in an efficient design, then the characteristic is similar to that of a DC motor.

Aerospace applications which have frequent starts and stops and frequent reversals of rotation with load on the motor, demand more torque than the rated torque.

This requirement comes for a brief period, especially when the motor starts from a standstill and during acceleration. During this period, extra torque is required to overcome the inertia of the load and the rotor itself. The motor can deliver a higher torque, maximum up to peak torque, as long as it follows the speed torque curve.

The speed is essentially controlled by the voltage, and may be varied by varying the supply voltage. The motor then draws just enough current to drive the torque at this speed. As the load torque is increased, the speed drops, and the drop is directly proportional to the phase resistance and the torque.

The voltage is usually controlled by a chopper or by a PWM logic. This gives rise to a family of torque-speed characteristics in the boundaries of continuous and intermittent operation. The continuous limit is usually determined by heat transfer and temperature rise.

The intermittent limit may be determined by the maximum ratings of semiconductor devices permitted in the controller, or by temperature rise.

In practice the torque-speed characteristic deviates from the ideal form because of the effects of inductance and other parasitic phenomena. The linear model of a DC motor torque-speed curve is a very good approximation.

3.3) Phase commutation

To simplify the explanation of how to operate a three phase BLDC motor, a typical BLDC motor with only three coils is considered. As previously shown, phases commutation depends on the hall sensor values.

When motor coils are correctly supplied, a magnetic field is created and the rotor moves. The most elementary commutation driving method used for BLDC motors is an ON-OFF switch scheme where, a coil D_i is either conducting or not conducting.

Only two windings are supplied at the same time and the third winding is floating. Connecting the coils to the power and neutral bus induces the current flow.

This, just exposed, is referred as trapezoidal commutation or block commutation.

Figure 31 shows the three phase bridge inverter previously exposed.

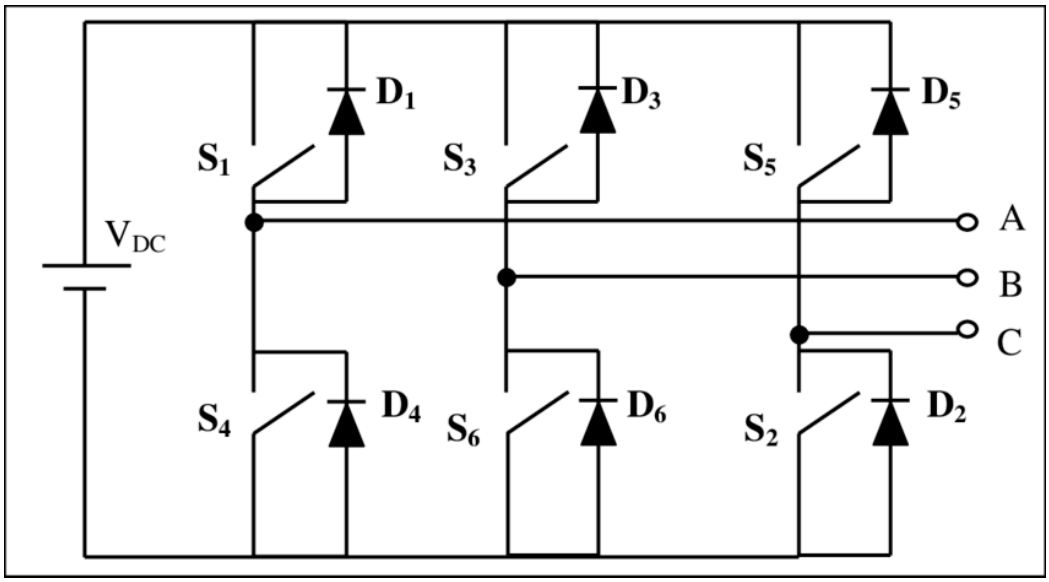

Figure 31: Three Phase Bridge Inverter

Figure 32 shows the equivalent circuit of a Y connection BLDC motor and the inverter topology.

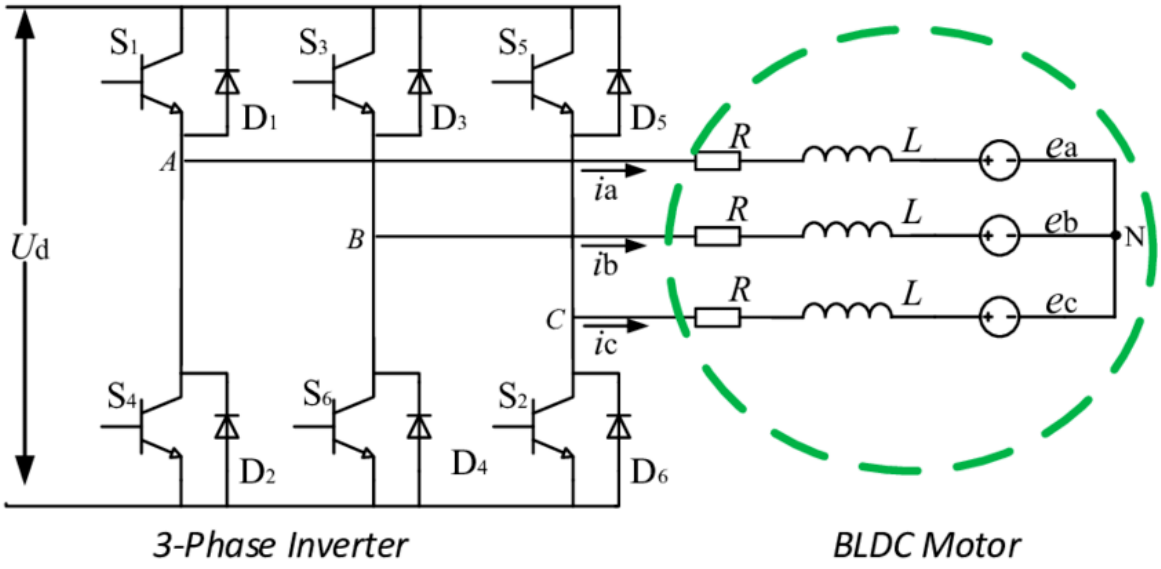

Figure 32: Circuit Diagrams of BLDC Motor with Inverter

Therefore to command brushless DC motors, a three phase bridges is used. For motors with multiple poles the electrical rotation does not correspond to a mechanical rotation. A four pole BLDC motor uses four electrical rotation cycles to have one mechanical rotation.

The back EMF of the BLDC Motor can drive the inverter by detecting the zero crossing point of the back EMF then commutate the inverter power switching devices.

The two power switching device turn ON at any instant for 60 degree and the commutation occurs by next pair conducted for the continuous operation of motor. The strength of the magnetic field determines the force and speed of the motor.

By varying the current flow through the coils, the speed and torque of the motor can be adjusted. The most common way to control the current flow is to control the average current flow through the coils.

PWM is used to adjust the average voltage and thereby the average current, inducing the speed. Table 1 shows the operation sequence of a BLDC motor with Hall Sensors.

Hall Sensors Values	Phase	Switches
101	U-V	Q1;Q4
001	U-W	Q1;Q6
011	V-W	Q3;Q6
010	V-U	Q3;Q2
110	V-W	Q5;Q2
100	W-V	Q5;Q4

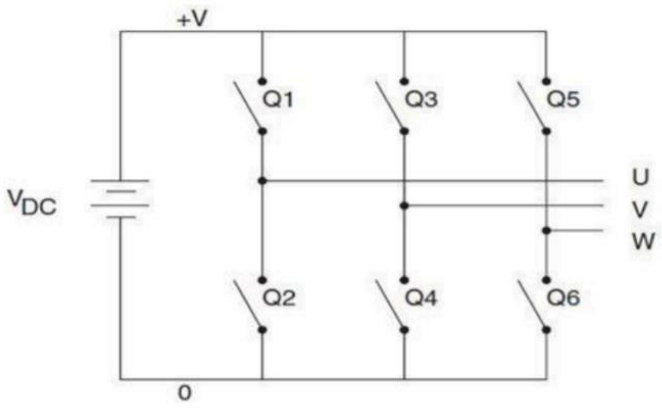

Table 1: Phase switches

The proposed scheme utilizes the back EMF difference between two phases for BLDC sensor less drive instead of using the phase back EMF.

The zero crossing points of the back EMF in each phase may be an attractive feature used for sensing, because these points are independent of speed and occur at rotor positions where the phase winding is not excited. However, these points do not correspond to the commutation instants.

Therefore, the signals must be phase shifted by 90 electrical degree before they can be used for commutation. The detection of the third harmonic component in back EMF, direct current control algorithm and phase locked loops have been proposed to overcome the phase-shifting problem.

Following Figure 33 shows the phase back EMF of BLDC motor. The commutation sequence with back EMF difference estimation method is that positive sign indicates the current entering into the stator winding and the negative sign indicates the current leaving from the stator winding. At any instant two stator windings are energized and one winding will be in floating.

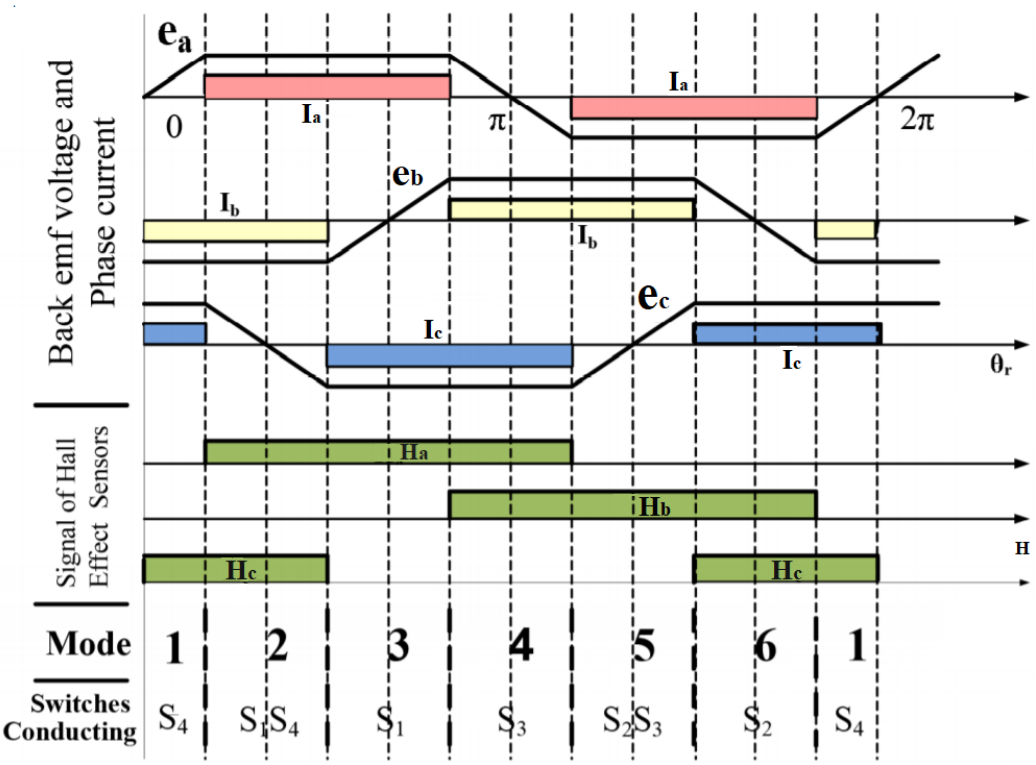

Figure 33: Phase Back EMF of BLDC Motor

3.4) Controls

Several different control modes are available for BLDC motors, depending on the controlled variables and the purpose of the regulation.

The most used is the speed control, employed in systems which receive an ON/OFF command such as hydraulic valves/pumps, reservoirs, compressors or as the inner loop of a position control mechanism like a servo-actuator.

In BLDC motor speed control, the actual speed is compared with the commanded speed and the error is sent inside a P.I.D. controller (Proportional – Integrative – Derivative).

This PID device calculates if the error lays inside a correct range, a zone with an upper limit and a lower limit, which represent the acceptable error of the system. If the speed is higher than the upper limit or lower than the lower limit, the control logic gives a step command to the motor to accelerate.

This acceleration is achieved modifying the voltage which powers the motor: usually a constant DC voltage is source is available and an efficient way of regulating the phase voltage is the implementation of a PWM logic, which applies high frequency pulses with a variable duty cycle.

Then, the signal is filtered by the circuit inductance resulting in a voltage that is intermediate between supply and ground, proportionally to the PWM duty cycle.

When the Pulse Width Modulation (PWM) signal is 1, the motor is forced to accelerate due to the positive voltage, when the duty cycle is 0 the applied voltage is 0.

The frequency of the PWM signal is proportional to the analogic signal wanted. A simple example of this method is shown in Figure 34.

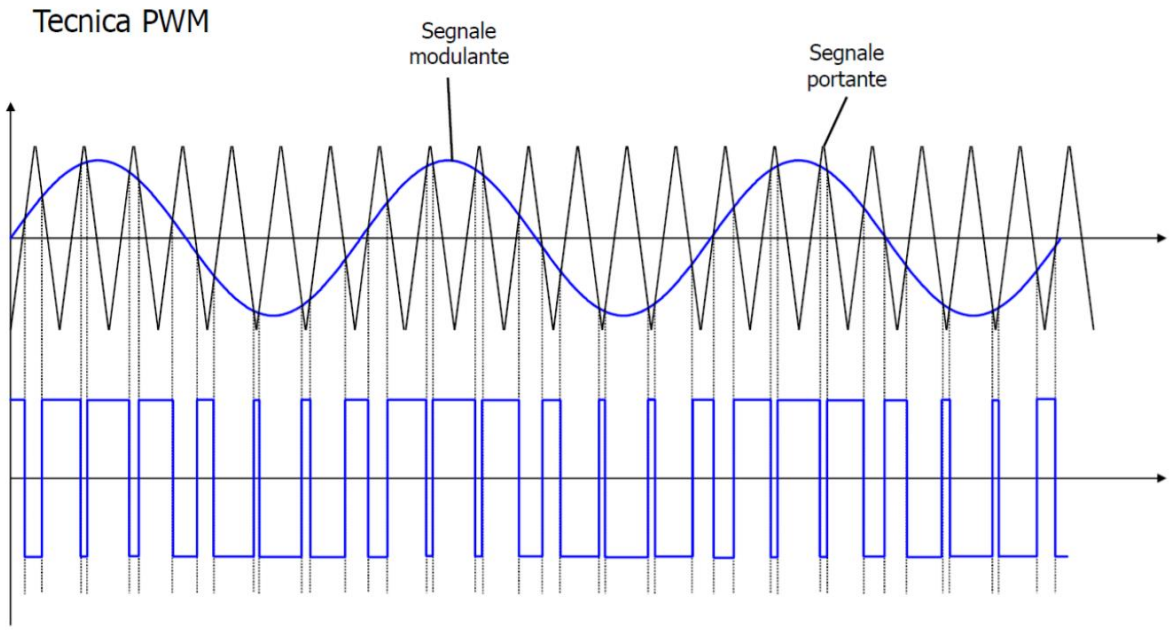

Figure 34: PWM control logic

The speed is evaluated using the signals of the Hall sensor or an encoder located properly on the moving shaft. The frequency of the PWM signal is given by the P.I.D. controller proportionally to the trend of the error: if this one is high, the signal will be 1 for a longer time than the case in which the error is small. A block diagram of a speed control loop is represented in Figure 35.

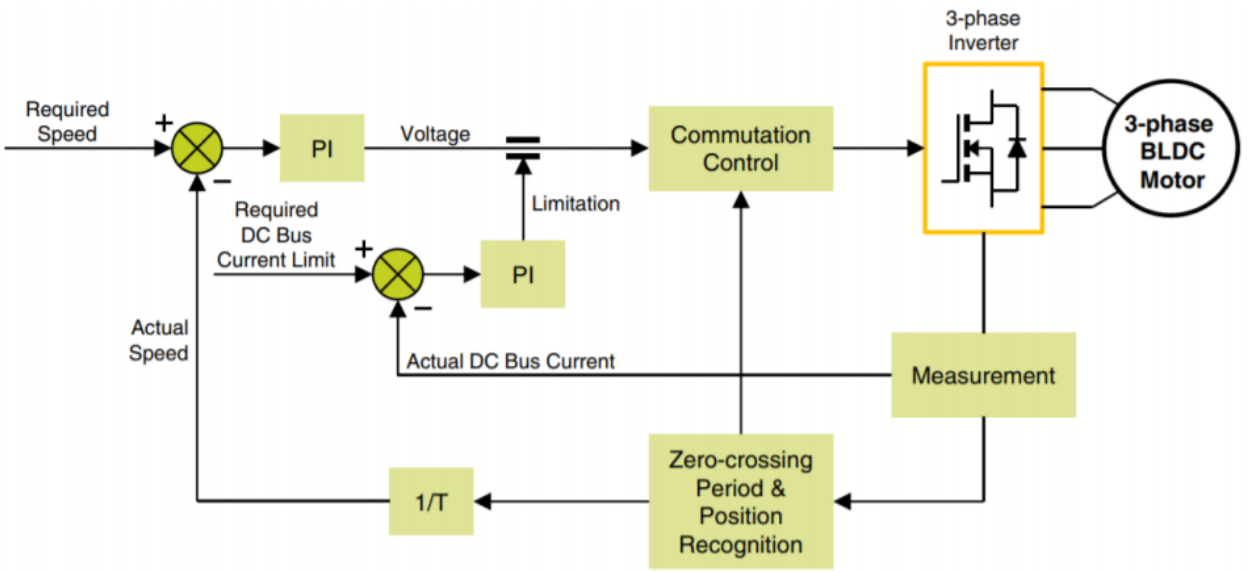

Figure 35: Speed control with current limitation

Another type of control loop is the torque control, where the motor can apply always the same output torque regardless to external load, position or speed. This control mode can be useful as inner loop of a position or speed control system. It is been said in paragraph 3.2. that the torque depends on the magnetic flux on the phase windings and it also depends on the current through the torque constant k_T. Hence, it's possible to control the torque modifying the current which flows in the phase windings. The block diagram for this type of control is shown in Figure 36.

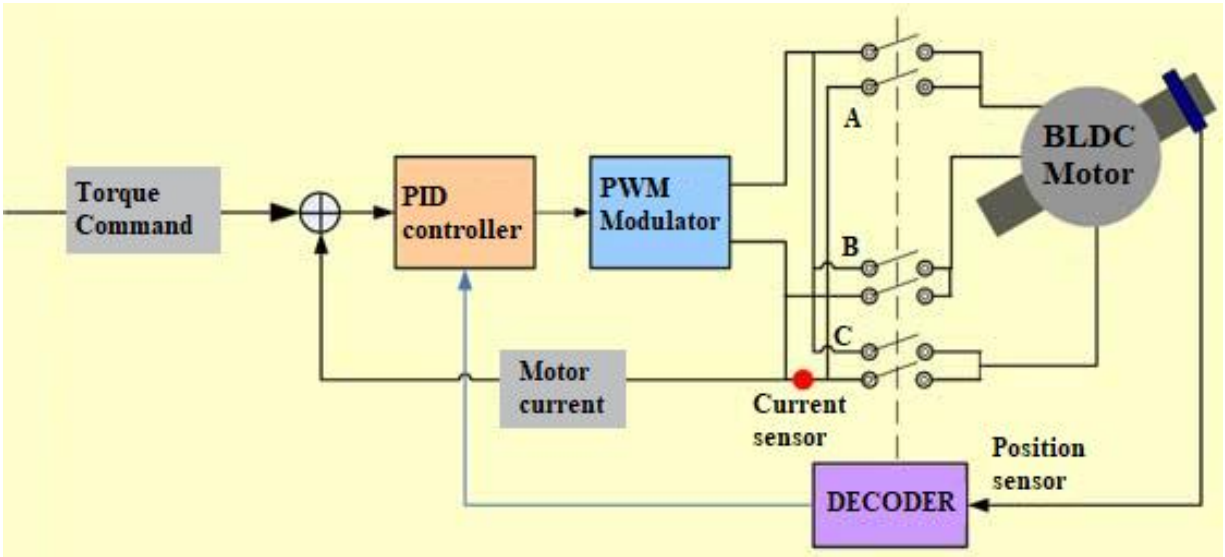

Figure 36: Block diagram for a torque control loop

It's possible estimate total current (due to the voltage drop) and the resulting value, multiplied by k_T is compared to the required torque command signal. The torque error is then sent to a PID controller which modifies the PWM duty cycle as in the speed control mode, regulating phase voltages and phase currents. Therefore, the only difference between torque and speed control mode is in the measured variable.

In a motor control design, it's important to ensure safety and reliability conditions developing a motor protection control logic. Some operating conditions can cause irreversible damages to the motor: for example, when a high external load causes the rotor to get stuck. In this case the current increases strongly, overheating the windings, damaging the coil insulation, demagnetizing rotor permanent magnets and possibly burning the power electronic devices driving the motor. To prevent a failure a motor protection control mode substitutes the normal control to preserve the system. The protection system manages peaks current, the maximum working current, under voltage conditions and Hall sensor's failures. Depending on the variable to be managed, the system works in the following ways:

- Peaks current condition, that is the maximum instantaneous current can flow in phase windings. When the windings cause a short circuit the control turn off the PWM signal in order to interrupt the power to the windings;

- Maximum working current condition, that is the extreme value of the output current when the motor needs to bear an overload. The control is implemented similar to a torque control;

- Under-voltage conditions, that is it's necessary to switch off the actuator when the voltage drop off a lower limit;

- Hall sensor's failure. Position and speed are determined using the signals provided by Hall sensors. If one of these devices break down, the commutation sequence will interrupt, and it can cause the rotor gets stuck or the growing of too high currents. The sensor failure could be detached via firmware, which controls if the logic of the sensor changes during the normal working activities.

4) Simulink reference models

Before to discuss Backlash models designed as purpose of this thesis it's necessary to analyse Simulink reference models which will be connected with Simscape models.

4.1) 2 D.O.F. Electro Mechanical Servo-Mechanism modeling

The first system has be analysed is the Electro Mechanical Servo-Mechanism with two degree of free represented in the following Figure 37 and subjected to external load T_R. In this structure there is a shaft with a certain compliance value between gearbox and final user.

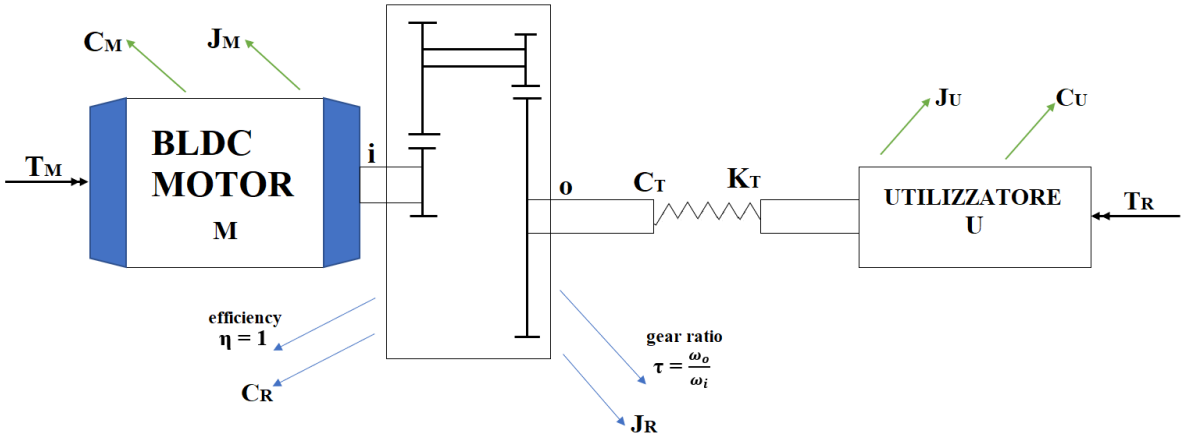

Figure 37: Schematic representation of the system

This model is used for secondary commands where it's necessary the presence of very long and flexible shafts like in Figure 38

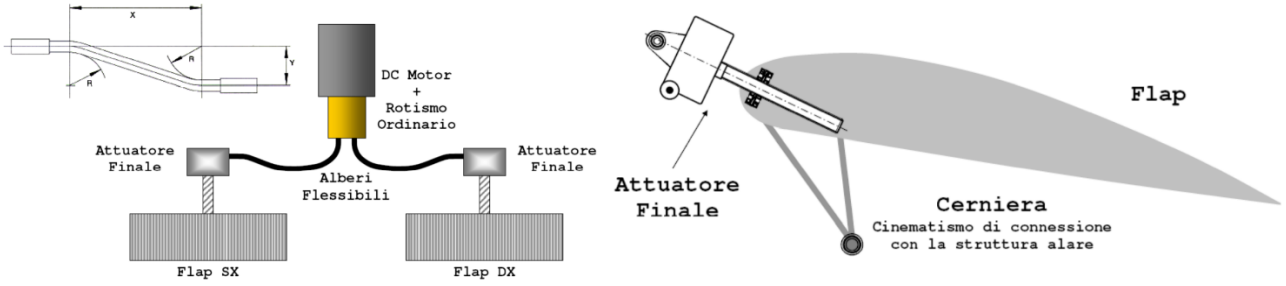

Figure 38: Actuation scheme for secondary commands

The system can divided into two zones:

- Fast shaft (Motor + Gearbox)
- Slow shaft (downstream of the Reducer)

First of all the torque TM is considered:

$$T_M = GM \cdot i$$

with *GM* the torque gain and *i* the current.

It supposes that this torque assumes values between TMM and –TMM, where TMM is the driving torque maximum.

Furthermore, it can possible write:

$$\mathrm{L} \cdot \frac{di}{dt} + R_i = \bar{V}$$

With *L* the inductance, R_i the resistance, $\bar{V}$ the voltage calculated as:

$$\bar{V} = V_A - K_{fcem} \cdot \omega_M$$

In which:

$$V_A = GA \cdot (\theta_{com} - \theta_u)$$

Where K_{fcem} is EMF constant, ω_M is angular speed of the rotor, GA is proportional gain, θ_{com} and θ_u are commanded and effective position respectively.

This voltage will assume values between VAM and –VAM, where VAM is supply voltage maximum.

It can also deduce the following relationship in which $\tau_{RL} = \frac{L}{R}$:

$$i = \frac{num(s)}{den(s)} = \frac{\frac{V_A - K_{fcem} \cdot \omega_M}{R}}{\tau_{RL} \cdot s + 1}$$

Now it's necessary to describe the mechanical system which is considered like a single degree of freedom model (infinitely rigid) where it derives the inertia and the damping coefficient. The aim of this treatment is to reduce the moment of user's inertia of the slow shaft at the fast shaft.

Because of upstream and downstream of the gearbox it must has the same power it can be possible to write:

$$J_U \cdot \dot{\omega}_U \cdot \omega_U = \bar{J}_U \cdot \dot{\omega}_i \cdot \omega_i$$

Where J_U is the user's inertia of the slow shaft, $\dot{\omega}_U$ and ω_U are angular acceleration and speed of the slow shaft respectively; instead $\bar{J}_U$ is the user's inertia of the fast shaft, $\dot{\omega}_i$and ω_i are angular acceleration and speed of the fast shaft respectively

Furthermore, it can establish with $\tau_R = \frac{\omega_o}{\omega_i}$ that:

$$\bar{J}_U = J_U \tau_R^2$$

So, it can write the total inertia J_T of the system as:

$$J_T = J_M + J_R + \bar{J}_U = J_M + J_R + J_U\tau_R^2$$

Where J_M is motor's inertia and J_R is the reducer's inertia at the fast shaft.
The same can be done for the viscous damping coefficients obtaining the following report:

$$C_T = C_M + C_R + \bar{C}_U = C_M + C_R + C_U\tau_R^2$$

Where C_M is the motor's viscous damping coefficient and C_R is the reducer's viscous damping coefficient at the fast shaft.
C_U and $\bar{C}_U$ are user's viscous damping coefficient at the slow shaft and at the fast shaft respectively.

Using relationships found previously it can produce the following Simulink model with elementary blocks which represents the system under consideration:

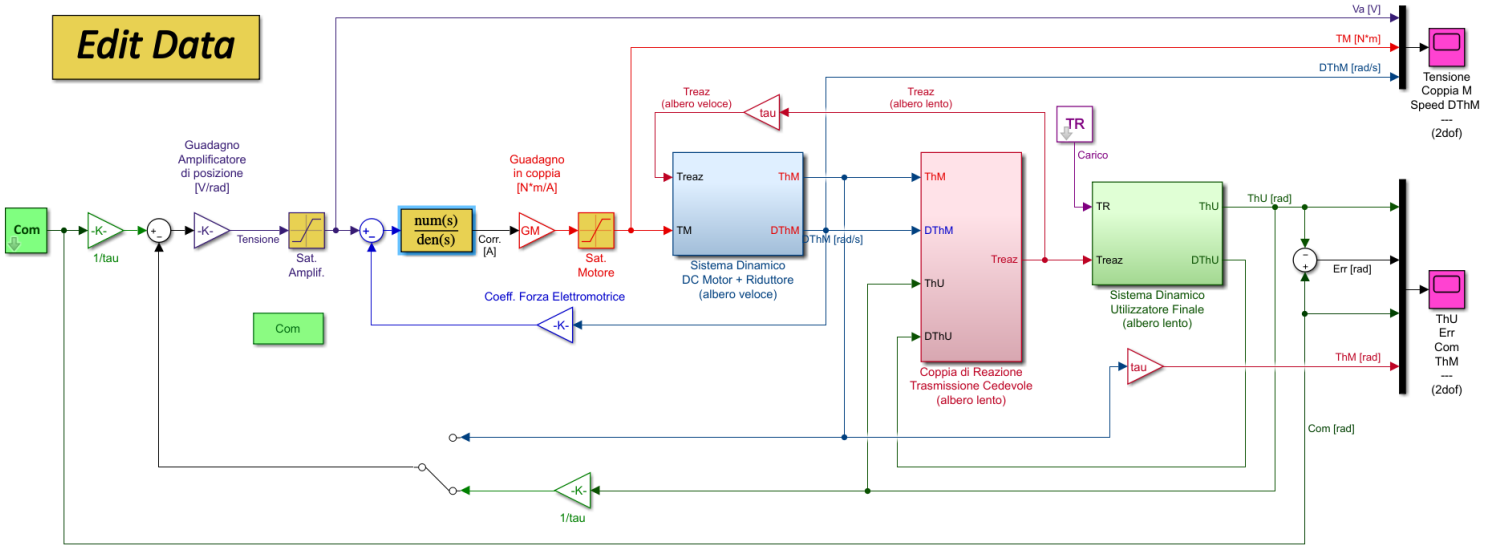

Figure 39: Simulink elementary blocks model

It sees that the model uses various colours to define its different parts:

- Control part is defined by blue and black lines;
- Cyan subsystem represents the BLCD + reducer complex;
- Red block defines flexible shaft model;
- Green block defines the end user's model.

It enters with a position command that is compared with the actual position, then there is an amplifier that generates a supply voltage which is reduced by the back-electromotive voltage and at the end it will produce the driving torque.

At this point the driving torque is applied inside cyan subsystem.

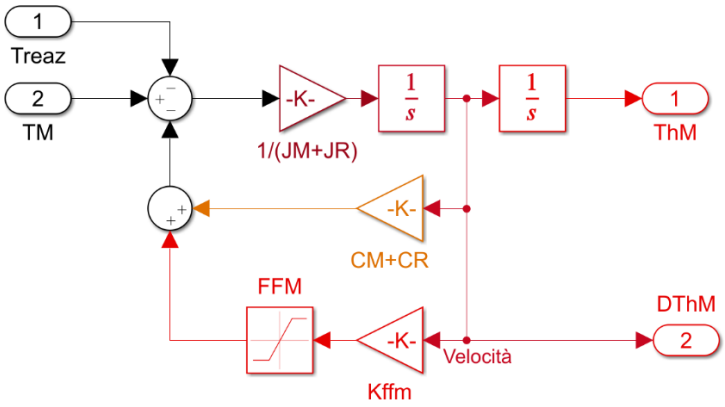

Figure 40: Cyan subsystem "BLCD + reducer"

"BLCD + reducer" block has a second order dynamics which provides angular position and speed. At the entrance there are the driving torque, a disturbing action (the reaction torque) and a viscous term; the difference between these torques is divided by the moment of inertia producing the acceleration. This result is integrated twice to obtain before angular speed and after the position. While the under part of the scheme models the friction.

Red block calculates the reaction torque according to the position and angular speed at the ends of the flexible shaft.

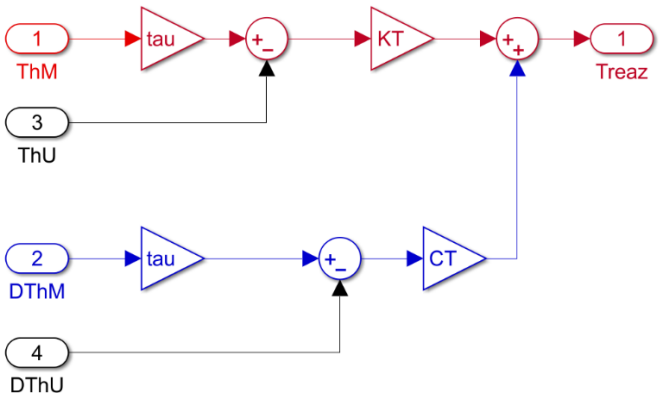

Figure 41: Red subsystem "flexible shaft model"

In the green block the input is the reaction torque which is opposed by external load and viscous effects, from the model comes out desired angular position and speed which are used to counter-react and correct the effective position.

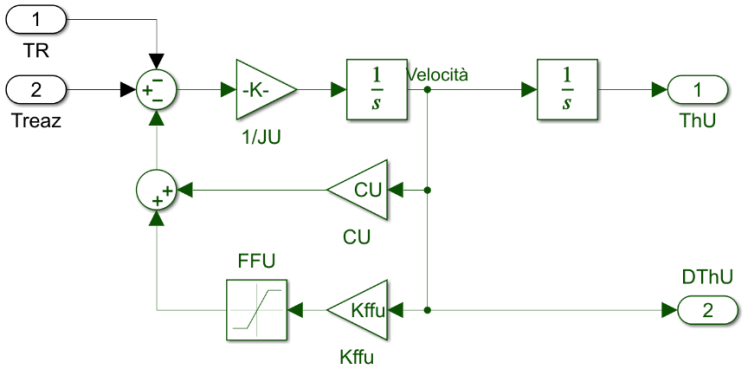

Figure 42: Green subsystem "end user"

A series of simulations can be performed using a step command and the numerical parameters shown in the Table 2:

```
Caratteristiche Comparatore-Amplificatore
DT=1e-5;        % Ampiezza passo d'integrazione (1e-6 x SMEMevo3)          [s]
TiBr=2;         % Istante arresto simulazione                              [s]
GAP=50;         % Guadagno Proporzionale Alimentatore/Amplificatore        [V/m]
GAD=0*50;       % Guadagno Derivativo Alimentatore/Amplificatore           [V*s/m]
GAS=0*50;       % Guadagno Anello di Velocità Alimentatore/Amplificatore   [V*s/m]
Vmax=25;        % Massima tensione di alimentazione Alimentatore/Amplificatore [V]

Caratteristiche DC Motor (M)
R=10;           % Resistenza ohmica delle bobine rotoriche DC Motor        [Ohm]=[V/A]
L=0.001;        % Induttanza delle bobine rotoriche DC Motor               [H]=[V*s/A]
tauRL=L/R
GM=20;          % Guadagno in coppia DC Motor                              [N*m/A]
JM=0.01;        % Momento d'inerzia del DC Motor ridotto all'albero rotorico [kg*m^2]
CM=0.02;        % Coefficiente di smorzamento viscoso dimensionale DC Motor [N*m*s/rad]
Kfcem=0.12;     % Coefficiente di Forza ControElettroMotrice (F.C.E.M.)    [V*s/rad]
TMM=50;         % Massima Coppia motrice erogata da DC Motor               [N*m]

FFM=1;          % Massima Coppia d'attrito secco DC Motor                  [N*m]
Kffm=1e4;       % Pendenza tratto lineare mod. Iperviscoso FF              [N*m/(rad/s)]

Caratteristiche riduttore (R)
JR=0.005;       % Momento d'inerzia del riduttore ridotto all'albero rotorico [kg*m^2]
CR=0.01;        % Coefficiente di smorzamento viscoso dimensionale riduttore [N*m*s/rad]
tau=1e-2;       % Rapporto di tramissione del riduttore                    [#]

Caratteristiche albero di trasmissione cedevole
KT=1e6%1e6;%1e8;% Rigidezza torsionale albero di trasmissione lento        [N*m/rad]
CT=500;         % Coefficiente di smorzamento viscoso dimensionale struttura [N*m*s/rad]

Caratteristiche utilizzatore (U)
JU=50;          % Momento d'inerzia del riduttore ridotto all'albero rotorico [kg*m^2]
CU=500;         % Coefficiente di smorzamento viscoso dimensionale riduttore [N*m*s/rad]

FFU=100;        % Massima Coppia d'attrito secco DC Motor                  [N*m]
Kffu=1e6;       % Pendenza tratto lineare mod. Iperviscoso FF              [N*m/(rad/s)]

Calcolo delle grandezze ridotte all'albero rotorico (veloce)
Jt=JM+JR+JU*tau^2
Ct=CM+CR+CU*tau^2

Coppie resistenti applicate
TR0=0;
TRC=2500;
TRs=1.4;

Comandi Predefiniti:
Com=[0 0 0];
TimeCom=[0 1 2];
```

Table 2: Simulation parameters

4.1.1) Simulation

The simulation starts clicking on the "Run" Simulink command and it produces the following trends.

On the first graph are reported the voltage, the drive torque and the angular speed.

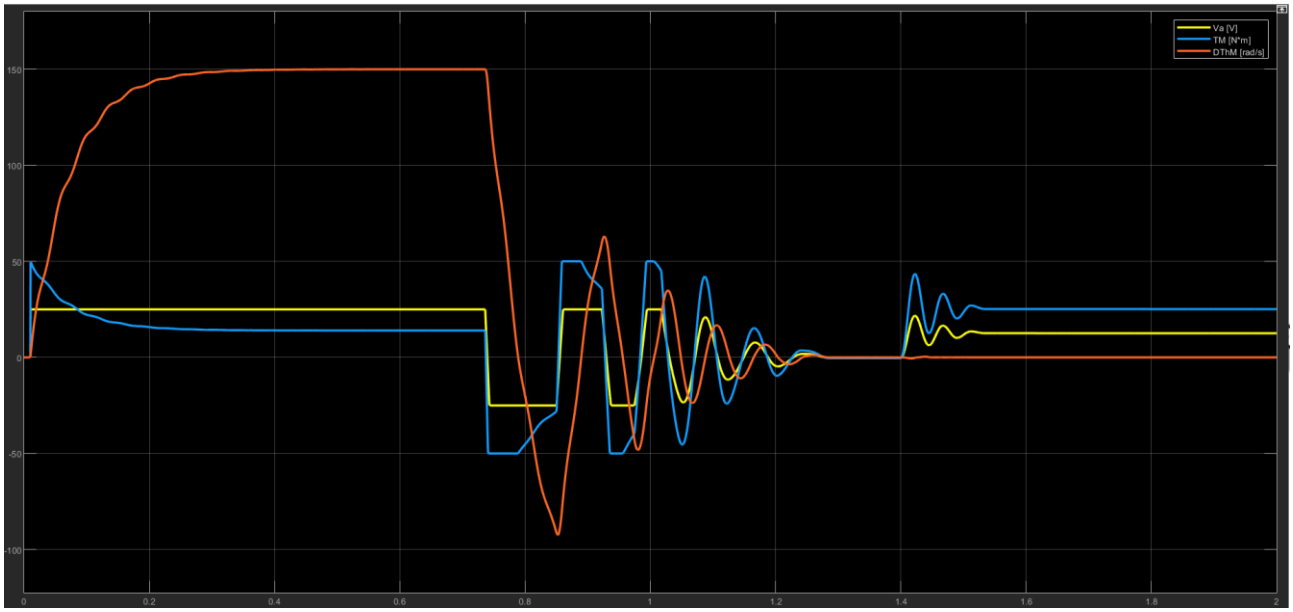

Figure 43: Voltage, drive torque and angular speed – external load

After selecting a step command, the simulation produces also the following graph where are plotted motor's and user's position and the relative error between these two signals.

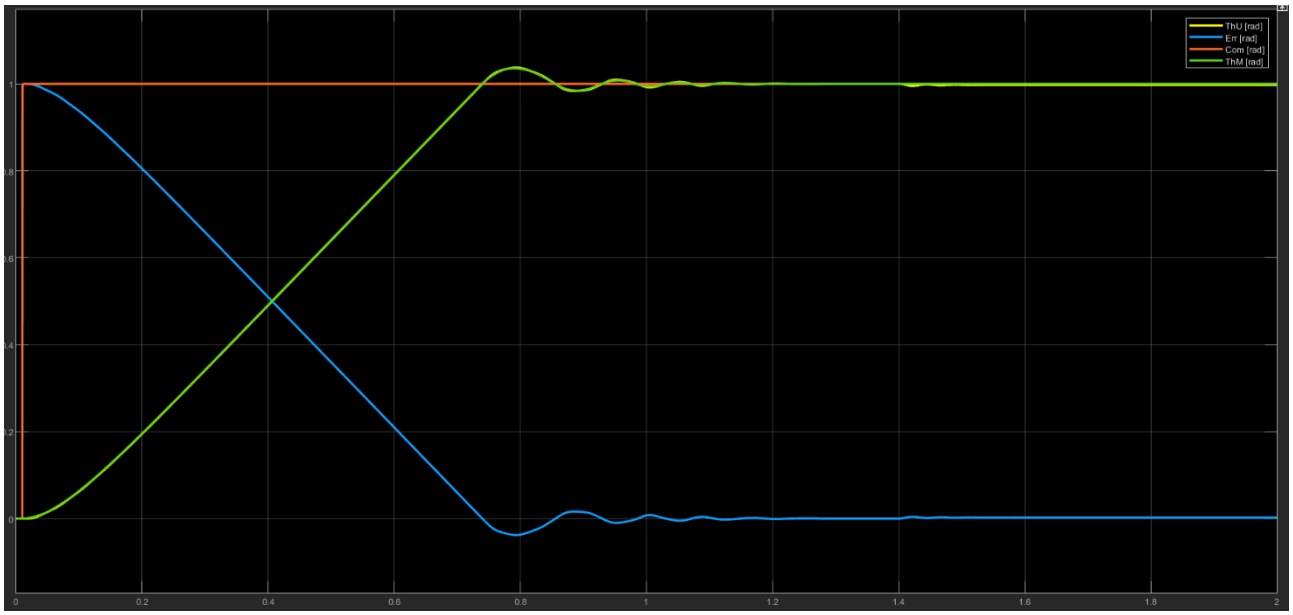

Figure 44: Command, positions and error

It seems that the motor's position ThM and the user's position ThU are similar but this is not the case.

In fact, when it applies the command, the two dynamics are not overlappes (this happens in the steady state) but they react in a distinct way: the user doesn't start

immediately, because motor and user have a certain inertia and because there is a shaft flexible in the middle between them.

As long as the differential torsion isn't high enough to overcome the friction and to apply an angular acceleration on the user, a position gap is created between the two elements which is gradually reduced as the user begins to move. This behaviour is visible on Figure 45.

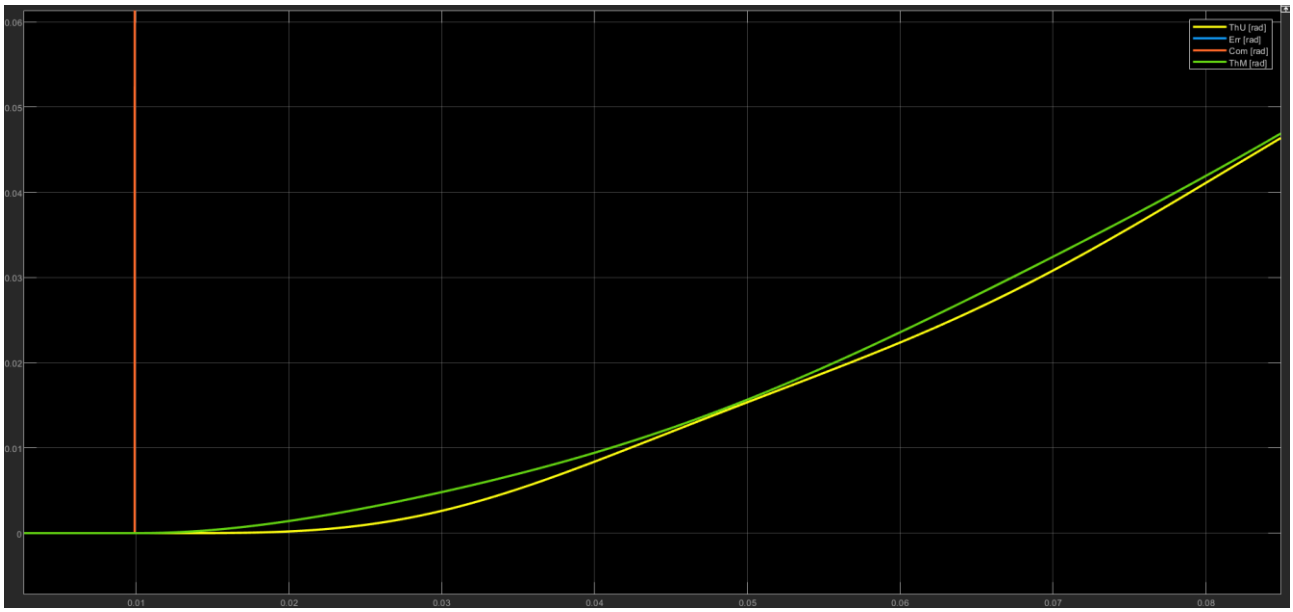

Figure 45: Two dynamics with no overlap

Zooming in to the following graph, it can see that the motor's response is always in advance, this is because the transmission shaft is slightly deformed in order to develop a reaction torque that compensates viscous losses.

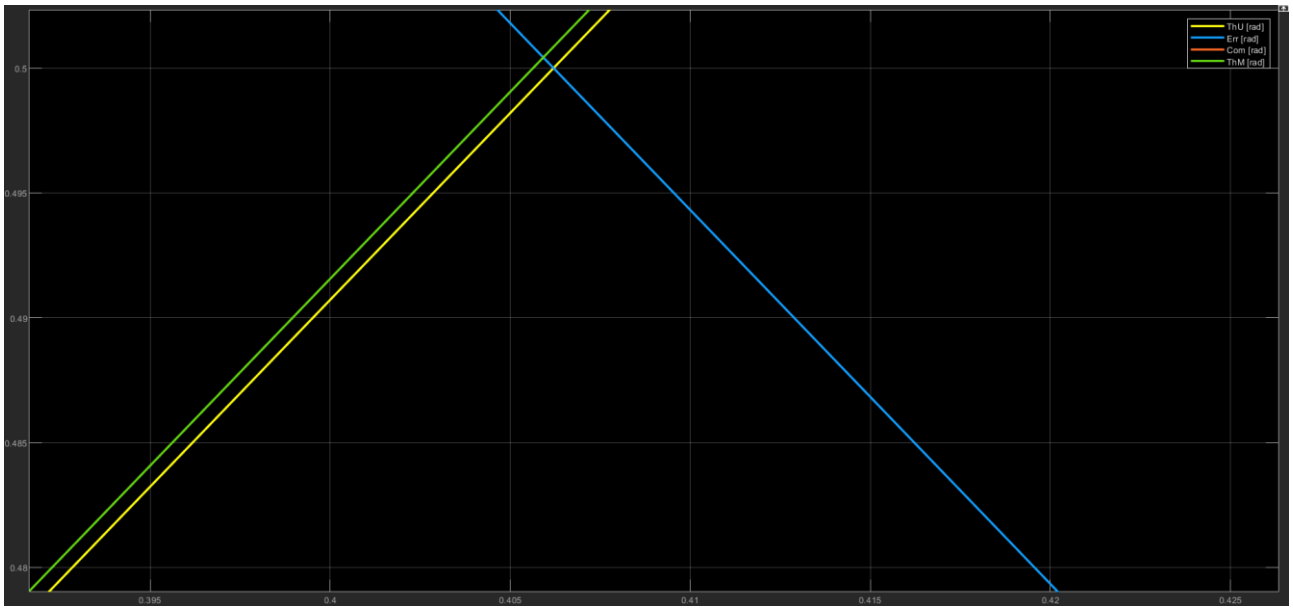

Figure 46: Two dynamics with one advanced

It see that the position of gearmotor and user stop not exactly on the commanded position and neither in a overlapped way: this event is due to a physical phenomenon,

in fact friction forces pose a system accuracy problem. Greater frictional forces, imply greater dispersion band around commanded position. This band it can be seen on Figure 47.

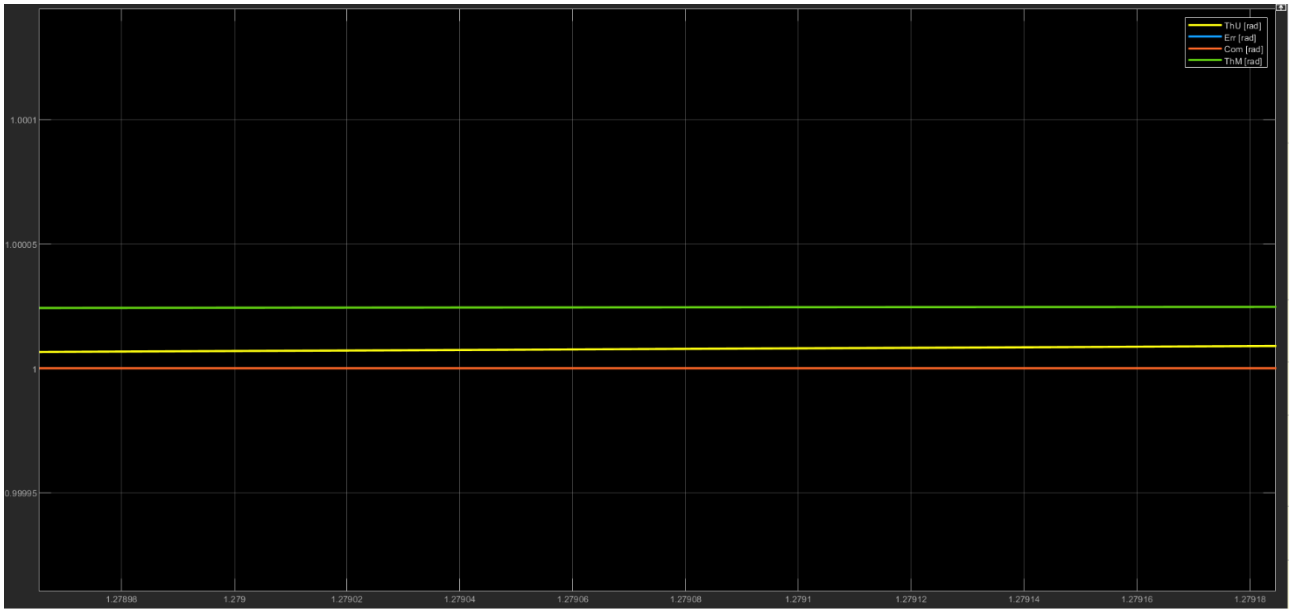

Figure 47: Band around commanded position

It's important to underline that the simulation uses a Euler first-order fixed-step resolution method (ode1), which is the simplest and most controllable possible.

The time step between an evaluation and the next is set at 10^{-5}s, at least two order less than the characteristic time, in order to observe precisely the dynamics of the system without numerical problems.

Moreover it's important to underline that the system moves away itself from the equilibrium position when the external aerodynamic load is applied.

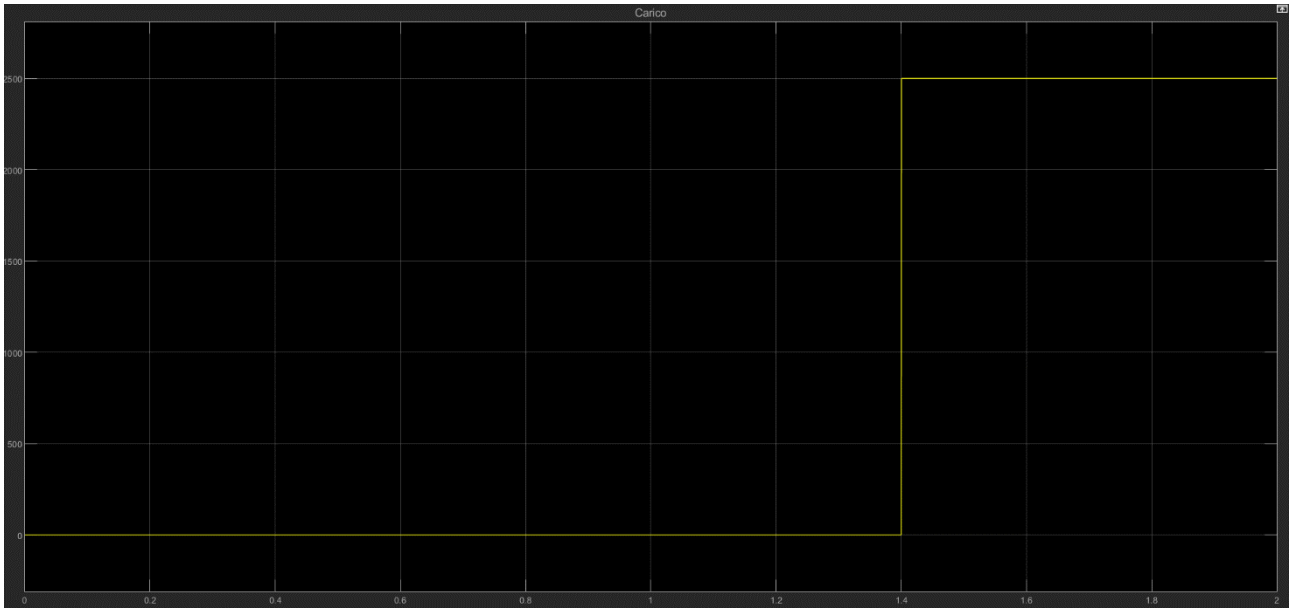

Figure 48: External load

4.2) EMA Low Fidelity for F-16 aircraft

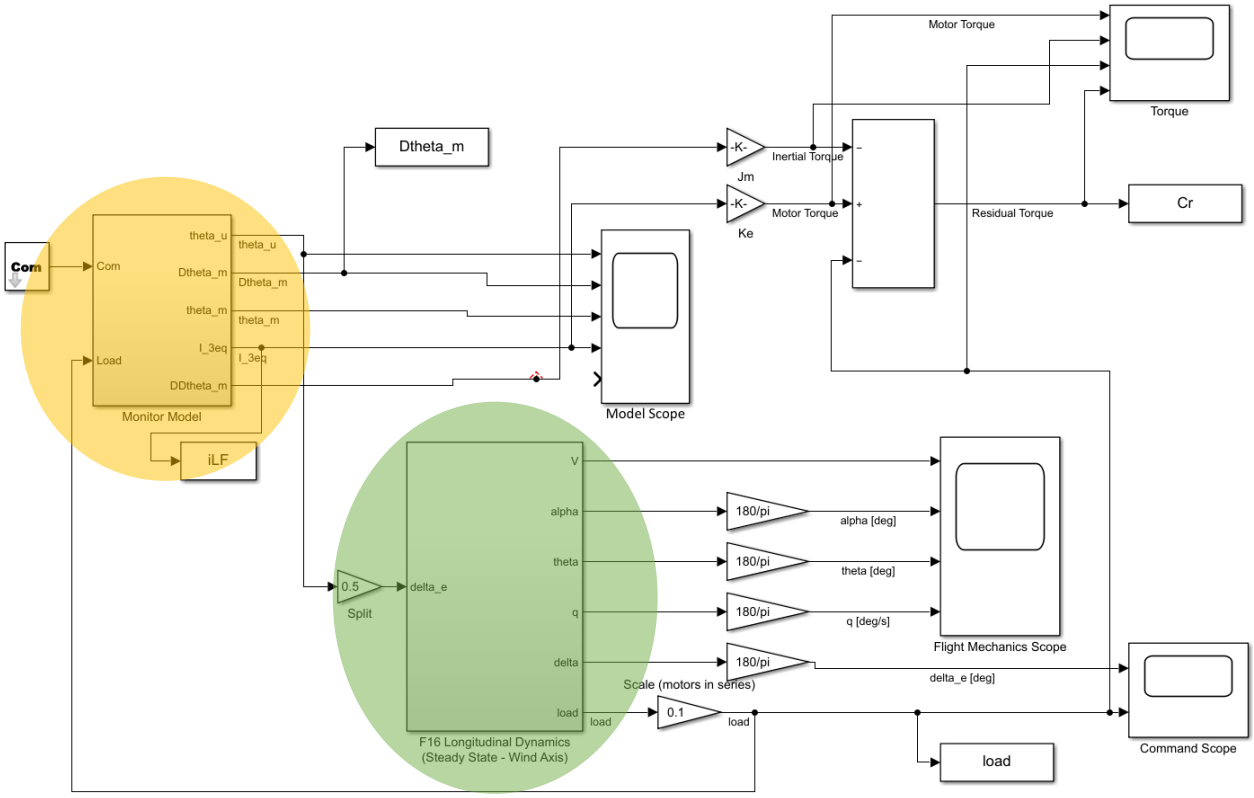

Figure 49: F-16 EMA Low Fidelity

The aim of this reference model is to simulate the real working behaviour of an electromechanical system, avoiding the necessity to have a real and expensive test bench.

This model is developed and implemented in a Matlab-Simulink environment and represents the response in time of a balancer control, which has a dynamic response in an intermediate range between a primary and a secondary flight control.

The model of the Electro-Mechanical Actuator has a high level of detail and it represents a highly non-linear dynamic.

Then Simscape environment will be used to model backlash mechanical phenomenon.

The simulation is very complex and computationally expensive, so a Euler first-order fixed-step resolution method, which is the simplest and most controllable possible, is employed.

The time step between an evaluation and the next is set at 10^{-5}s, at least two order less than the characteristic time, in order to observe precisely the dynamics of the system without numerical problems.

It's not recommended using second order methods as Runge-Kutta or Dormand-Price, because during the simulation they will interpolate data during the recursive evaluation of the error, causing non-linearity convergence problems especially for motor torque's and inertial torque's trends.

It can choose one of the following position command signals:

- Step control
- Sinusoidal command
- Ramp control
- Chirp command: signal in which the frequency varies linearly with time, growing up (up-chirp) or decreasing (down-chirp).

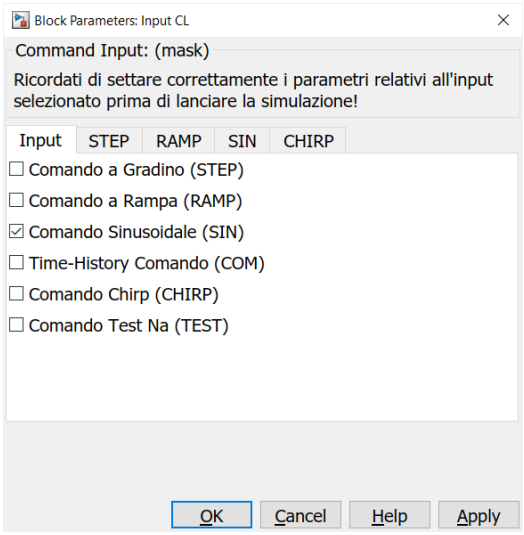

Window 1: command signal

Now it's necessary to analyse each block which is contained inside the model during following paragraphs.

The main blocks which have to considered are:

1) *Inside Monitor Model (yellow circle on Figure 49): Controller, Electrical model, Mechanical model*
2) *F-16 Longitudinal Dynamics model (green circle on Figure 49)*

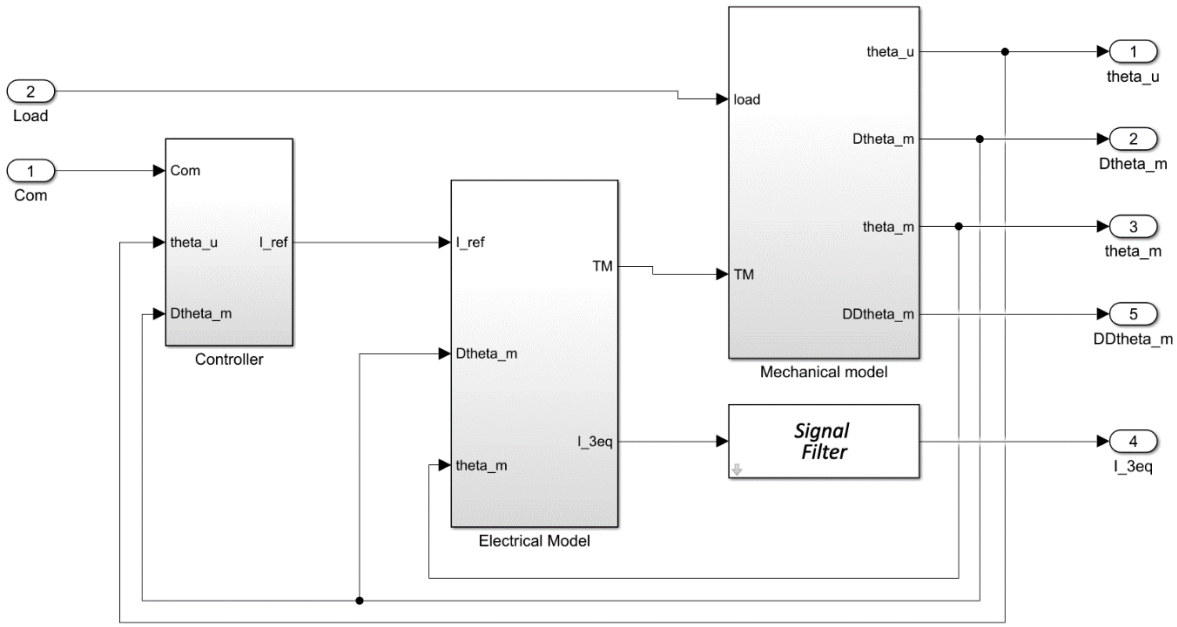

Figure 50: Inside Monitor Model

To use a simpler current signal and not analyse too high frequencies, a filter with a time constant of $5 \cdot 10^{-4}$ s is used.

Now it is explained how the I_{3eq} (equivalent single-phase current) is obtained: given the three-phase brushless motor, the equivalent single-phase current is evaluated as the sum of the modules of the three currents, subsequently divided by 2 (only two are the active phases) and therefore this value is multiplied by the sign of the torque.

4.2.1) Motor's control block

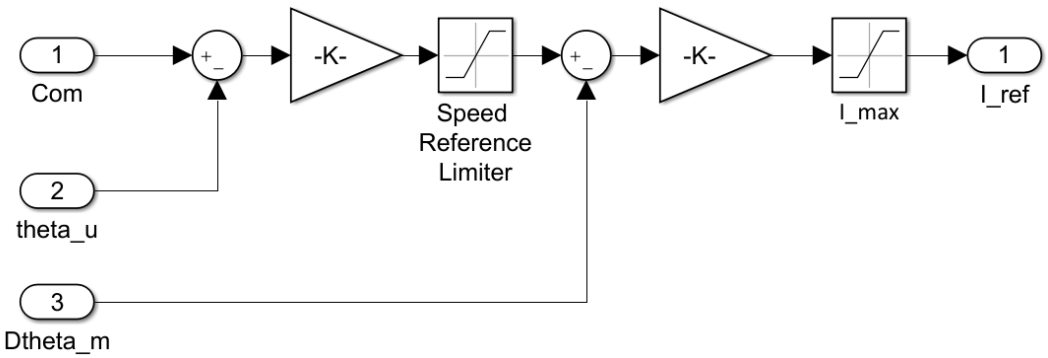

Figure 51: Motor's control block

This block receives as input the position command given to the actuator *Com*, the actual position feedback of the actuator *theta_u*, the motor speed feedback (*Dtheta_m*). After comparing the command and the actual position of the actuator, the position error is generated and this is suitably amplified by multiplying it by the gain *GAPm1 = 1e5*.

The signal is then transformed into a speed and enters the saturation block, which limits this value between its maximum and *minimum* $[\omega_{min}, \omega_{max}] = \pm 8000$ *rpm*. Once the reference speed is compared with the actual motor feedback *Dtheta_m*, the error is multiplied by a gain *GAPm2 = 0.05* which replaces a PID type controller.

The division by the torque constant *Kv = 0.0752* allows to obtain the reference current: this parameter must be saturated to not exceed the maximum current value $I_{max} = 22.5$ *A* to avoid breakages or faulty conditions of the motor like overheating.

4.2.2) Motor's electrical block

On the model below, the transformation from reference current to reference torque performed by the motor is modeled referring to an equivalent single-phase.

The control is based on the current feedback: the error between the electrical parameters I_{ref} and I_{3eq} (reference current and current flowing in the equivalent single-phase respectively) is sent in a saturation block.

To obtain the actual voltage acting on the motor rotor, the current's error is multiplied by the nominal supply voltage value of the inverter $V_{dcm} = 48$ *V*. The voltage, thanks to the sum block, is also purified from the negative effects that lead to malfunction conditions of the motor, that is: the short circuit of the stator windings (turn-to-turn short circuit) and the eccentricity of the rotor.

The effective supply voltage of the motor is the input model's signal and the current is its output. The motor is represented by a first order transfer function:

$$G = \frac{\frac{1}{Rm}}{\tau_{RLm}+1}$$

where Rm is the resistance of the windings expressed in [Ω] and τ_{RLm} is the ratio between the resistance Rm and the inductance Lm, which represents the time constant of the system. The output current must again take into account the possible short circuit (with a division by the percentage of non-defective coils) because the absorbed current, because of Rm and Lm decrease after a winding short circuit, must be greater than the rated condition.

The torque of the model is subsequently obtained after multiplying by the torque gain $GT = 0.07322\ Nm\ /\ A$ and subsequently subjecting it to the limitation in torque of the motor between its maximum value and its minimum value with the saturation block $[TMMmin, TMMmax] = \pm 1{,}689\ Nm$.

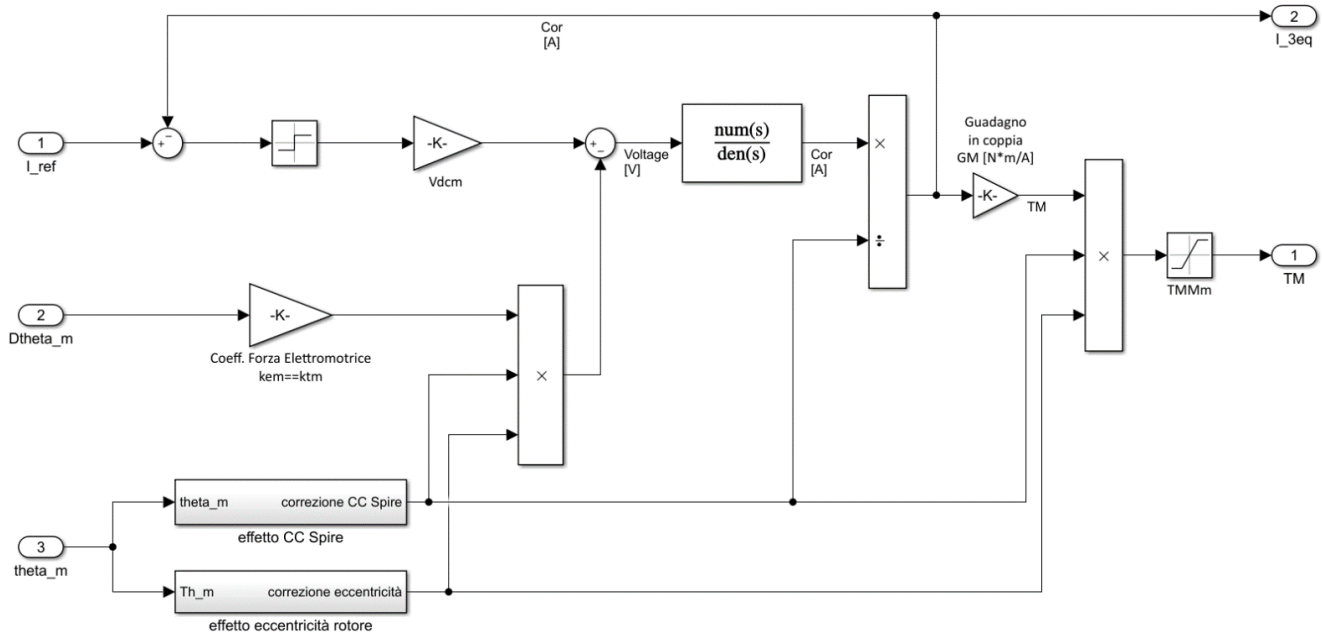

Figure 52: Motor's electro-mechanical block

4.2.3) Coils effect and eccentricity

During the normal operating life of a motor, repeated over-currents and the resulting over-temperatures generated could lead to a degradation of the polymeric insulating parts of the circuits.

If this event occurs in the stator near the copper windings, the phase coils come into direct contact (the windings are therefore no longer separated from the insulation), allowing the current to bypass a part of the winding (short circuit). In this case, the resistance and inductance of the coil decreases, so with the same voltage acting on the winding, the passing current is higher. If the motor absorbs a higher value of current, the dissipation of energy increases and the heat generated by the Joule effect increases, thus leading to a complete system failure.

In this Simulink subsystem only the predictable coil-to-coil short circuit is implemented but from the reference model it is impossible to distinguish which phase is shorted, because three currents are evaluated for an equivalent single-phase actuator. Therefore, for the model the short circuit percentage is the average between the three reference coefficients:

$$N_{equiv} = (N_a + N_b + N_c) / 3$$

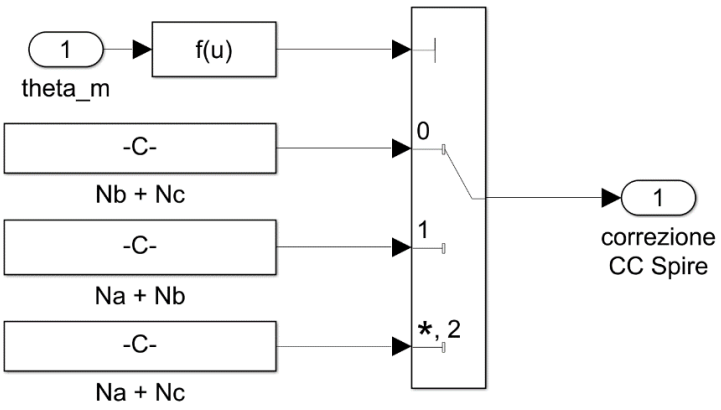

Figure 53: Coils effect

Now phenomenon of eccentricity and its effects will be discussed.

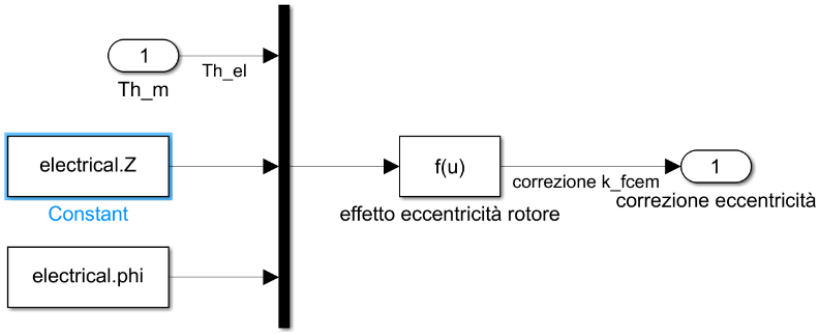

Figure 54: Eccentricity effect

The eccentricity defect consists in the misalignment that is created between the rotation axis and the symmetry axis of the stator. The main causes of the rotor eccentricity defect are attributable to: support bearing degradation, manufacturing tolerances, unbalanced load, incorrect assembly, rotor shaft flexure/torsion and mechanical usury that occurs during the normal operating life of the motor. Eccentricity, which causes a variation in the position of the air gap between the stator and the rotor, can be evaluated with current and speed trends. When an eccentricity error occurs, unbalanced magnetic forces are created, because the permanent magnets are closer to the windings, generating an attractive force that acts on rotor. The magnetic coupling between rotor and stator therefore changes and when the eccentricity becomes too large, the result of the magnetic forces could cause friction from stator to rotor, causing possible damage.

Furthermore, the torque coefficient and the counter electromotive force coefficient increase and decrease according to the angular position.

4.2.4) Mechanical block

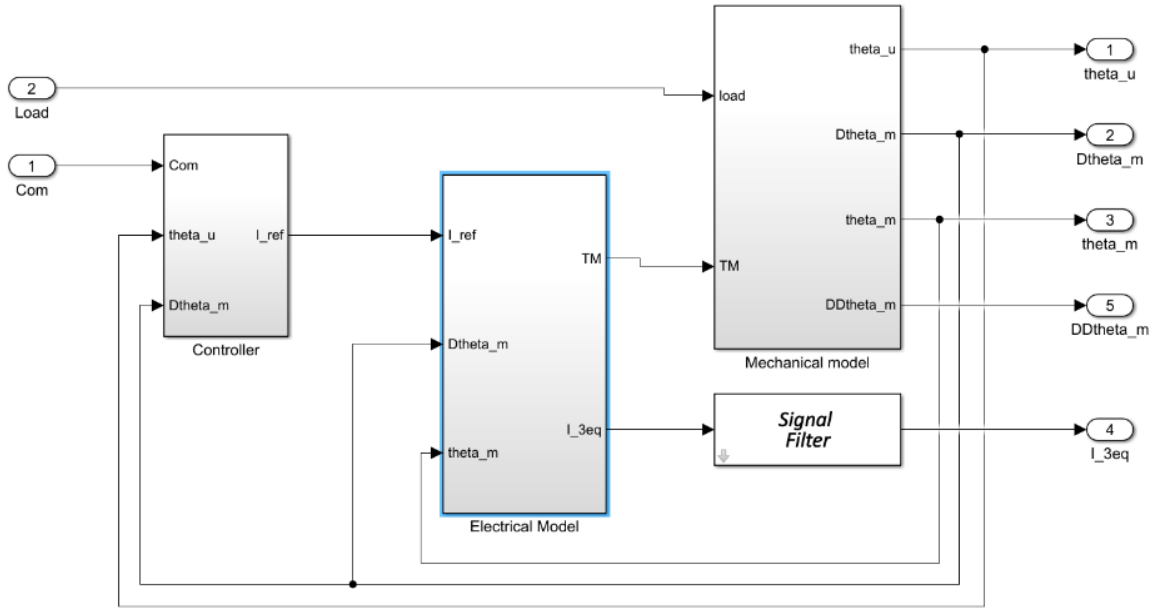

Figure 55: Mechanical block

The actuator's dynamics which moves the mobile surface is implemented in this block.

As shown in the figure above, motor torque *TM* and resistant external aerodynamic *load* are the inputs of a second order dynamic system that provides as output:

- the position of the user: actuator *theta_u*
- the actual angular position *theta_m* of the motor and its speed and acceleration *Dtheta_m* and *DDtheta_m* respectively.

Then these parameters are manipulated to reach the desired actuator position and motor speed.

Now it examines in detail how the mechanical model of the actuator is structured.

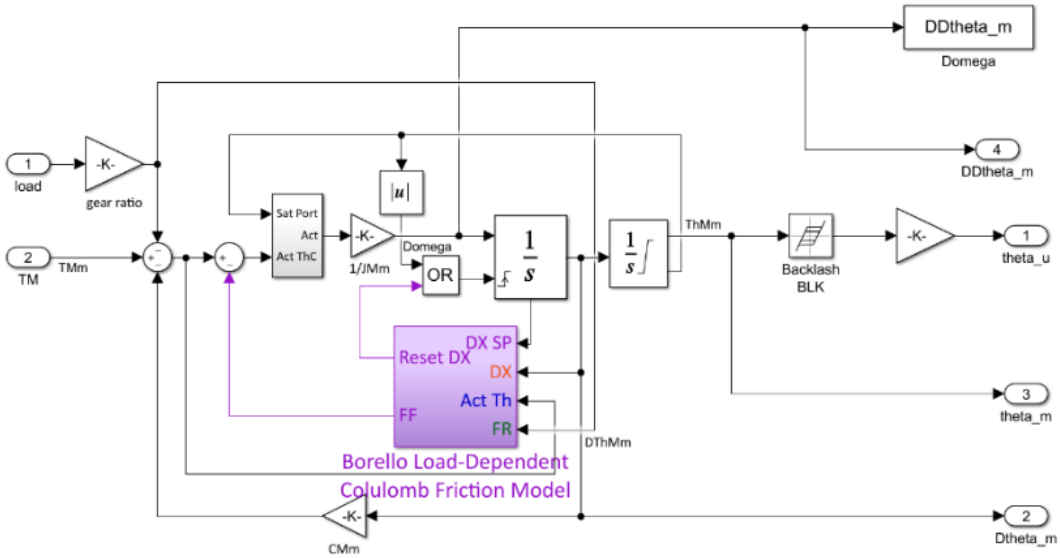

Figure 56: Mechanical block in details

The actual value of the net drive torque (calculated as the algebraic sum between the motor torque *TM*, the resisting torque *load* multiplied by *gear ratio 1/500* and the friction torque *Dtheta_m* multiplied by viscous friction coefficient *Cm= 5.172e-5*) is

processed by a control subsystem designed to simulate the effect of the friction and mechanical hard-stops involving the servomechanism.

The drive torque is then divided by the total inertia *Jm = 2.5e-5* (which is the sum of the inertia of the motor and the actuator-user) and this value is subsequently integrated twice to find the speed and position of the actuator.

Obviously the position will then be subjected to the modeling of the mechanical phenomenon of backslash (recovery of mechanical backlashes that lead to mechanical hysteresis) and then finally obtain the position of the actuator. A saturation port will model and manage the cases in which the actuator will reach its limit positions and the case in which these mechanical limits have not yet been reached.

4.2.5) Friction Borello block

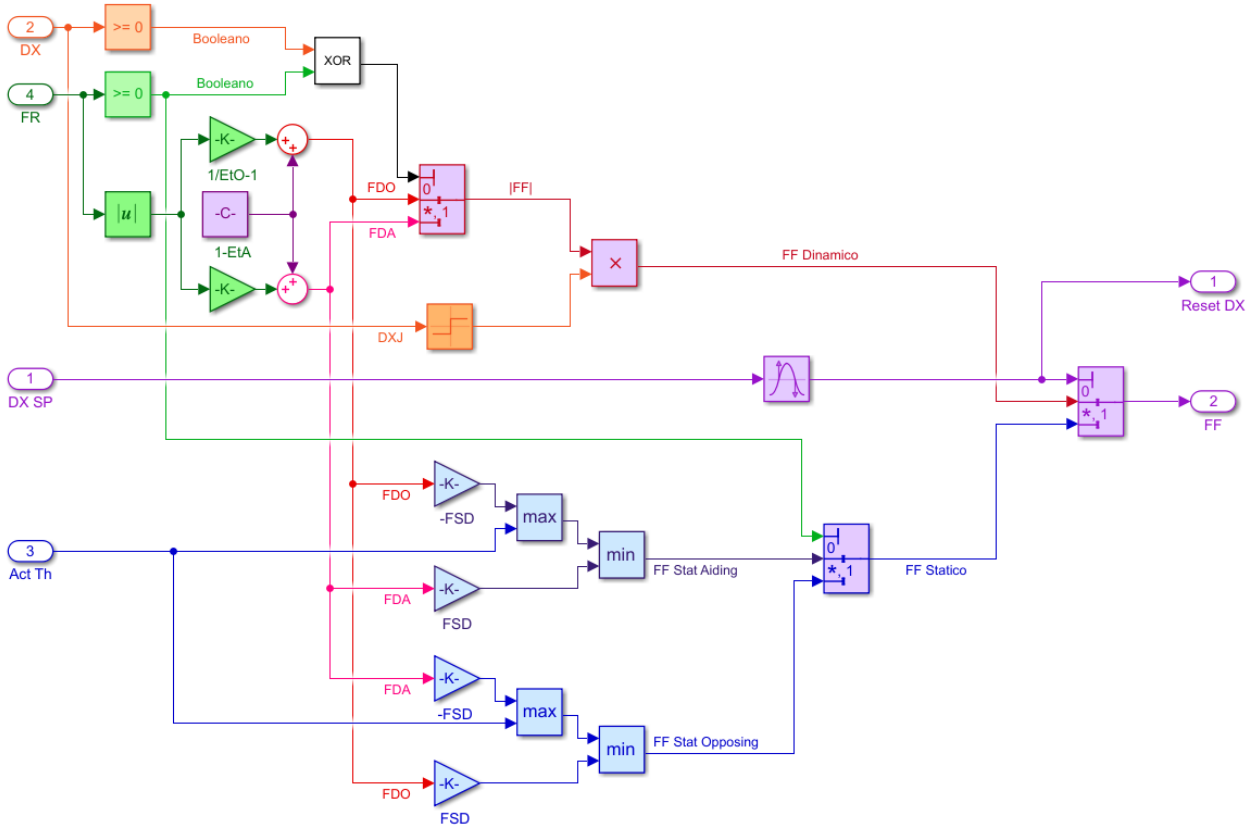

Figure 57: Friction Borello model

Borello Model's friction block uses a switch to go through between two conditions: in this case they are the static and dynamic friction conditions.

During the evaluation of the speed, the central purple line with the "hit crossing" block verifies if the speed maintains the same sign between two successive instants. If this condition is true, the total friction FF is evaluated using the red lines of the subsystem, which represents the dynamic friction condition; otherwise total FF is evaluated using the blue lines, which correspond to the static friction condition. This model is more complicated than the conventional Borello Friction model: in fact it considers also the dependence to the dynamic external load (in opposition and in aiding) trough two different transmission efficiencies.

The generic friction force can be found in relation to the active force module according to the following mathematical model which takes into account the conditions in which the actuator is stationary and the conditions in which the actuator movement occurs:

$$F_f = \begin{cases} F_{act} & x = 0 \wedge |\dot{F}_{att}| \leq F_{sj} \\ F_{sj} \cdot sgn(F_{act}) & \dot{x} = 0 \wedge |F_{att}| > F_{sj} \\ F_{dj} \cdot sgn(\dot{x}) & \dot{x} \neq 0 \end{cases}$$

where Ff is the evaluated generic friction force (so the torque coming as model output in Figure 57), $Fact$ is the active force applied to the actuator system (so the torque TM), Fsj the static friction force and Fdj the friction force under dynamic conditions.

The produced output friction torque performing in those conditions is finally subtracted (or could be added, whether aiding conditions would be considered) to the torque TM.

4.2.6) Dynamics block and numerical data

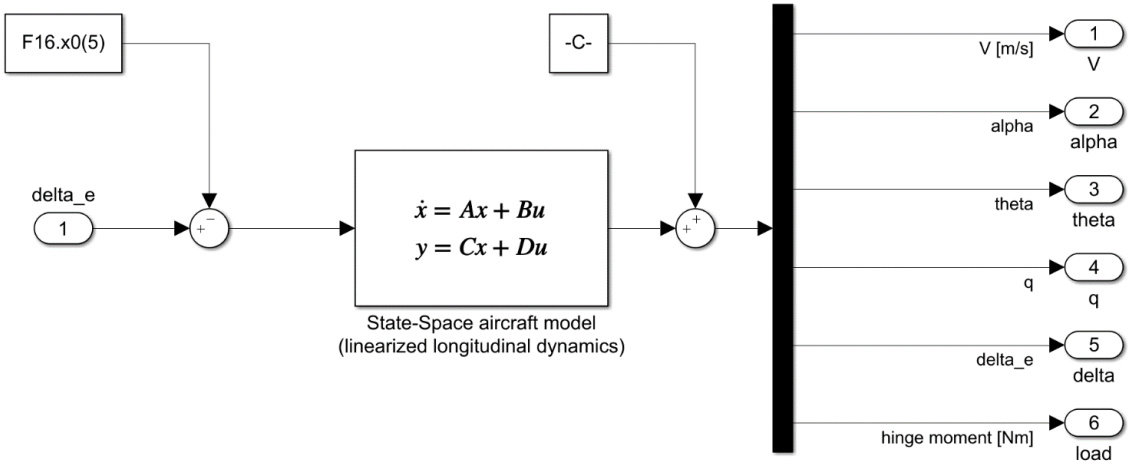

Figure 58: F-16 Longitudinal Dynamics model

The Simulink's model reproduces the response of the longitudinal dynamics of the F-16 aircraft to a balancer *delta_e* deflection command. This is represented by the system of state-space equations in the matrix form:

$$\begin{cases} \dot{\bar{x}}(t) = A\bar{x}(t) + B\bar{u}(t) \\ \bar{y}(t) = C\bar{x}(t) + D\bar{u}(t) \end{cases}$$

where:

- A is "state variables matrix" ($n \times n$)
- B is "control matrix" ($n \times m$)
- C is "observation matrix" ($l \times n$)
- D is "output matrix" ($l \times m$)

Using the scope, the trend of all state variables characteristic of the linearized longitudinal dynamics under consideration is displayed during the time.

The main parameters of the reference model are shown in Table 3 and Table 4 below:

```
   F16 aerodynamic model (linearized longitudinal dynamics, constant thrust)
   state and command matrices

% state vector x = [DV Dalpha theta q]'
% y = [DV Dalpha theta q delta_e Mh_e]'

F16.x0 = [153.0096 0.03961 0 0 -0.0132435583641 -457.33]';

F16.A = [-1.9311e-2   8.8157e+0 -3.2170e+1 -5.7499e-1
     -2.5389e-4  -1.0189e+0  0.0000e+0  9.0506e-1
      0.0000e+0   0.0000e+0  0.0000e+0  1.0000e+0
     -1.1415e-12 -8.2225e-1  0.0000e+0 -1.0774e+0];

F16.B = [ 1.7370e-1
     -2.1499e-3
      0.0000e+0
      1.7555e-1];

F16.C = [eye(4); zeros(1,4); -5.9978e+0 -8.9812e+3  0.0000e+0 -2.6102e+2];

F16.D = [0 0 0 0 1 9.4643e+3]';
```

Table 3: F-16 Longitudinal Dynamics parameters

```
   Definizione parametri LF model
   parametri simulazione
simulation.TiBr      = 5;             % [s]            durata simulazione
simulation.DT        = 1e-5;          % [s]            passo di integrazione
simulation.initPos   = 0;             % [rad]          posizione iniziale (albero lento)

simulation.tauFilter = 5*1e-4;        % [s]           tempo caratteristico filtro I_3eq

simulation.timeCom   = [0 0.1 0.1+simulation.DT simulation.TiBr];   % parametri comando 'Com'
simulation.com       = [0 0 0.1 0.1];
   controller
controller.GAPm1     = 1e5;           % [1/s]          guadagno proporzionale controller          == controller.Gprop
controller.GAPm2     = 0.05;          % [Nms/rad]      guadagno proporzionale PID                 == controller.PID.GAP
controller.W_refMax  = 8000*pi/30;    % [rad/s]        saturazione errore posizione
controller.I_Max     = 22.5;          % [A]            saturazione I_ref
   electrical model
electrical.Z         = 0;             % []             modulo eccentricità                        == 0.42 * BLDC.zeta
electrical.phi       = 0;             % [rad]          fase eccentricità                          == BLDC.phi
electrical.P         = 2;             % []             numero paia poli                           == BLDC.P
electrical.Nabc      = [1 1 1];       % []             frazione spire attive                      == BLDC.N_abc

electrical.Vdcm      = 48;            % [V]            tensione di alimentazione                  == inverter.Hbridge.Vdc

electrical.Rm        = 2.130;         % [ohm]          resistenza motore                          == BLDC.Rs
electrical.Lm        = 720*1e-6;      % [H]            induttanza motore                          == BLDC.Ls

electrical.Kv        = 0.0752;        % [Nm/A]         valore nominale                            == 2 * BLDC.Ke
electrical.Ke        = 0.07648;       % [Nm/A]         costante forza controelettromotrice        (valore calibrato)
electrical.GT        = 0.07322;       % [Nm/A]         guadagno in coppia                         (valore calibrato)

electrical.TMM       = 1.689;         % [Nm]           saturazione coppia motore                  == BLDC.TMM
   mechanical model

mechanical.Jm        = 2.5e-5;        % momento di inerzia totale                                 == dynamics.JM+dynamics.JU
mechanical.Cm        = 5.172e-5;      % coefficiente attrito viscoso                              (valore calibrato)

mechanical.BLK       = 1e-5;          % [rad]          backlash width (albero lento)              == dynamics.BLK
mechanical.tau       = 1/500;         % []             rapporto di trasmissione                   == dynamics.tau

% mechanical.FST       = 0.1;           % []           coefficiente di attrito statico
mechanical.FSJ       = 0.1;           % []             coefficiente di attrito statico
% mechanical.FDT       = 0.05;          % []           coefficiente di attrito dinamico

mechanical.FSD       = 2;             % Static-to-Dynamic Friction Ratio
mechanical.FDJ       = mechanical.FSJ/mechanical.FSD; % Dynamic Load Indipendent Friction
mechanical.EtO       = 0.85;          % Rendimento trasmissione in Opposition
mechanical.EtA       = 0.60;          % Rendimento trasmissione in Aiding

mechanical.ThUmin    = -1;            % [rad]          finecorsa inferiore                        == dynamics.ThUmin
mechanical.ThUmax    = 1;             % [rad]          finecorsa superiore                        == dynamics.ThUmax

save 'LFdata.mat'
```

Table 4: EMA Low Fidelity parameters

4.2.7) Simulation

To start the simulation, a unit step command is imposed on the actuator which reaches the commanded position at about 1.3 s (at the same time the motor reaches its commanded position of 500 rad). The simulation time is 5 s.

Reaching the required position of the user and the motor has a certain delay in time for their different inertia and because the motor is subject to a resistant torque and to a dynamic friction force which have to be overcome.

For this reason, the maximum speed attainable by the motor decreases (from 600 rad/s to about 220 rad/s) and then settles at zero once the desired equilibrium position is reached.

The current flowing in the equivalent single-phase motor reflects the considerations just discussed: the motor must be powered more intensively to reach and maintain the maximum rotation speed, so I_3eq immediately reaches its maximum value of 18 A. It is clear that this condition is undesirable because the loss of power due to the Joule effect is very significant and the consequent increase in temperature can cause problems of expansion of the material and therefore of blocking and malfunction.

The current then settles at the steady state value of 14 A once the commanded position has been reached.

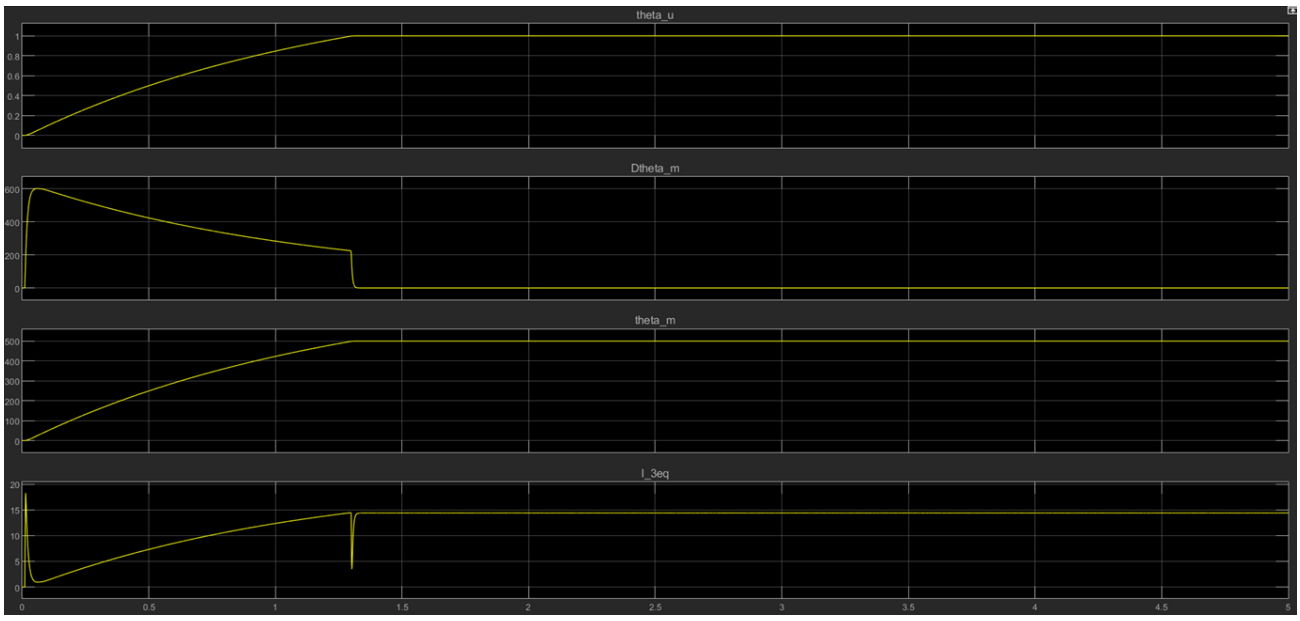

Figure 59: position, speed and current trends

External aerodynamic load reaches its peak at around 1.3 seconds; for this reason, at this instant of time, it is necessary to:

- a driving torque that decreases due to the resistant load
- an inertial torque that decreases as the ω of the motor decreases (which reduces in this way its position)
- a current that suddenly decreases (the motor decelerates so less current is needed).

It can be noted that the driving torque obviously immediately reaches its maximum value of 1.4 Nm in correspondence with the maximum speed reached by the motor and the peak current. Consequently, the maximum rotation speed of the rotor corresponds

to the ω_{max} of the shaft with a maximum inertial torque of 1.5 Nm (generated by the angular acceleration of the mass of the shaft and rotor integral to it). The torque then settles to its speed value at the position command reached with zero inertial torque.
It is also possible to graph the residual torque (the torque that continues to act on the system after it has been stopped) and the trend over time of the external resistant aerodynamic load

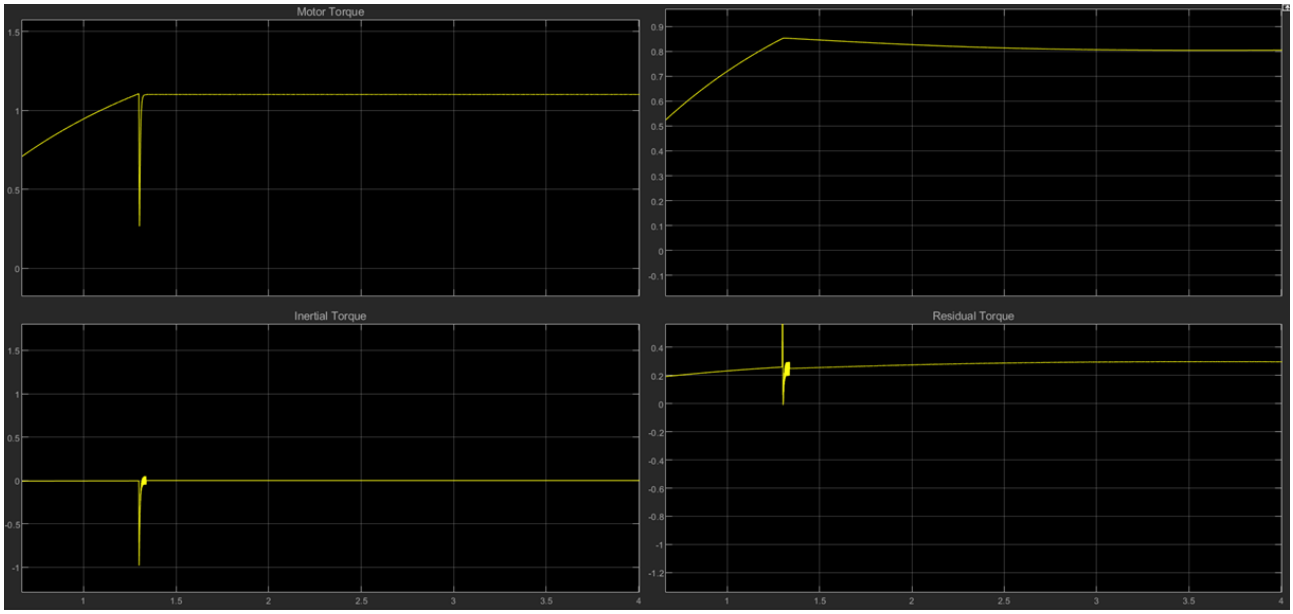

Figure 60: torques trends

It can see an increasing external aerodynamic load with an increase of the delta_e in order to balance it. Once the equilibrium position is reached, the load remains constant and the balancer has reached its maximum value of deflection commanded by the actuator.

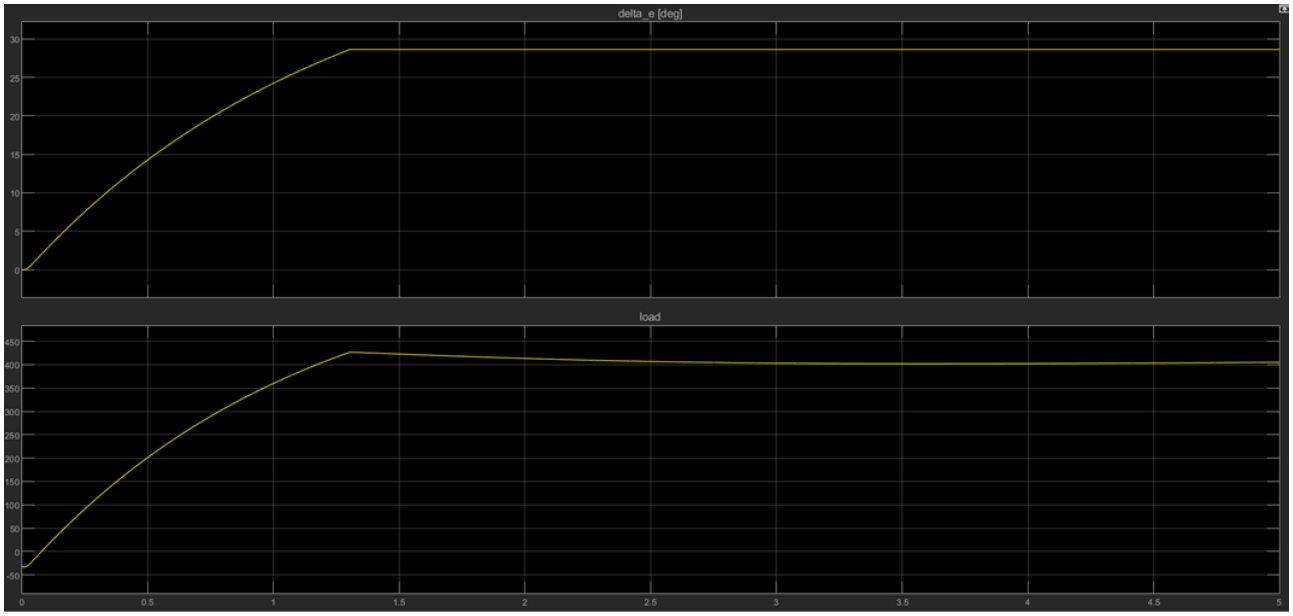

Figure 61: position and external load trends

The speed V remains almost constant up to 1.5 seconds at about 153 m/s and then decreases to about 142 m/s but with a slow and not sudden rate of climb.

The alpha attitude angle rapidly increases from its minimum incidence value of 2.3 deg to its maximum of about 5 deg. The incidence therefore varies within contained values as expected from a military-aerobatic aircraft which thus minimizes wave and shape resistances. The pitch speed *q* increases and then settles at a constant value once the balancer is locked in equilibrium.

The theta pitch angle varies suddenly from 0 to 12 deg; a sign that the longitudinal dynamics are suitably stressed.

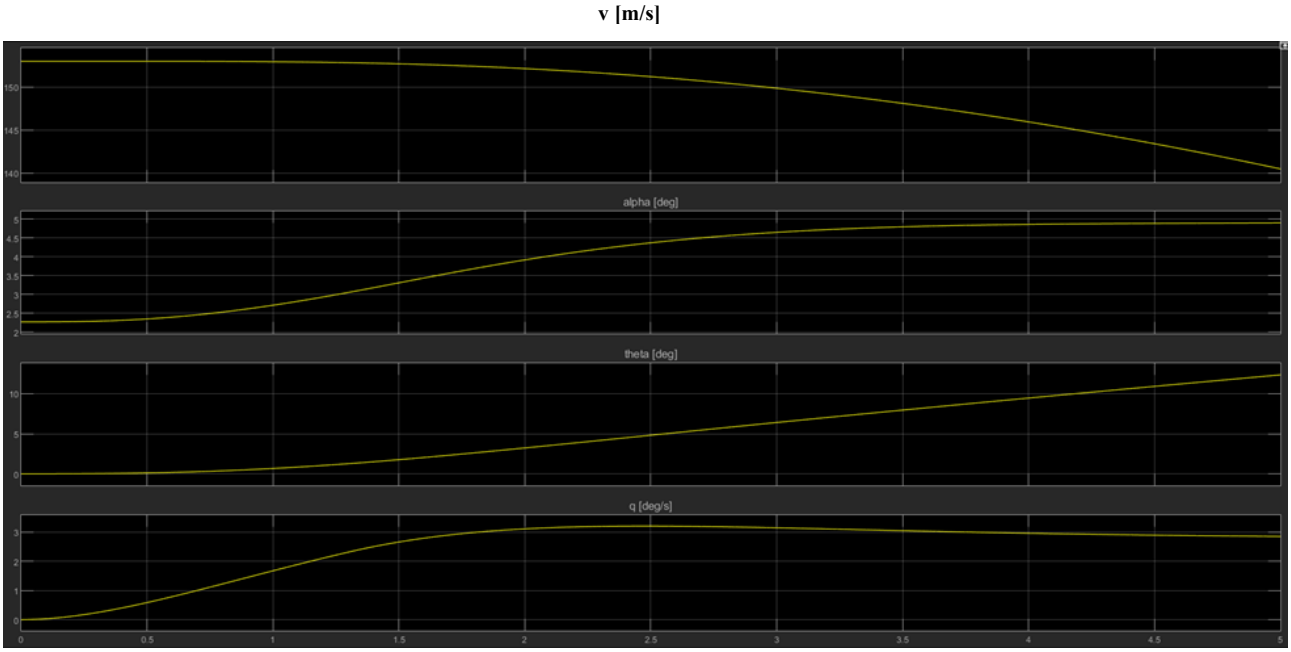

Figure 62: longitudinal dynamics trends

5) Simscape environment

The main difference which exists between Simscape and Simulink is that the first gives a “realistic” and more intuitive overall vision of the modeled system where the connection between physical blocks are correctly dimensioned. Also, it uses some blocks that allows the integration of networks from different physical domains. Simulink, instead, uses block diagram approach where the signal flow is unidirectional. Moreover, Simscape’s signal flow is bi-directional between blocks.

5.1) Backlash phenomenon and mechanical transmission

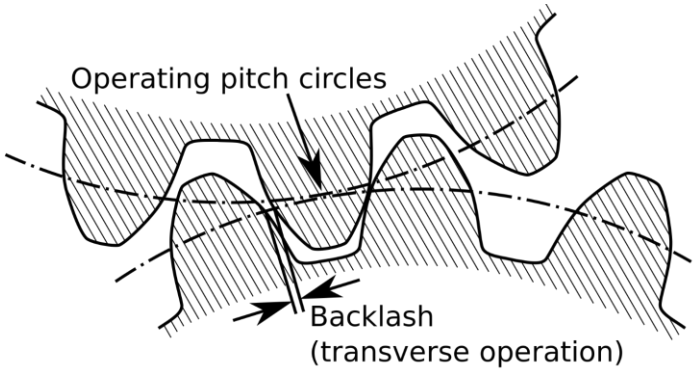

Figure 63: Mechanical Backlash

When it analyse mechanical assemblies such as ball screws, gearboxes, reducers and gear motors, it’s important to know the amount of backlash that is present. Backlash is a movement or amount of “play or lash” visible in a mechanical system which is caused by a gap between parts that make contact. Some amount of backlash is unavoidable in nearly all reversing mechanical couplings and, depending on the application, backlash may or may not be desirable. In fact, in some ways a certain amount of backlash is desirable, too much can lead to a mechanical failure. It can be defined as "the maximum distance or angle through which any part of a mechanical system may be moved in one direction without applying appreciable force or motion to the next part in mechanical sequence" which is necessary to prevent jamming phenomenon.

Unwanted backlash can have many causes. One of the major contributing factors is poor lubrication. In a well-built machine, backlash is minimized by design, but a certain amount must be present to allow for lubrication between the moving parts. If lubrication is not present or either poor quality or contaminated the rubbing of parts creates undesired clearances which contributes to adds backlash. Another cause of backlash is poor manufacturing (like manufacturing errors) of the gears to begin with, especially when gear teeth are cut too deep.

Backlash is also one of those things that increases due to the age of the system. Too much backlash in a system can cause many different type of failures such as gear slip. Other types of failures can be more catastrophic: for example destroying or losing manufactured parts which is a waste of material and time for repairs. Moreover, when there is too much backlash the machine will no longer be as precise as it once was

because the there is a loss of position as it moves in both directions. This loss will cause the machine to travel and undershoot its target position and create undesirable results in what it was designed to do.

Other reasons for the presence of the backlash in mechanical linkages are the possibility of having a greater tolerance towards deflection under load and thermal expansion.

Considering a typical mechanical linkages that contemplates backlash, like gearbox, the transmission ratio is the following:

$$\tau = \frac{\dot{\theta}_m}{\dot{\theta}_u} = \frac{T_u}{T_m\,\eta_m}$$

where $\dot{\theta}_m$ and T_m are the motor angular speed and torque, $\dot{\theta}_u$ and T_u are referred to the user angular speed and torque and η_m the transmission mechanical efficiency.
On EMAs actuators, a high transmission ratio is needed in order not to use an oversized motor that needs convert its high RPMs to useful torque to counterbalance surface loads. Typical motor speed rating is about from thousands to tens of thousand of RPM, while the required speed by a slow shaft that moves the flight control surface is about tens of degrees per second. This requirement is typically expressed in angular terms (50- 60°/s on primary flight commands and 5-6°/s on secondary flight commands).

5.2) Simscape blocks used

Figure 64: Inertia block

The Inertia block represents an ideal mechanical translational inertia, described with the following equation:

$$T = J\,\frac{d\omega}{dt}$$

where:

- T is inertia torque
- J is inertia
- ω is angular velocity
- t is time.

By default, the block has one mechanical translational conserving port. The block positive direction is from its port to the reference point. This means that the inertia torque is positive if inertia is accelerated in positive direction.

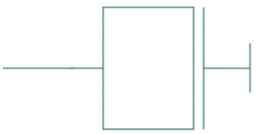

Figure 65: Mass block

The Mass block represents an ideal mechanical translational mass, described with the following equation:

$$F = m\frac{dv}{dt}$$

where:

- F is inertia force;
- m is mass;
- v is velocity and t is time.

By default, the block has one mechanical translational conserving port. The block positive direction is from its port to the reference point. This means that the inertia force is positive if mass is accelerated in positive direction.

Figure 66: Spring block

The Translational Spring block represents an ideal mechanical linear spring, described with the following equations:

$$F = Kx$$
$$x = x_{init} + x_R - x_C$$
$$v = \frac{dx}{dt}$$

where:

- F is the force transmitted through the spring;
- K is the spring rate and x is the relative displacement (spring deformation);
- x_{init} is the spring initial displacement (initial deformation); the spring can be initially compressed ($x_{init} > 0$) or stretched ($x_{init} < 0$)
- x_R, x_C are the absolute displacements of terminals R and C, respectively
- v is the relative velocity and t is the time.

The block positive direction is from port R to port C. This means that the force is positive if it acts in the direction from R to C.

Figure 67: Rotational Damper block

The Rotational Damper block models a faultable linear rotational viscous damper. From the start of the simulation, the block uses the nominal damping coefficient. If it enables faults for the block, the damping coefficient changes in response to one or both of these triggers:

- Simulation time: A fault occurs at a specified time.
- Simulation behaviour: If the magnitude of the rotational acceleration exceeds a specified maximum value, the block increments the number of shocks by one. A fault occurs if the number of shocks exceeds a specified maximum number of shocks.

If a fault trigger event occurs, the block uses the faulted damping coefficient for the remainder of the simulation. It can program the block to issue a fault report as a warning or error message.

The defining equations are

$$T = D\,\omega$$

and

$$\omega = \omega_R - \omega_C,$$

where

- T is the torque transmitted through the damper.
- D is the damping (viscous friction) coefficient.
- ω is the relative velocity.
- ω_R and ω_C are the absolute velocities of terminals R and C, respectively.

The positive block direction is from port R to port C. Therefore, the torque is positive if it acts in the direction from R to C.

Figure 68: Rotational Friction block

The Rotational Friction block represents friction in contact between rotating bodies. The friction torque is simulated as a function of relative velocity and is assumed to be the sum of Stribeck, Coulomb, and viscous components, as shown in the following figure.

The Stribeck friction, T_S, is the negatively sloped characteristics taking place at low velocities. The Coulomb friction, T_C, results in a constant torque at any velocity. The viscous friction, T_V, opposes motion with the torque directly proportional to the relative velocity. The sum of the Coulomb and Stribeck frictions at the vicinity of zero velocity is often referred to as the breakaway friction, T_{brk}.

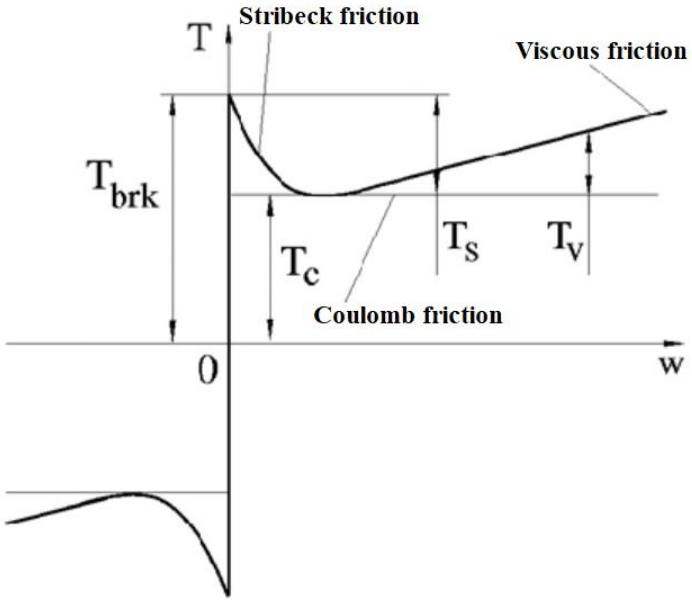

Figure 69: Friction graph

The friction T is approximated with the following equations:

$$T = \sqrt{2e}\,(T_{brk} - T_C) \cdot \exp\left(-\left(\frac{\omega}{\omega_{St}}\right)^2\right) \cdot \frac{\omega}{\omega_{St}} + T_C \cdot \tanh\left(\frac{\omega}{\omega_{Coul}}\right) + f\omega$$

$$\omega_{St} = \omega_{brk}\sqrt{2}$$

$$\omega_{Coul} = \omega_{brk}/10$$

$$\omega = \omega_R - \omega_C$$

where:

- ω_{brk}: Breakaway friction velocity
- ω_{St}: Stribeck velocity threshold
- ω_{Coul}: Coulomb velocity threshold
- ω_R, ω_C: Absolute angular velocities of terminals R and C, respectively
- ω: Relative velocity
- f: Viscous friction coefficient.

The exponential function used in the Stribeck portion of the force equation is continuous and decays at velocity magnitudes greater than the breakaway friction velocity.

The hyperbolic tangent function used in the Coulomb portion of the force equation ensures that the equation is smooth and continuous through $\omega = 0$, but quickly reaches its full value at nonzero velocities.

The block positive direction is from port R to port C. This means that if the port R velocity is greater than that of port C, the block transmits torque from R to C.

Figure 70: Rotational Spring block

The Rotational Spring block represents an ideal mechanical rotational linear spring, described with the following equations:

$$T = K \cdot \varphi$$

$$\varphi = \varphi_{init} + \varphi_R - \varphi_C$$

$$\omega = \frac{d\varphi}{dt}$$

where:

- T: Torque transmitted through the spring
- K: Spring rate
- φ: Relative displacement angle (spring deformation)
- φ_{init}: Spring preliminary winding (spring offset)
- φ_R, φ_C: Absolute angular displacements of terminals R and C, respectively
- ω: Relative angular velocity
- t: Time

The block positive direction is from port R to port C. This means that the torque is positive if it acts in the direction from R to C.

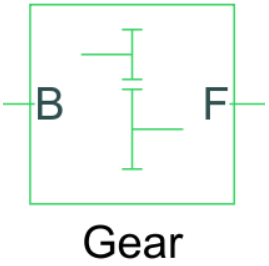

Figure 71: Simple Gear block

The Simple Gear block represents a gearbox that constrains the connected driveline axes of the base gear, *B*, and the follower gear, *F*, to corotate with a fixed ratio that it

specifies. It chooses whether the follower axis rotates in the same or opposite direction as the base axis. If they rotate in the same direction, the angular velocity of the follower, ω_F, and the angular velocity of the base, ω_B, have the same sign. If they rotate in opposite directions, ω_F and ω_B have opposite signs.
The kinematic constraint that the Simple Gear block imposes on the two connected axes is

$$r_F \omega_F = r_B \omega_B$$

where:

- r_F is the radius of the follower gear
- ω_F is the angular velocity of the follower gear
- r_B is the radius of the base gear
- ω_B is the angular velocity of the base gear.

The follower-base gear ratio is

$$g_{FB} = \frac{r_F}{r_B} = \frac{N_F}{N_B}$$

where:

- N_B is the number of teeth in the base gear
- N_F is the number of teeth in the follower gear

Reducing the two degrees of freedom to one independent degree of freedom yields the torque transfer equation

$$g_{FB}\, \tau_B + \tau_F - \tau_{loss} = 0$$

where:

- τ_B is the input torque.
- τ_F is the output torque.
- τ_{loss} is the torque loss due to friction.

For the ideal case, $\tau_{loss} = 0$.

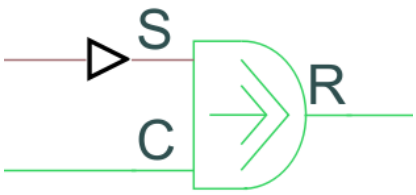

Figure 72: Ideal Torque Source block

The Ideal Torque Source block represents an ideal source of mechanical energy that generates torque proportional to the input physical signal. The source is ideal in a sense that it is assumed to be powerful enough to maintain specified torque regardless of the angular velocity at source terminals.

Connections R and C are mechanical rotational conserving ports. Port S is a physical signal port, through which the control signal that drives the source is applied. It can use

the entire variety of Simulink signal sources to generate the desired torque variation profile. Positive signal at port S generates torque acting from C to R. The torque generated by the source is directly proportional to the signal at the control port S.

The block positive direction is from port C to port R. This means that the torque is positive if it acts in the direction from C to R. The relative velocity is determined as $\omega = \omega_R - \omega_C$, where ω_R, ω_C are the absolute angular velocities at ports R and C, respectively, and it is negative if velocity at port R is greater than that at port C. The power generated by the source is negative if the source delivers energy to port R.

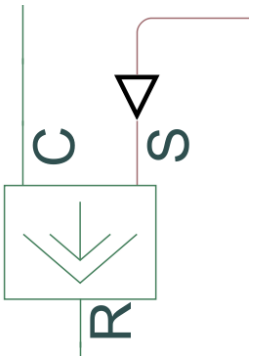

Figure 73: Ideal Force Source block

The Ideal Force Source block represents an ideal source of mechanical energy that generates force proportional to the input physical signal. The source is ideal in a sense that it is assumed to be powerful enough to maintain specified force at its output regardless of the velocity at source terminals.

Connections R and C are mechanical translational conserving ports. Port S is a physical signal port, through which the control signal that drives the source is applied. It can use the entire variety of Simulink signal sources to generate the desired force variation profile. Positive signal at port S generates force acting from C to R. The force generated by the source is directly proportional to the signal at the control port S.

The block positive direction is from port C to port R. This means that the force is positive if it acts in the direction from C to R. The relative velocity is determined as $v = v_C - v_R$, where v_R, v_C are the absolute velocities at ports R and C, respectively, and it is negative if velocity at port R is greater than that at port C. The power generated by the source is negative if the source delivers energy to port R.

Figure 74: Mechanical Rotational Reference block

The Mechanical Rotational Reference block represents a reference point, or frame, for all mechanical rotational ports. All rotational ports that are rigidly clamped to the frame (ground) must be connected to a Mechanical Rotational Reference block.

Figure 75: Mechanical Translational Reference block

The Mechanical Translational Reference block represents a reference point, or frame, for all mechanical translational ports. All translational ports that are rigidly clamped to the frame (ground) must be connected to a Mechanical Translational Reference block.

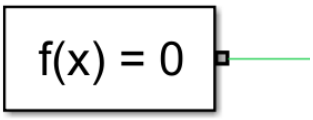

Figure 76: Solver Configuration block

Each physical network represented by a connected Simscape block diagram requires solver settings information for simulation. The Solver Configuration block specifies the solver parameters that your model needs before you can begin simulation.

Each topologically distinct Simscape block diagram requires exactly one Solver Configuration block to be connected to it.

Figure 77: Simulink-PS Converter block

The Simulink-PS Converter block converts the input Simulink signal into a physical signal. It uses this block to connect Simulink sources or other Simulink blocks to the inputs of a Physical Network diagram.

Figure 78: Backlash block

The Backlash block represents a double-sided mechanical rotational hard stop that restricts motion of a body between upper and lower bounds. Both ports of the block are of mechanical rotational type. The impact interaction between the slider and the stops is assumed to be elastic. The stop is implemented as a spring that comes into contact with the slider as the gap is cleared. The spring opposes slider penetration into the stop with the torque linearly proportional to this penetration. To account for energy dissipation and nonelastic effects, the damping is introduced as a block parameter, thus making it possible to account for energy loss.

The basic hard stop model, `Full stiffness and damping applied at bounds, damped rebound`, is described with the following equations:

$$T = \begin{cases} K_p \cdot (\varphi - g_p) + D_p \cdot \omega & \text{for } \varphi \geq g_p \\ 0 & \text{for } g_n < \varphi < g_p \\ K_n \cdot (\varphi - g_n) + D_n \cdot \omega & \text{for } \varphi \leq g_n \end{cases}$$

$$\omega = \frac{d\varphi}{dt}$$

Where

- T is interaction torque between the slider and the case
- g_p is the initial gap between the slider and upper bound
- g_n is the initial gap between the slider and lower bound
- φ is the slider angular position
- K_p is contact stiffness at upper bound
- K_n is contact stiffness at lower bound
- D_p is damping coefficient at upper bound
- D_n is damping coefficient at lower bound
- ω is the slider angular velocity
- t is time.

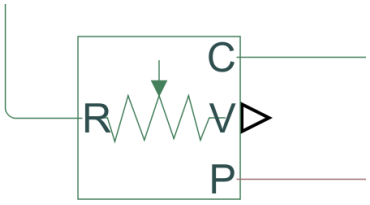

Figure 79: Ideal Translational Motion Sensor block

The Ideal Translational Motion Sensor block represents a device that converts an across variable measured between two mechanical translational nodes into a control signal proportional to velocity or position. It can specify the initial position (offset) as a block parameter. The sensor is ideal since it does not account for inertia, friction, delays, energy consumption, and so on.

Connections R and C are mechanical translational conserving ports that connect the block to the nodes whose motion is being monitored. Connections V and P are physical signal output ports for velocity and position, respectively.

The block positive direction is from port R to port C. This means that the velocity is measured as $v = v_R - v_C$, where v_R, v_C are the absolute velocities at ports R and C, respectively.

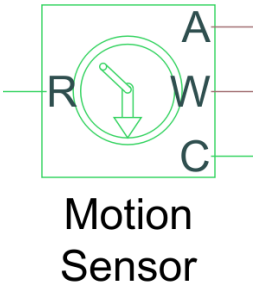

Figure 80: Ideal Rotational Motion Sensor block

The Ideal Rotational Motion Sensor block represents an ideal mechanical rotational motion sensor, that is, a device that converts an across variable measured between two mechanical rotational nodes into a control signal proportional to angular velocity or angle. It can specify the initial angular position (offset) as a block parameter.

The sensor is ideal since it does not account for inertia, friction, delays, energy consumption, and so on.

Connections R and C are mechanical rotational conserving ports that connect the block to the nodes whose motion is being monitored. Connections W and A are physical signal output ports for velocity and angular displacement, respectively.

The block positive direction is from port R to port C. This means that the velocity is measured as $\omega = \omega_R - \omega_C$, where ω_R, ω_C are the absolute angular velocities at ports R and C, respectively.

The **Wrap angle to [0, 2*pi]** parameter lets to control the angular displacement output range. When set to On, it keeps angular displacement within the range from 0 to 2π radians (360 degrees), regardless of the number of revolutions performed by the object and the direction of rotation. When set to Off, the output range is unrestricted.

5.3) Simscape VS Simulink

Before to discuss mechanical backlash on Simscape it's important focusing about the Simscape's precision on representing dynamics developed thanks to Simulink (regarding parameter settings, initial conditions and blocks which have to be used).

To compare Simscape and Simulink development environments it's necessary start with the representation of the dynamics of two typical systems:

- mass-spring-damper system;
- two mass-spring-damper system.

The first is a simple physical system used for the initial approaches to modeling while the second, as a first approximation, it can be representative of different mechanisms like a hydraulic jack adapted to move a mobile surface, subjected to any external load, through a yielding shaft.

5.3) MCK's system Simulink VS Simscape

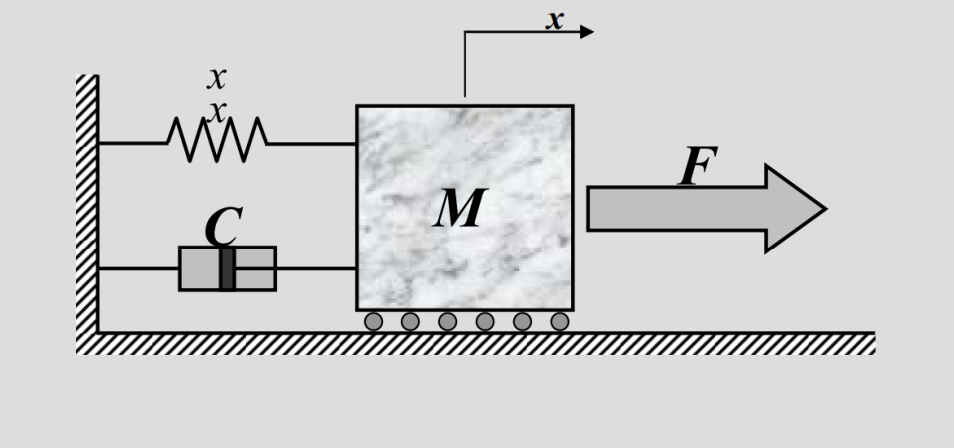

Figure 81: MCK system

The system consists of a mass M moving in a plane smooth horizontal without friction due to the combined action of a external forcing F, of the elastic return force produced by an ideal spring with stiffness K and the due damping force to a viscous damper.

The spring has a constant stiffness with respect to elongation x and the damper has a dimensional damping coefficient C.

This is a linear problem described by a second order dynamics through the differential equation:

$$M \cdot \frac{d^2x}{dt^2} + C \cdot \frac{dx}{dt} + K \cdot x = F$$

To model the elementary block diagram the differential equation must be rewritten as follows in order to obtain the expression for the mass linear acceleration:

$$\frac{d^2x}{dt^2} = \frac{F - C \cdot \frac{dx}{dt} - K \cdot x}{M}$$

Simulink elementary block model is described by the following figure:

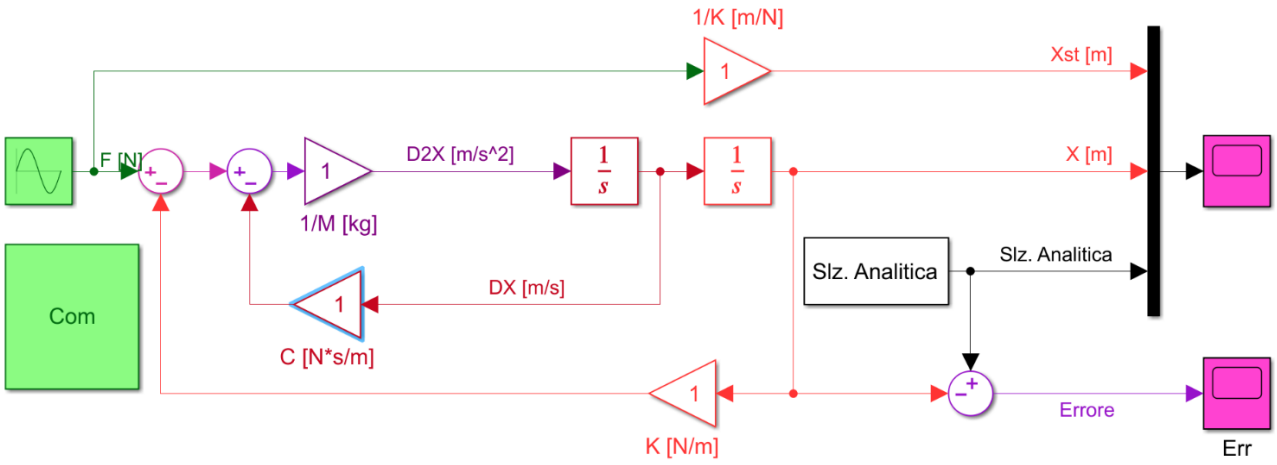

Figure 82: MCK Simulink model

Now it's showed the correspondent Simscape model (all green in the model's top left part) and how Simulink and Simscape dynamics are represented:

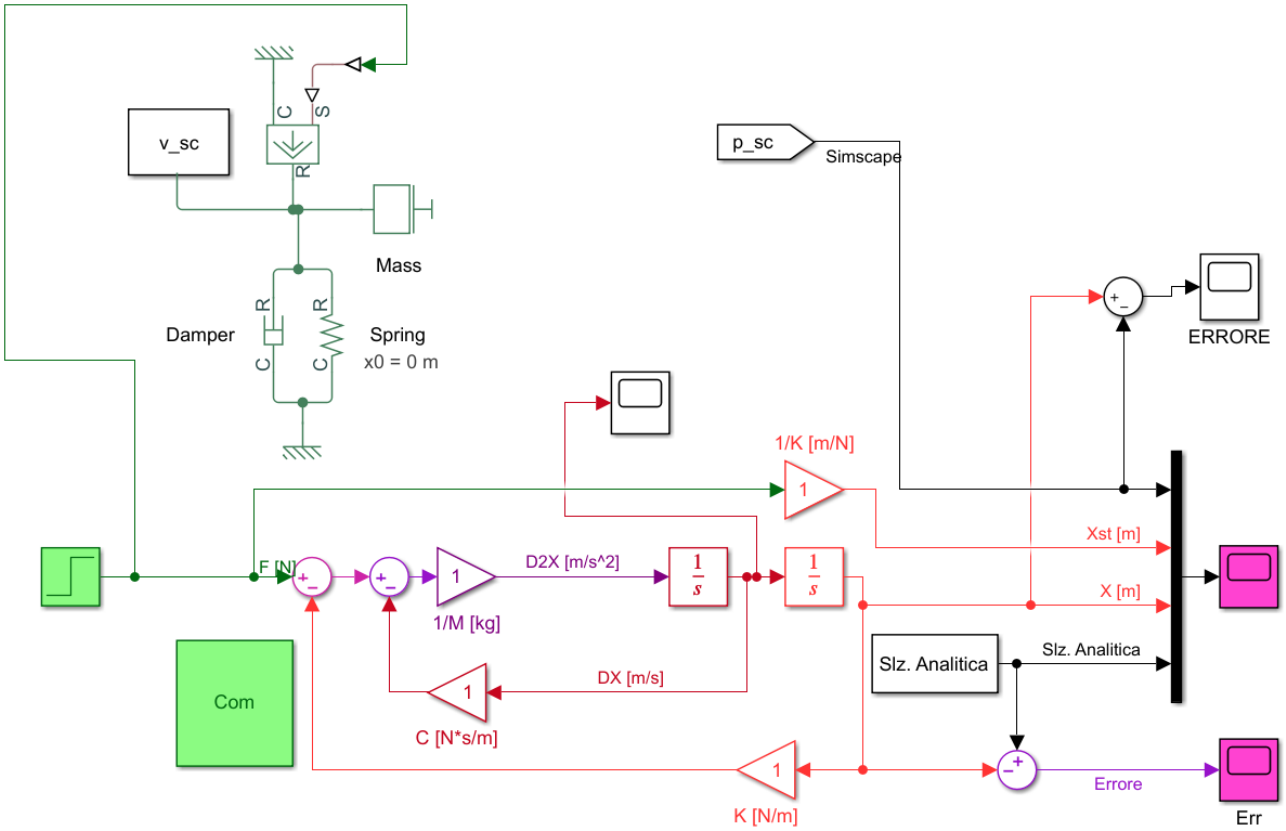

Figure 83: MCK Simascape model

It's important to keep in mind that the "**p_sc**" block contains the following structure equipped with a sensor to estimate the linear position of the mass:

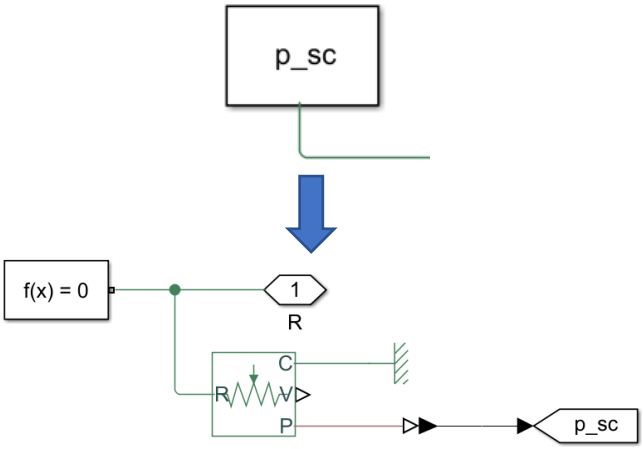

Figure 84: Inside p_sc block

The mass initial position has been setted to 0 m. Using both development environments it's possible to see that the mass dynamics are described identically: in fact the position's curves on Simulink (red) and Simscape (yellow) are exactly superimposed.

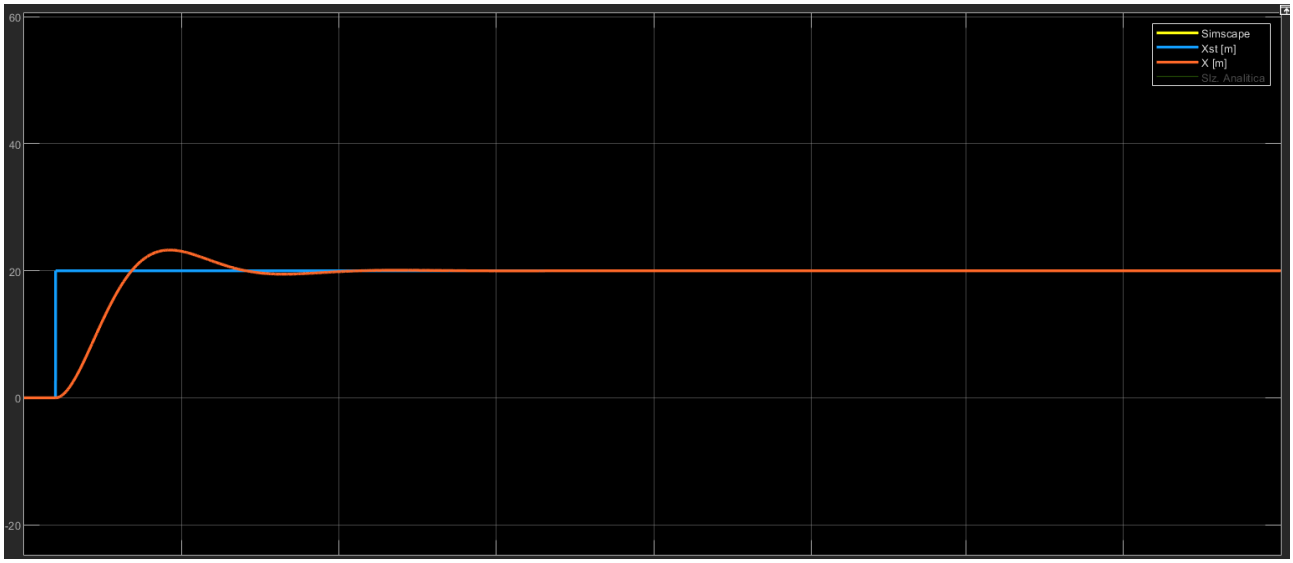

Figure 85: Simulink superimposed dynamics

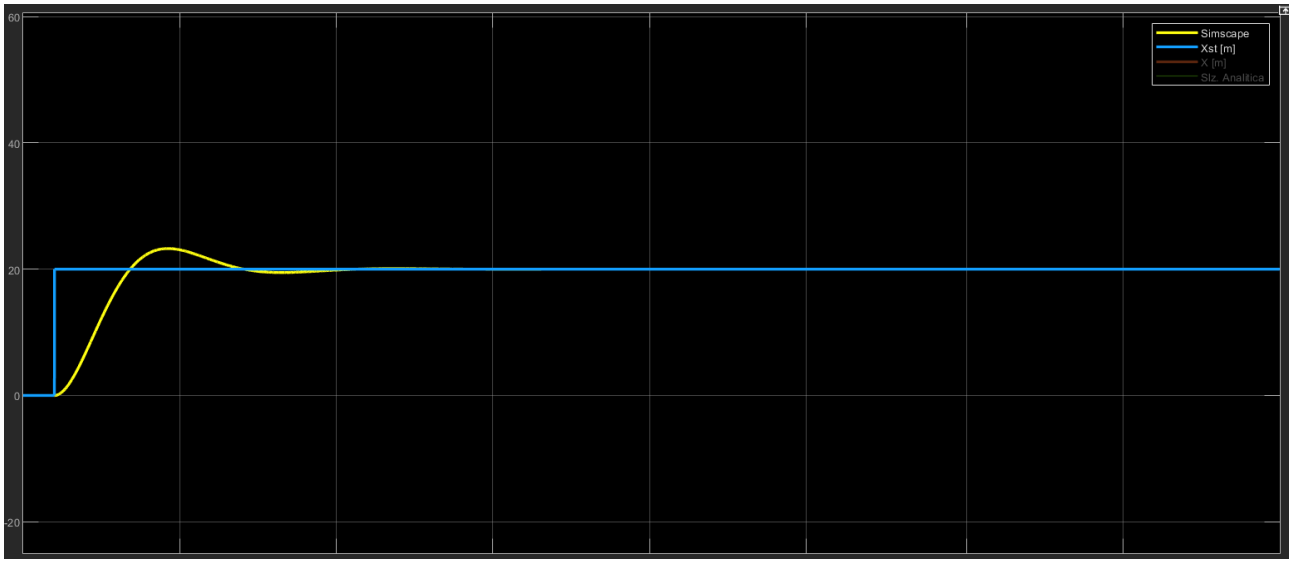

Figure 86: Simscape superimposed dynamics

The system is linear and its response is characterized by a first climb when the force F is applied and by a following overshoot where the system is at rest. Then, since the elastic return is greater than the force F, the position drops (given that the static x has been exceeded) and finally the oscillatory dynamics is established which attenuates and then settles on the position value commanded to infinity.

As a verification that the two dynamics are superimposed it can possible see the position error calculated between Simulink and Simscape position. This error is of the order of 10^{-15}.

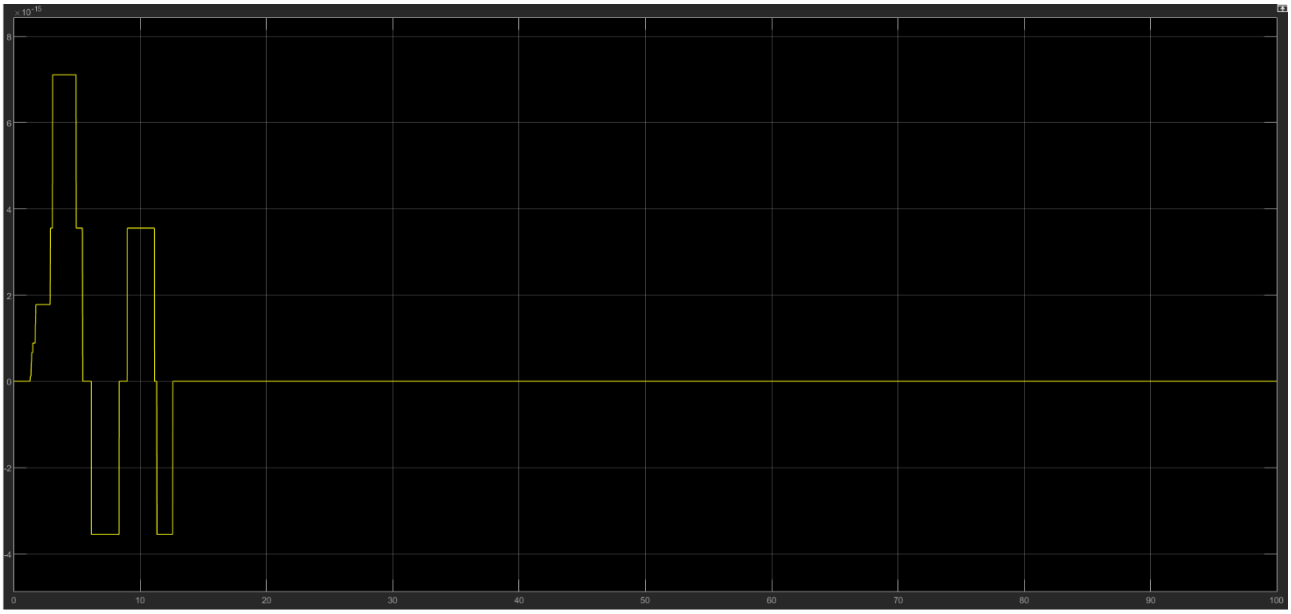

Figure 87: Error between Simulink and Simscape

5.4) MCK 2 D.O.F. system Simulink VS Simscape

This paragraph describes a harmonic oscillator: a system consisting of two masses connected to each other by means of an ideal spring and an ideal damper. Therefore, in this MCK system with 2 degrees of freedom, the stiffness K_R is constant and independent of its relative deformation and the dimensional viscous damping coefficient C_R is constant and independent of the corresponding relative speed.

The "commanded" driving force F_M is applied to the first mass, while the external load F_R acts on the second one. The entire system is subjected to absolute damping by means of a viscous damper that connects the first mass to a fixed reference.

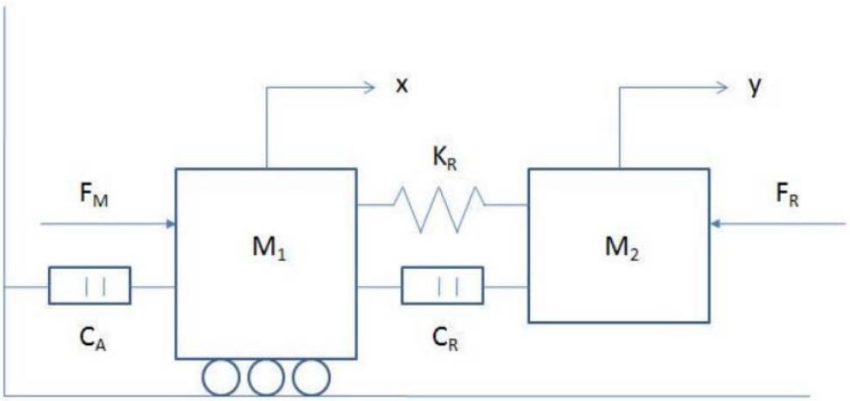

Figure 88: Harmonic oscillator physical system

The system is characterized by two translational degrees of freedom relating, for example, to the instantaneous position of the centre of gravity of the two masses *x* and *y*.

The dynamics of the system can be described by the following differential equations:

$$M_1 \cdot \ddot{x} + C_a \cdot \dot{x} = F_M - K_r \cdot (x - y) - C_r \cdot (\dot{x} - \dot{y})$$

$$M_2 \cdot \ddot{y} = K_r \cdot (x - y) + C_r \cdot (\dot{x} - \dot{y}) - F_R$$

In order to obtain the system's elementary block model it's necessary to introduce a third equation: it can be assumed that the force F_M applied to the mass M_1 is proportional, thanks to a gain GM, to the position error Err.

$$F_M = G_M \cdot (Com - y)$$

This error consists to the difference between a hypothetical commanded position Com (the command input of the dynamic system) and the corresponding instantaneous position y of the mass M_2.

The Simulink model of the mechanical system examined is the following:

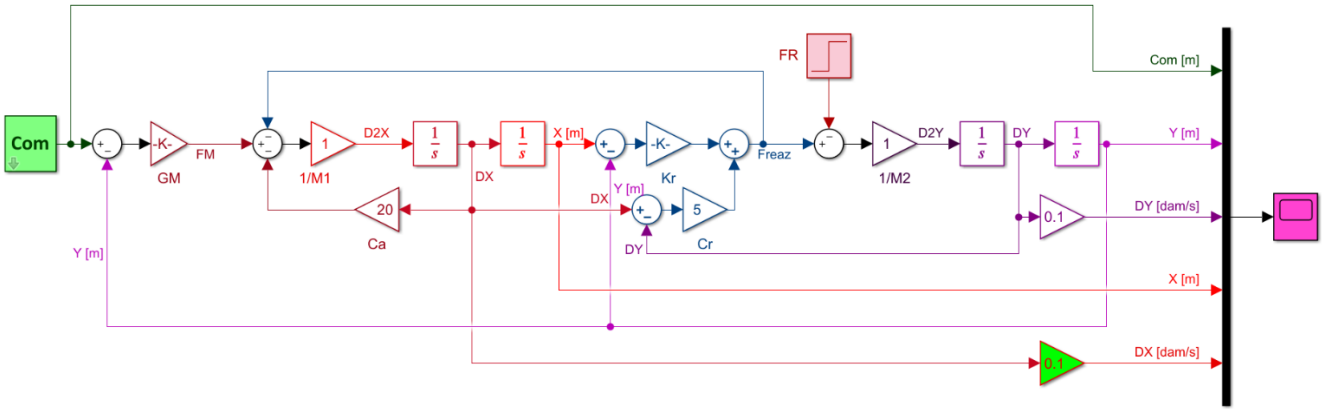

Figure 89: Harmonic oscillator Simulink model

Thanks to the step command mass M_1 begins to move and due to an elastic recall effect the mass M_2 also begins to move (at the beginning it starts quite slowly).

An oscillatory dynamics of the two masses is established, which tends to decrease: in about 1.5 second the oscillations of x and y (M_1 and M_2 respectively) are almost the same.

Then the system is at rest and reaches the commanded position.

When the load F_R is applied the system, which was at rest, starts again and both the mass M_1 and the mass M_2 move from the position reached.

The final equilibrium positions where both masses are stopped will not be the same. Final equilibrium positions will be a little further from the commanded position and this difference is determined by the external load F_R and by the relative stiffness between the mass M_1 and M_2.

In fact with a decreasing of the K_R of the spring the deviation will be less.

Now it's showed the correspondent Simscape model (all green in the model's top part) and how Simulink and Simscape dynamics are represented:

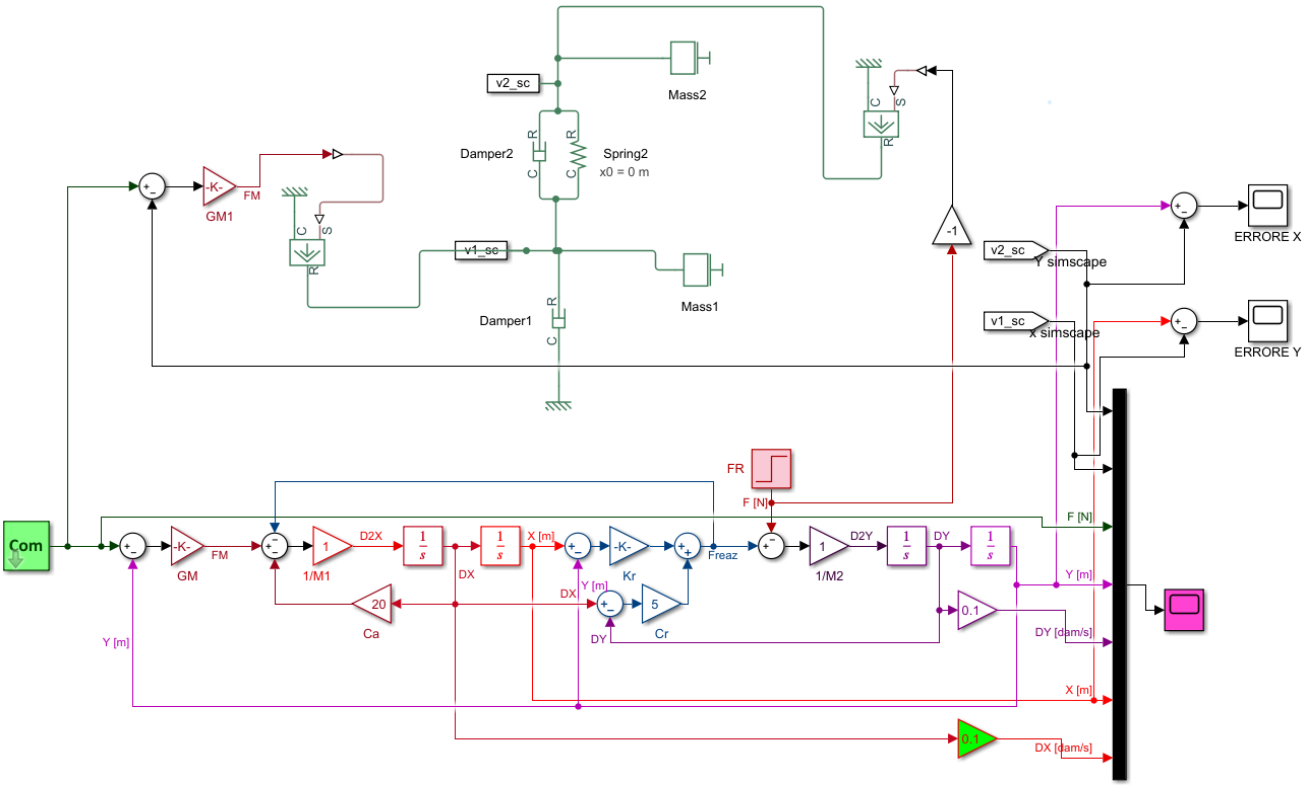

Figure 90: Harmonic oscillator Simascape model

The masses initial positions have been both settled to 0 m.

It's clear that the dynamics of the two masses described through Simulink and Simscape are identically: in fact the position's curves on Simulink (cyan for *x* and green for *y*) and Simscape (blue for *x* and yellow for *y*) are exactly superimposed.

Figure 91: Simulink superimposed dynamics

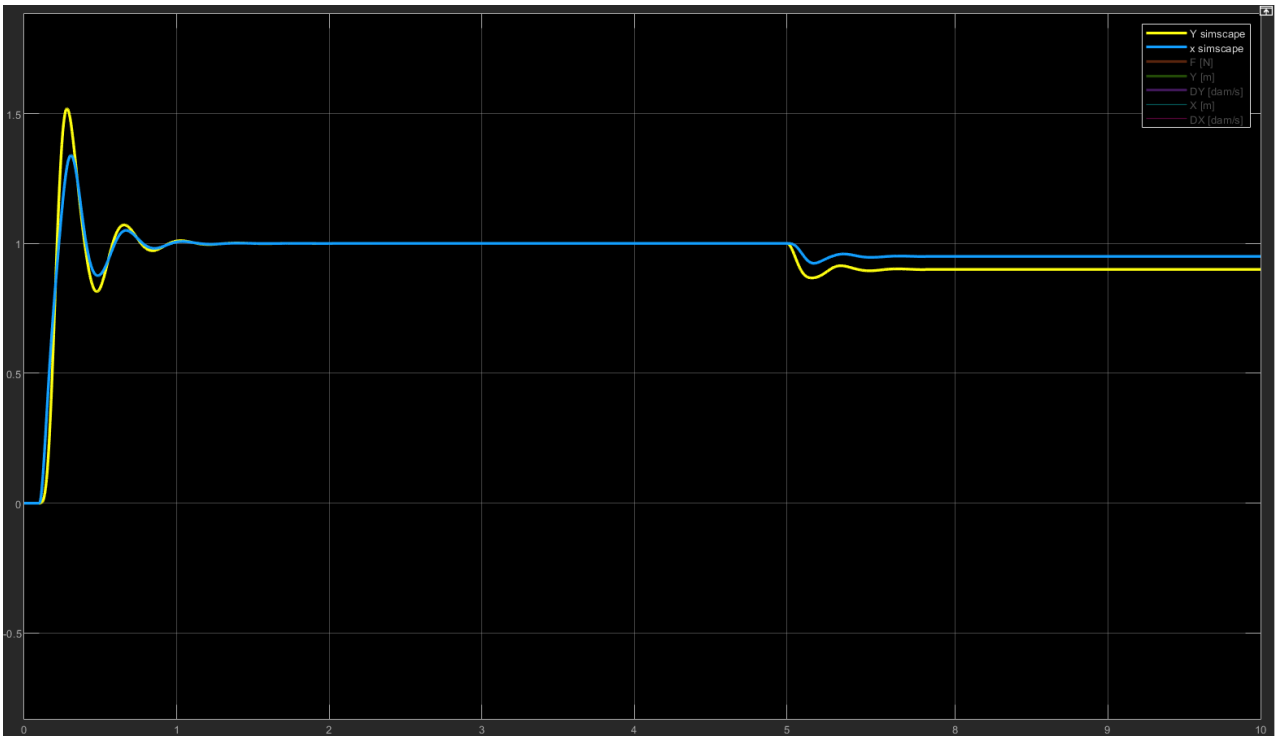

Figure 92: Simscape superimposed dynamics

As a verification that the two dynamics are superimposed it can possible see the position error about x and y calculated between Simulink and Simscape position respectively.

For x this error is of the order of 10^{-13} .

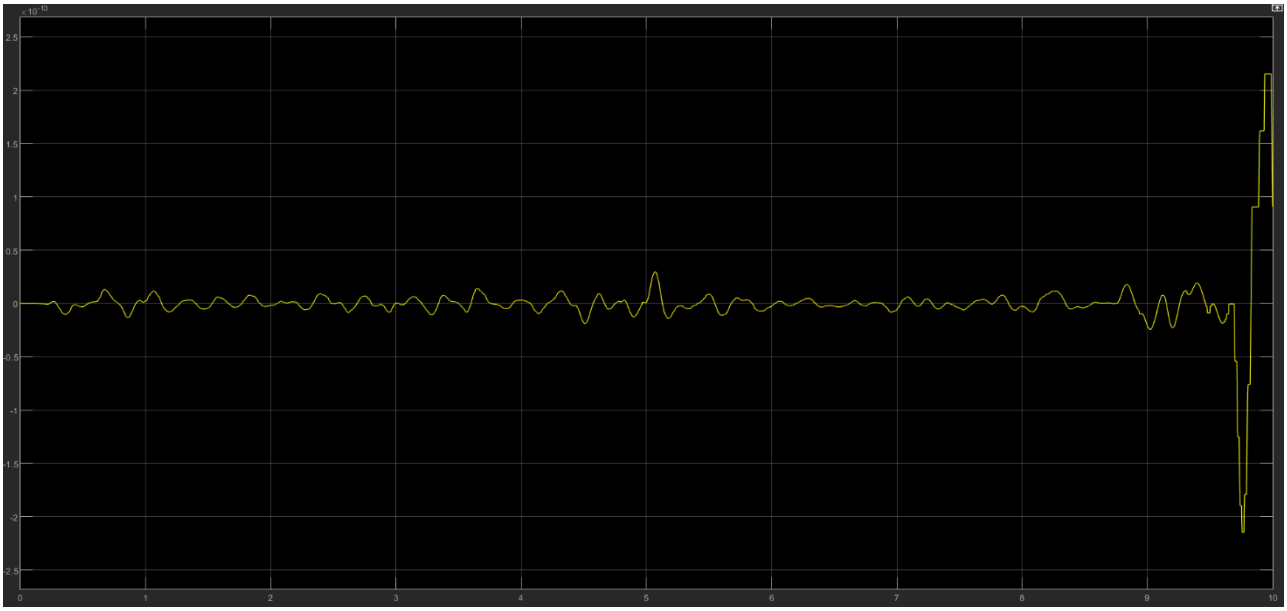

Figure 93: Error for x

For y this error is of the order of 10^{-14}.

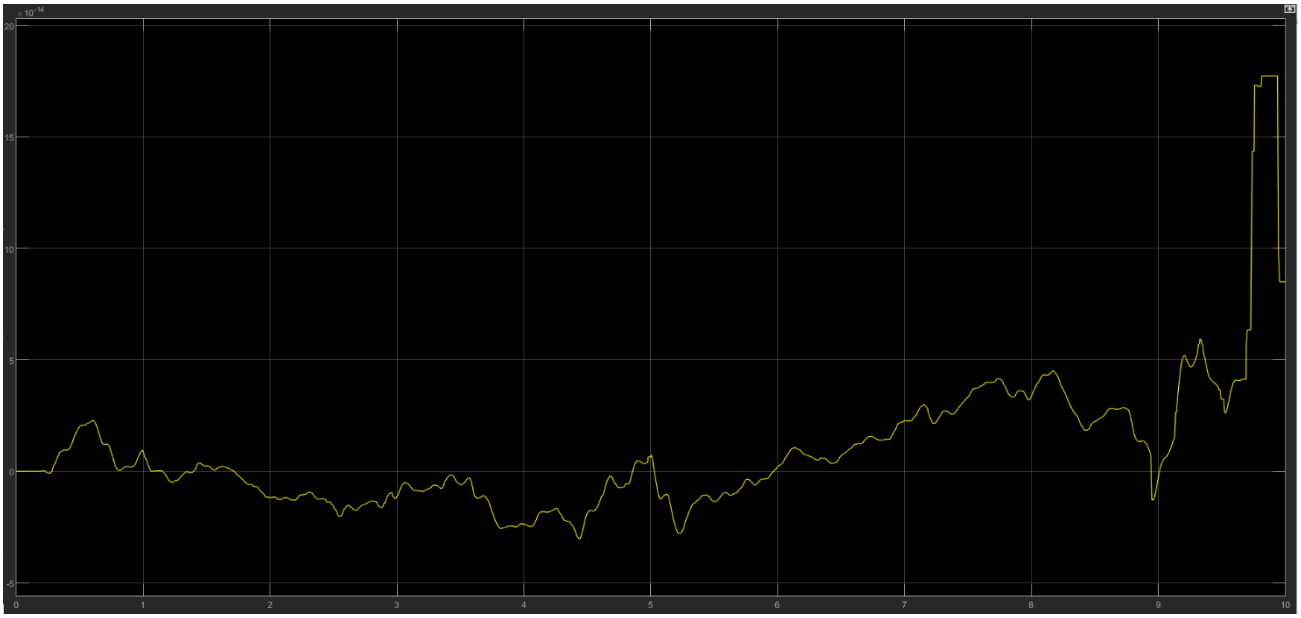

Figure 94: Error for y

6) Simscape modeling

6.1) Simscape model mechanical transmission with backlash

Before analysing backlash modeling in Simscape models linked to the Simulink models shown in chapter 5, it is necessary to study easier mechanical transmission models such as in paragraphs 6.2 and 6.3

6.2) Simscape model with only driven torque

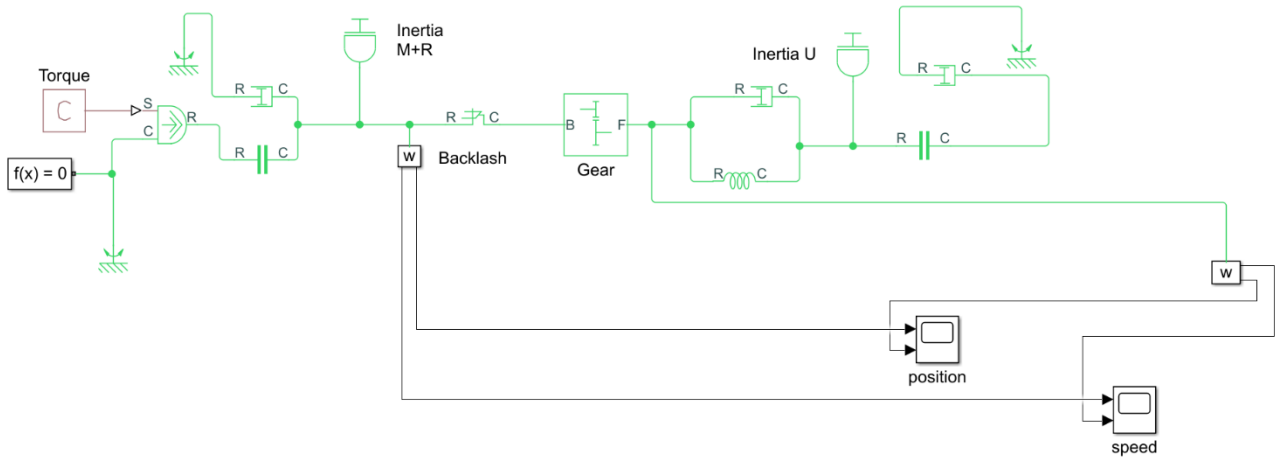

Figure 95: First Simscape mechanical model

The first mechanical model developed through Simscape represents a mechanical transmission with backlash where the drive torque delivered by the motor drives the gearbox which moves a moving surface at low speed and high torque. No viscosity is considered inside the friction model of the system.

It is possible to examine positions and speeds trends of the motor and user measured over time:

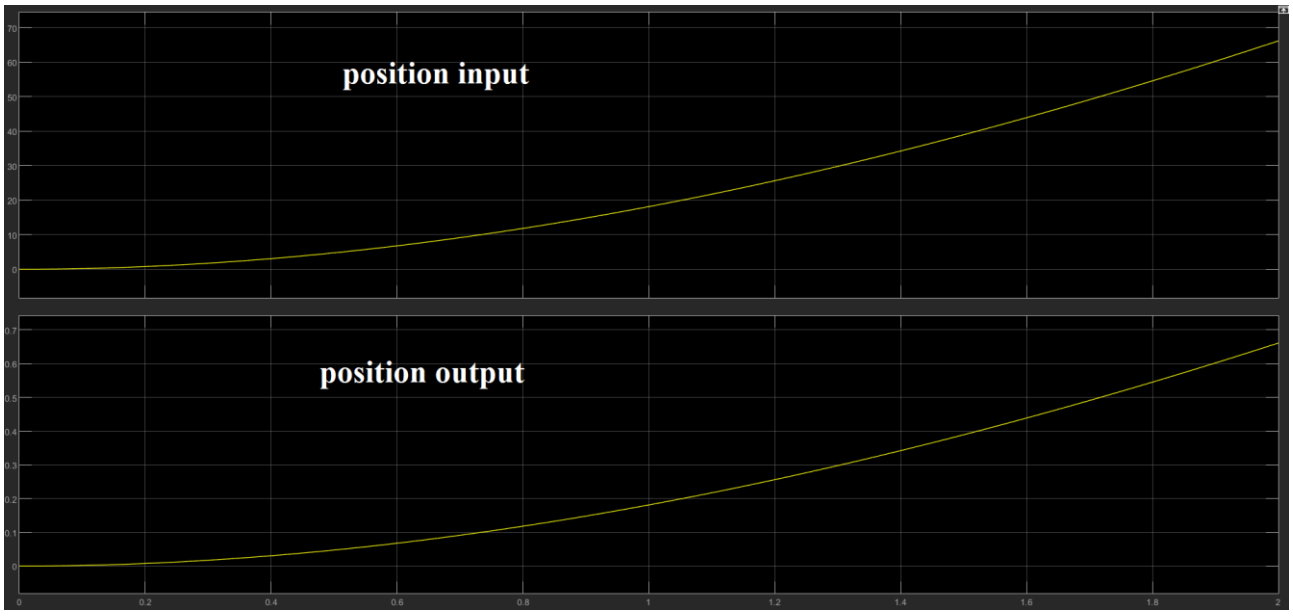

Figure 96: Positions of motor and user

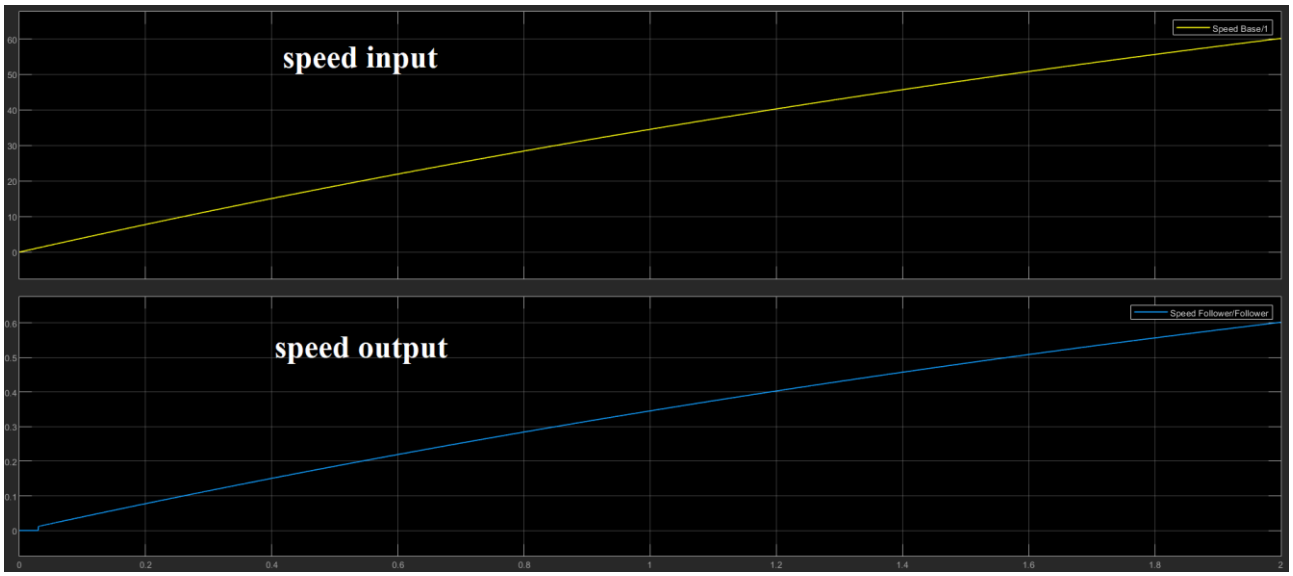

Figure 97: Speeds of motor and user

It is clear that, on Figure 96 and Figure 97, positions and speeds trends are consistent to the transmission ratio τ.

Furthermore, from the positions graph, it is possible to notice during initial instants the backlash phenomenon (Figure 98): an amount of space between the two mechanical parts must be overcome before the drive wheel and the driven wheel can be in contact. So the user starts to move itself 0.0275 s after the motor.

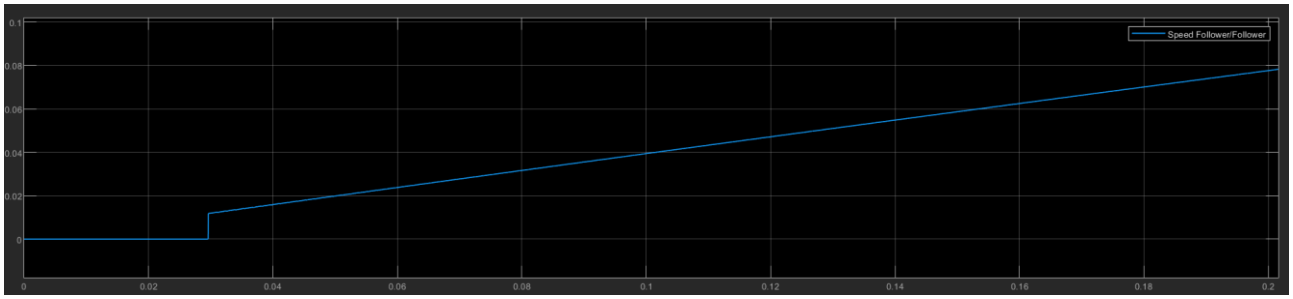

Figure 98: Backlash

The system is characterized by the following data:

Input	***Value***
Torque	4 Nm
Motor	***Value***
Inertia	0.085 kg· m^2
Damping	0.03 N·m/(rad·s)
Breakaway friction torque	5 Nm
Breakaway friction velocity	0.1 rad/s
Coulomb friction torque	5 Nm
Viscous friction coefficient	0 N·m/(rad·s)
Gear	***Value***
Teeth ratio	100

User	***Value***
Inertia	50 kg· m^2
Damping	100 N·m/(rad·s)
Breakaway friction torque	500 Nm
Breakaway friction velocity	0.1 rad/s
Coulomb friction torque	500 Nm
Viscous friction coefficient	0 Nm/(rad·s)
Yielding drive shaft	***Value***
Spring	1e5 Nm/rad
Damping	500 N·m/(rad·s)
Backlash	***Value***
Upper bound	1 deg
Lower bound	-1 deg

Table 5: Data's model

Zooming positions graphs it's possible to see the motor with its inertia starts at 0.005 second and also the backlash phenomenon for the user.

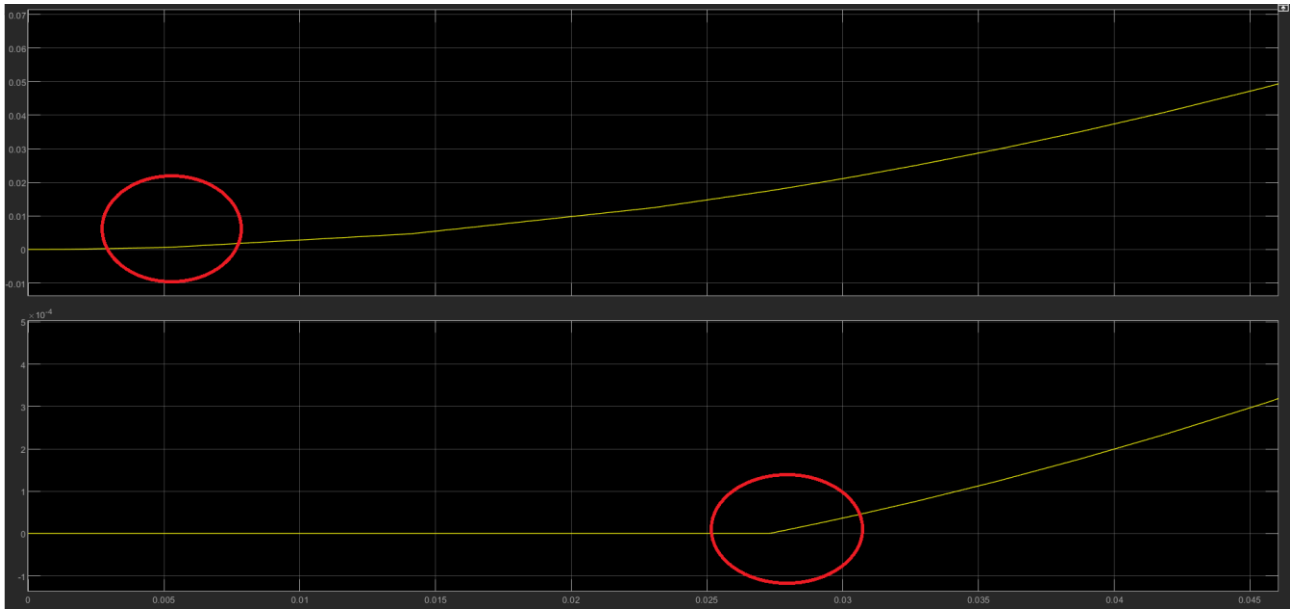

Figure 99: Zooming positions graphs

6.3) Simscape model with driven torque and external load

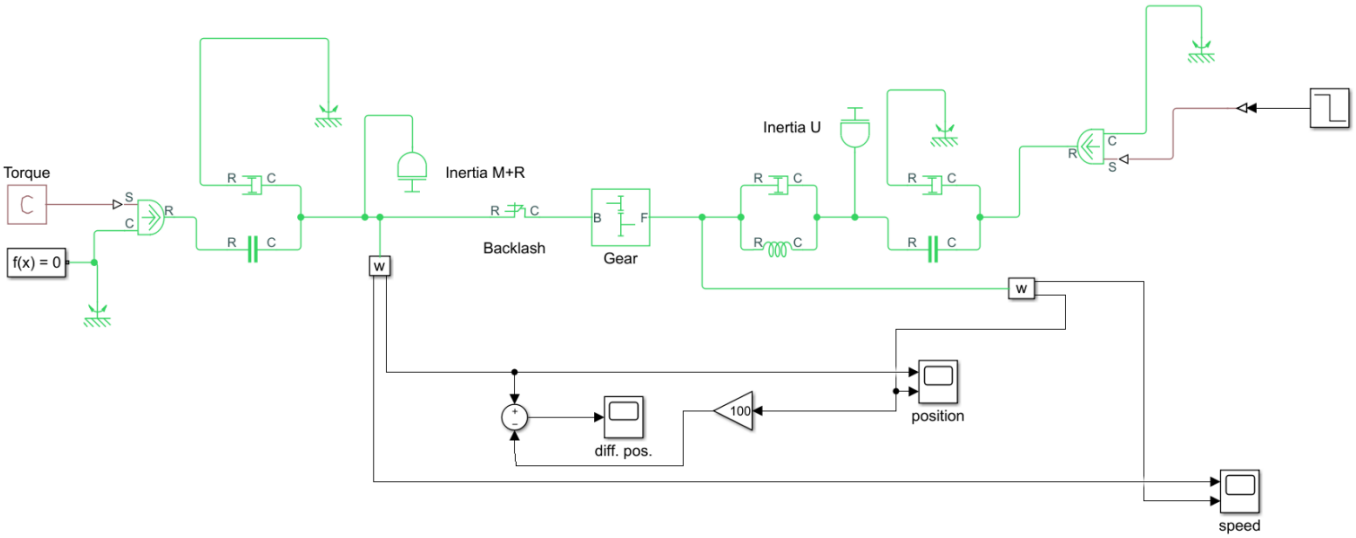

Figure 100: First Simscape mechanical model

The second mechanical model developed through Simscape adds an external load T_R= 2500 Nm applied at 1.4 s.

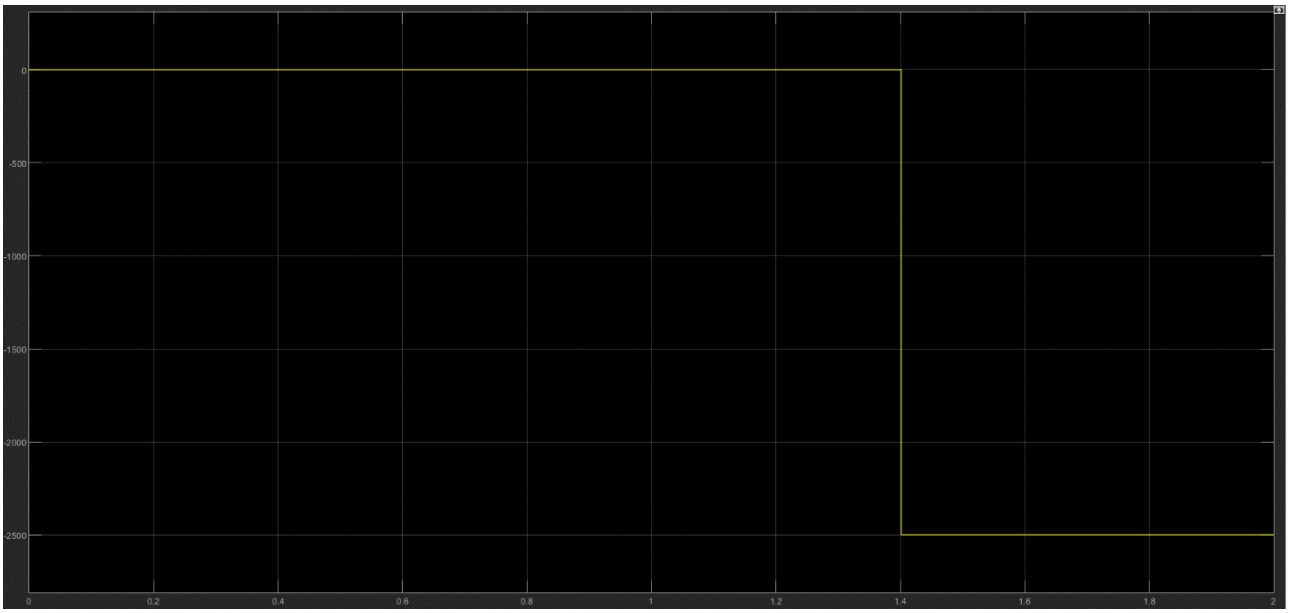

Figure 101: External load

Data used in this model are the same of the model described in the previous paragraph.

In this system there is also the calculation of the position difference between input and output at the same shaft in order to make some considerations. It is important to note that the measurements of positions and speeds are made through sensors contained inside **"w"** blocks.

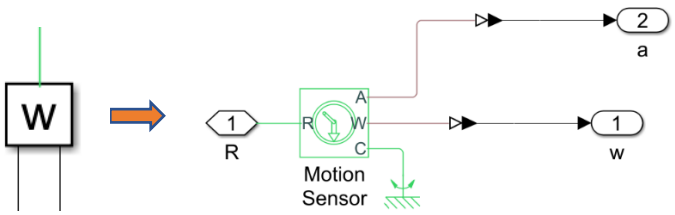

Figure 102: Inside "w" blocks

Now it analyses positions and speeds trends:

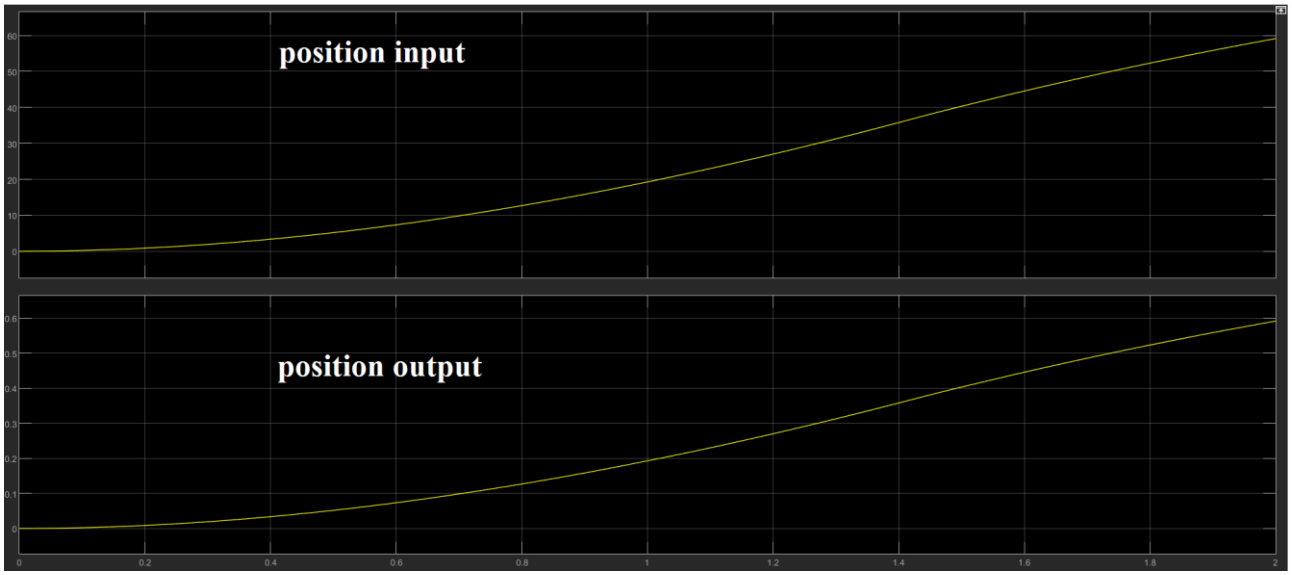

Figure 103: Positions of motor and user

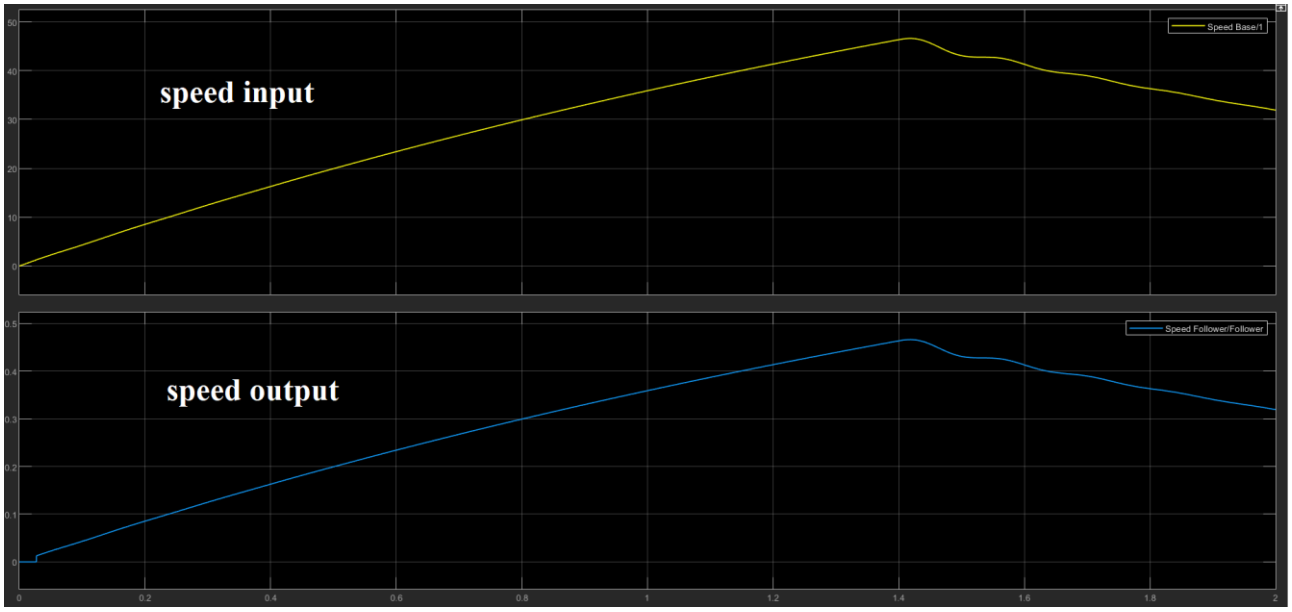

Figure 104: Speeds of motor and user

It is clear that, on Figure 103 and Figure 104, positions and speeds trends are consistent to the transmission ratio τ. Now it is possible to see mechanical backlash in the following figure:

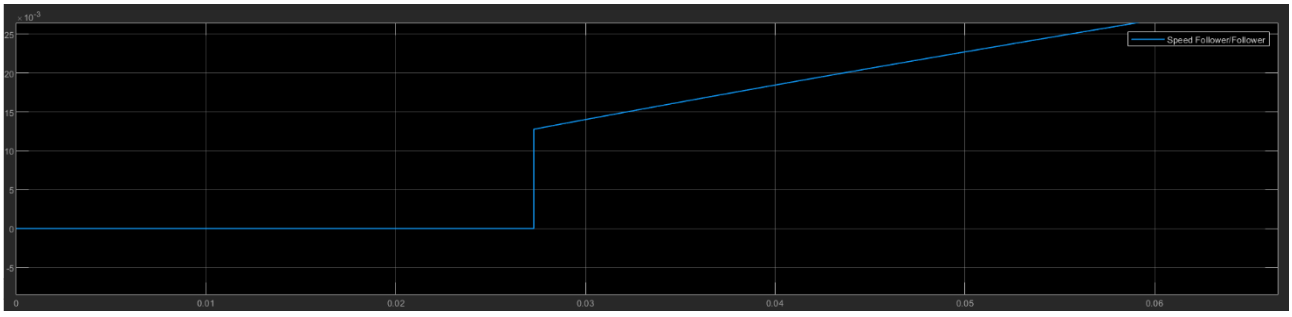

Figure 105: Backlash

The positions increase but, when the external load is applied, with a lower rate of growth. On the other hand the speeds before increase and then decrease due to the load.

Furthermore, from the positions graph, it is possible to notice during initial instants the backlash phenomenon (Figure 105): an amount of space between the two mechanical parts must be overcome before the drive wheel and the driven wheel can be in contact. So the user starts to move itself 0.0275 s after the motor.

Zooming positions graphs it's possible to see the motor with its inertia starts at 0.005 second and also the backlash phenomenon for the user.

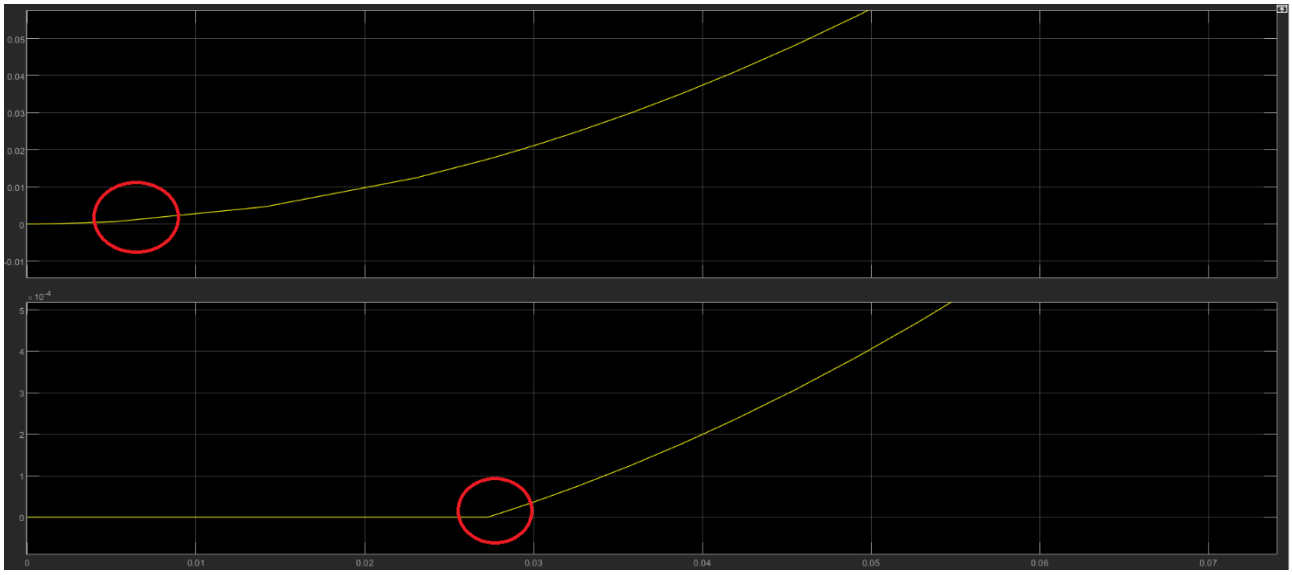

Figure 106: Zooming positions graphs

The difference between positions initially increases, therefore motor and user positions have different growth rates. Then the difference becomes constant because motor and user increase with the same rate.

The difference at the same shaft calculated is of the order of 10^{-3} .

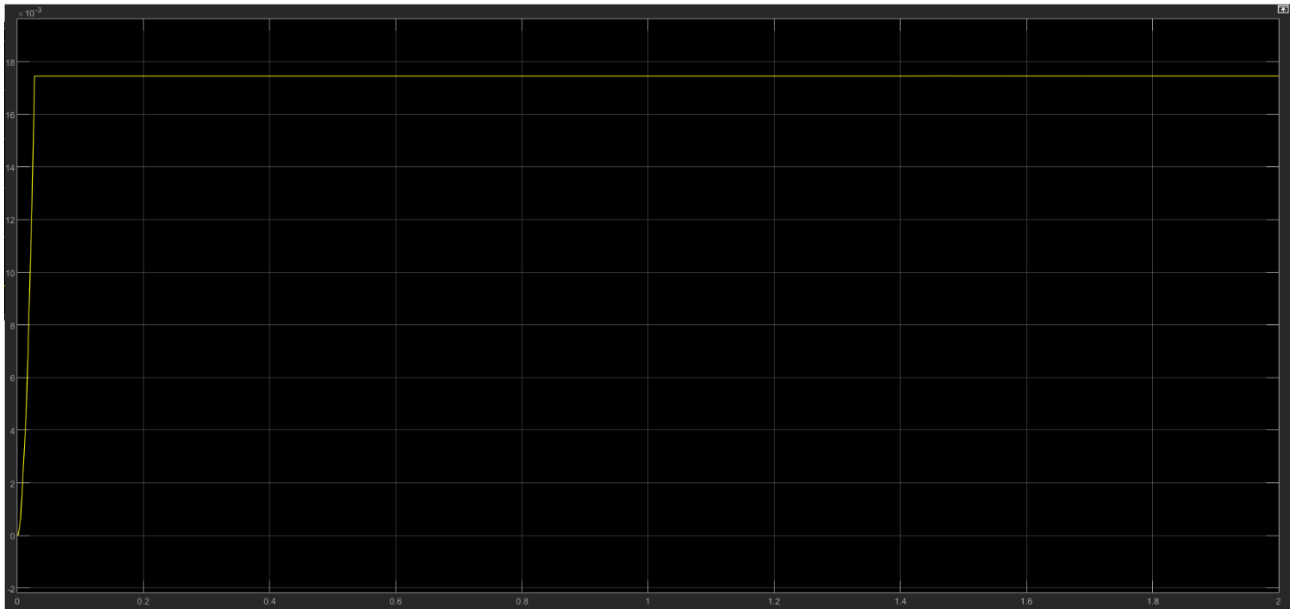

Figure 107: Position difference at the same shaft

6.4) Analysis of several friction models

In order to model correctly the following two models on Simscape, in next paragraphs 6.5 & 6.6, it's necessary to discuss about the friction models on Simulink and their adaptation on Simscape.

First of all, it can start with a Mass-Spring-Damper rotational system (Figure 108) which contains the Borello Friction model (Figure 109):

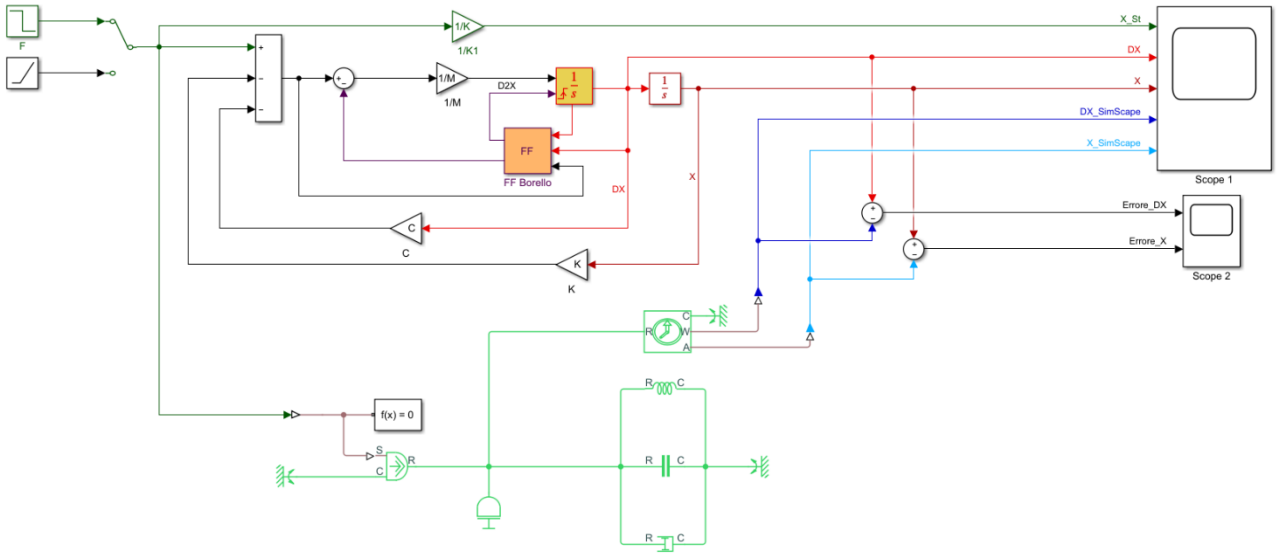

Figure 108: Mass-Spring-Damper with Borello model

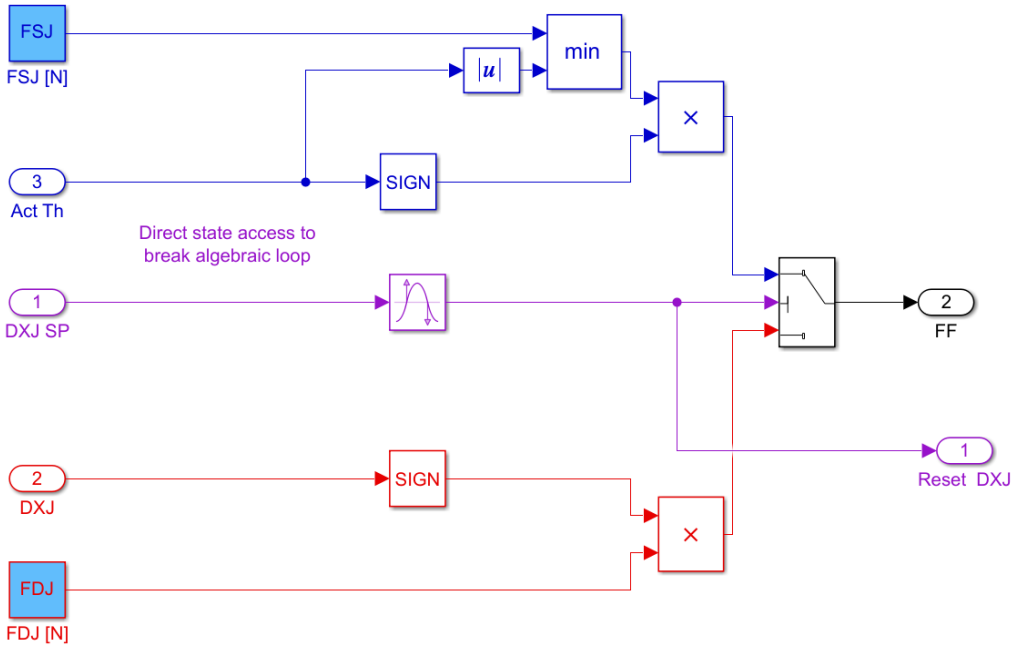

Figure 109: Borello Friction Model

The model proposed:

- Distinguishes the friction torque sign in function of the speed direction;
- Discriminates adherence from dynamic conditions (indeed two different values can be assigned to the friction torque: FSJ for statical condition and FDJ for dynamical ones);

- Evaluates the eventual stoppage of the mechanical component, moving at the beginning;
- Assesses the eventual element restart, still at the beginning;
- Correctly keeps arrested (or in motion) the mechanical component;
- Takes into account the presence of eventual mechanical end-stops, against which a completely inelastic shock is supposed to occur.

The considered model, starting from the classical Coulomb formulation, describes the dry friction effects as a function of speed and active torque according to the the same mathematical expression of the paragraph 4.2.5.

The system is characterized by the following data:

Mass	***M = 1 Kg***
Damper	***C = 1 N·m/(rad·s)***
Spring	***K = 10 Nm/rad***
Initial position	***X0 = 0 m***
Initial Rotational Force value	***F0 = 10 Nm***
Finale Rotational Force value	***F1 = -10 Nm***
Step Time	***TimeF = 10 s***
Stop Time	***TiBr = 20 s***
Static Friction Rotational Force	***FSJ = 0.5 Nm***
Dynamic Friction Rotational Force	***FDJ = 0.25 Nm***

Table 6: Data's model

The optimum value that makes overlap the Borello Friction Model with the Simscape Friction Model (which considers instead the Stribeck curve) is the ***Breakaway friction velocity: 0.00060623 rad/s***

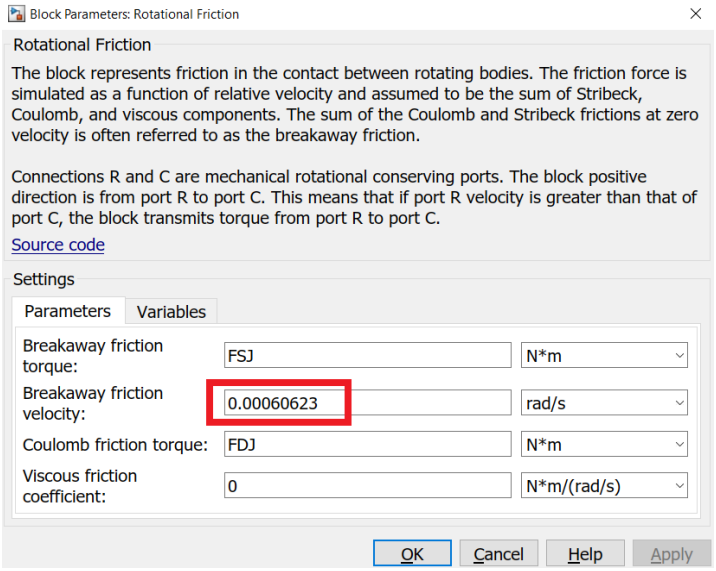

Window 2: Breakaway friction speed chosen

In fact the position and the speed error between Simulink and Simscape are minimized and they are of the magnitude's order of 10^{-6} and 10^{-5} respectively.

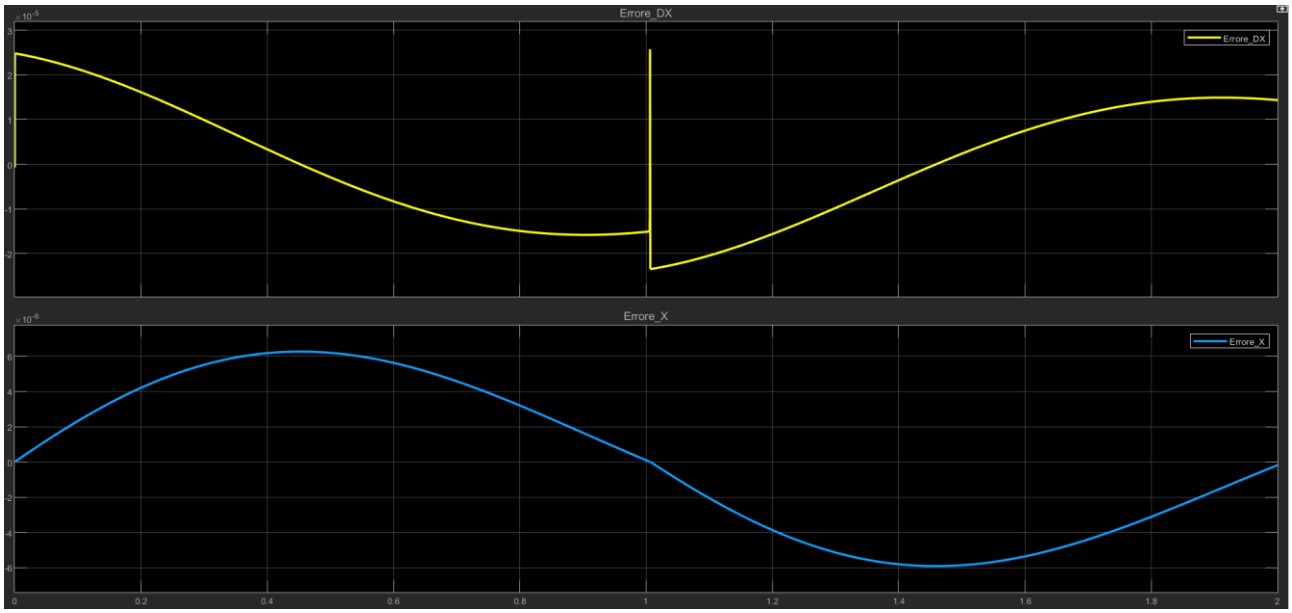

Figure 110: Errors

Secondary, it's necessary to consider, in the same Mass-Spring-Damper rotational system, the Saturated Hyper viscous Friction model (separately for motor and user) showed in the following figures.

In the first model are used a F0=50 Nm and a F1= -50 Nm while in the second model are used a F0= 200 Nm and a F1= -200 Nm

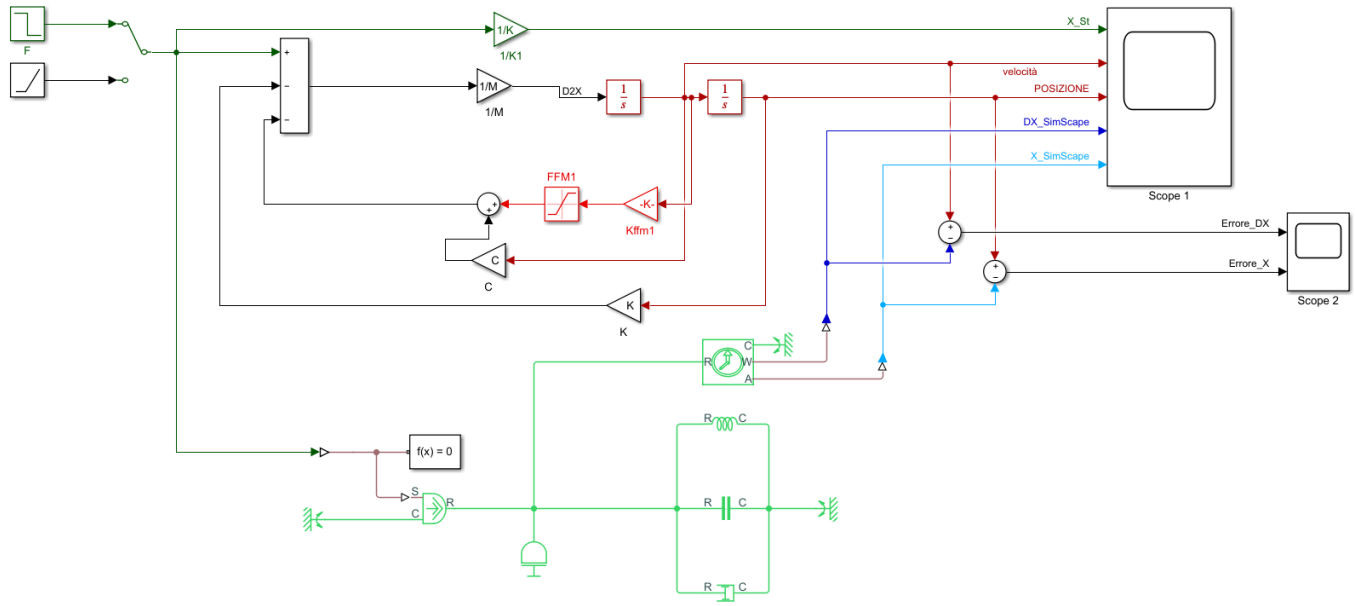

Figure 111: Motor's Saturated Hyper viscous model

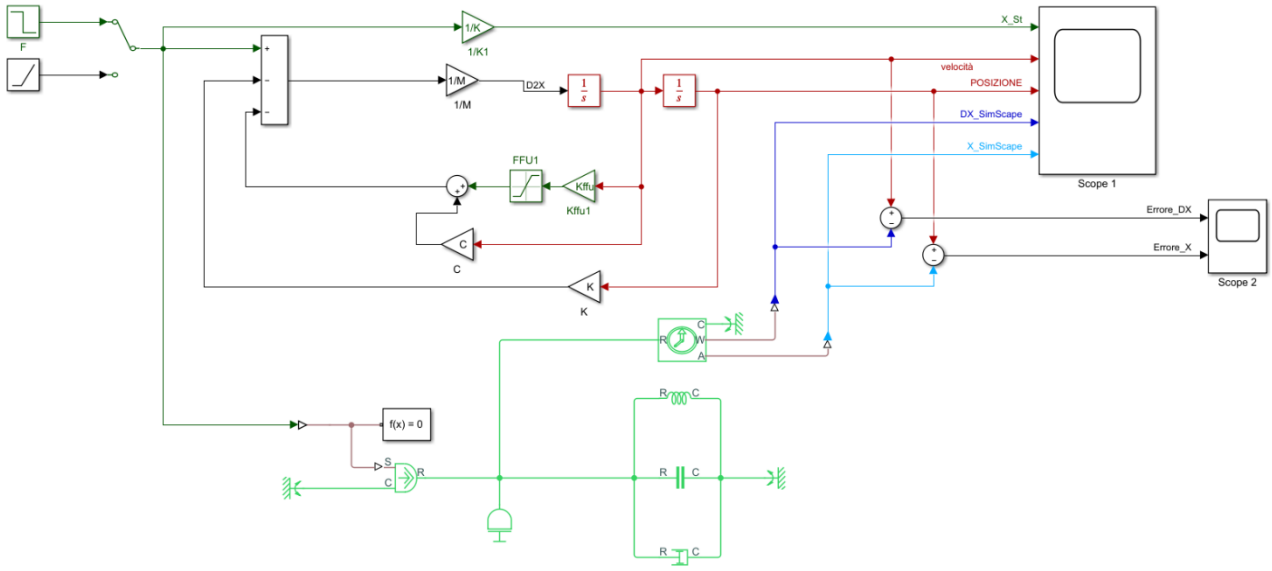

Figure 112: User's Saturated Hyper viscous model

The Saturated Hyper viscous Friction model is a simplified model of dry friction derived from the Coulombian model where it is:

- eliminated the discontinuity in the origin (for null values of the relative speed v);

- approximated the trend using a saturated hyper viscous friction model (i.e. with a viscous dimensional coefficient plus as high as possible, compatibly with the stability of the calculation process).

To eliminate the discontinuity in a small range of the origin in the speed axis having half-width equal to ε, a linearization of the relation that connects the force (or torque) of friction at speed is performed.

It's possible to see in Figure 113 a Saturated Hyper viscous Friction model graphic representation.

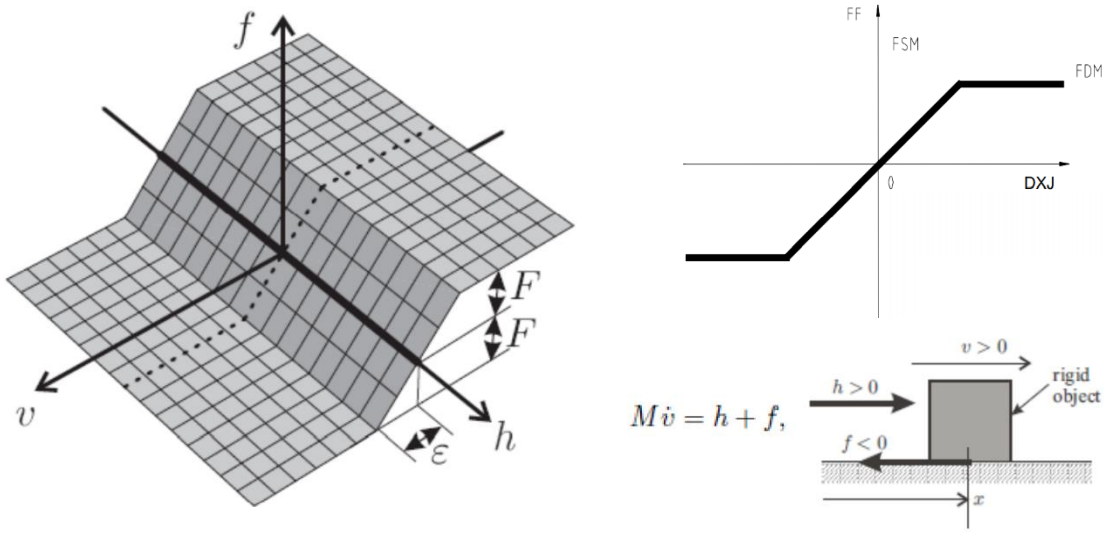

Figure 113: Saturated Hyper viscous Friction graphic representation

The thick black line represents the value of attraction force in static conditions (v = 0), f is the friction force [N], F is the maximum dynamic friction force [N], v is the relative

speed [m/s], h is the load in the direction of motion [N] and ε is the dead band speed or saturation speed [m/s].

The so said hyper viscous friction algorithm can be described as follow:

$$FF = \begin{cases} F \cdot v / \varepsilon & if \quad |v| \le \varepsilon \\ F \cdot \mathrm{sgn}(v) & otherwise \end{cases}$$

The optimum value that makes overlap the Saturated Hyper viscous Friction Model with the Simscape Friction Model (for both motor and user) is always the ***Breakaway friction velocity: 0.00060623 rad/s***

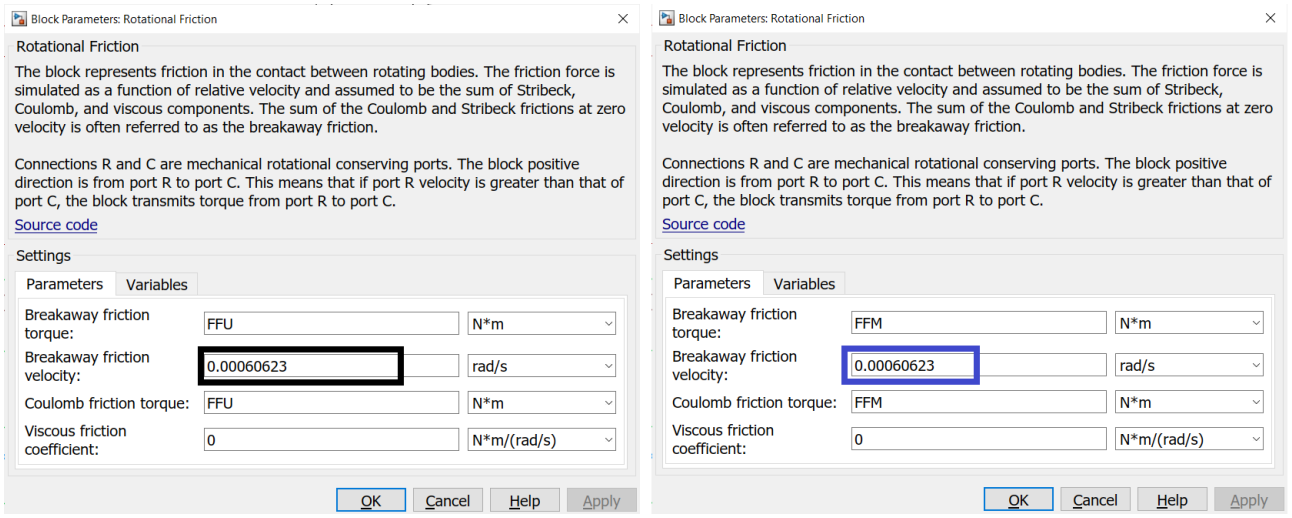

Windows 3: Breakaway friction speed chosen

In fact the position and the speed error between Simulink and Simscape are minimized and they are:

- for the motor both errors are of the magnitude's order of 10^{-6};
- for the user both errors are of the magnitude's order of 10^{-6} .

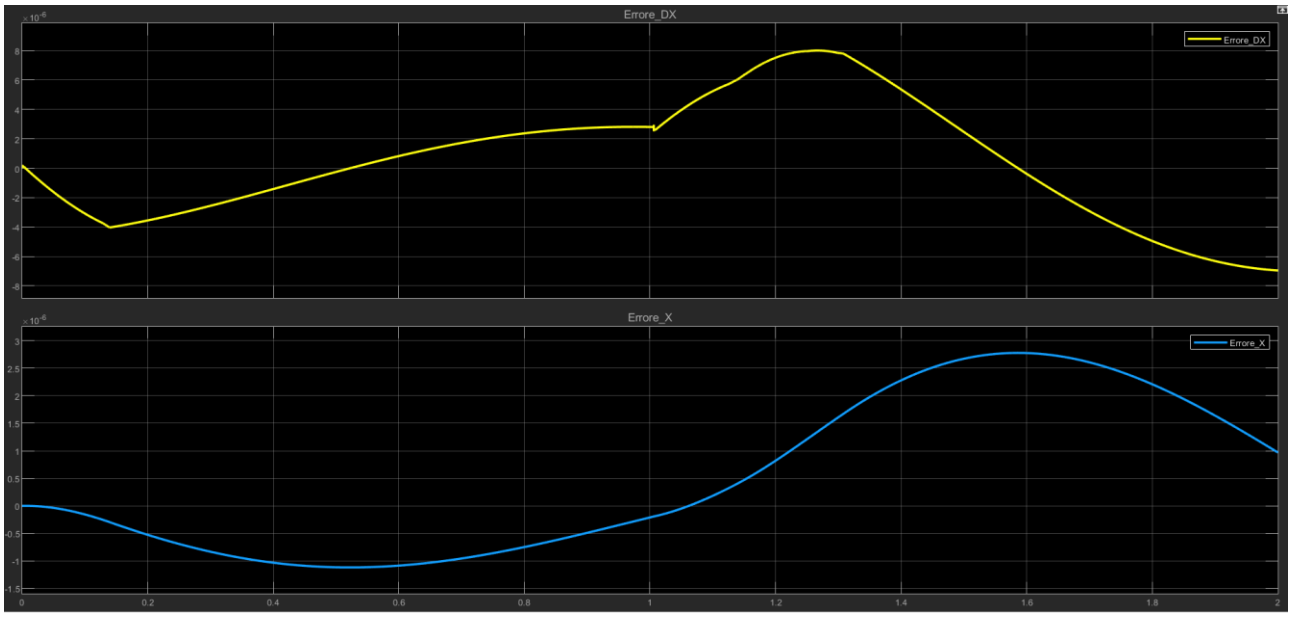

Figure 114: Errors

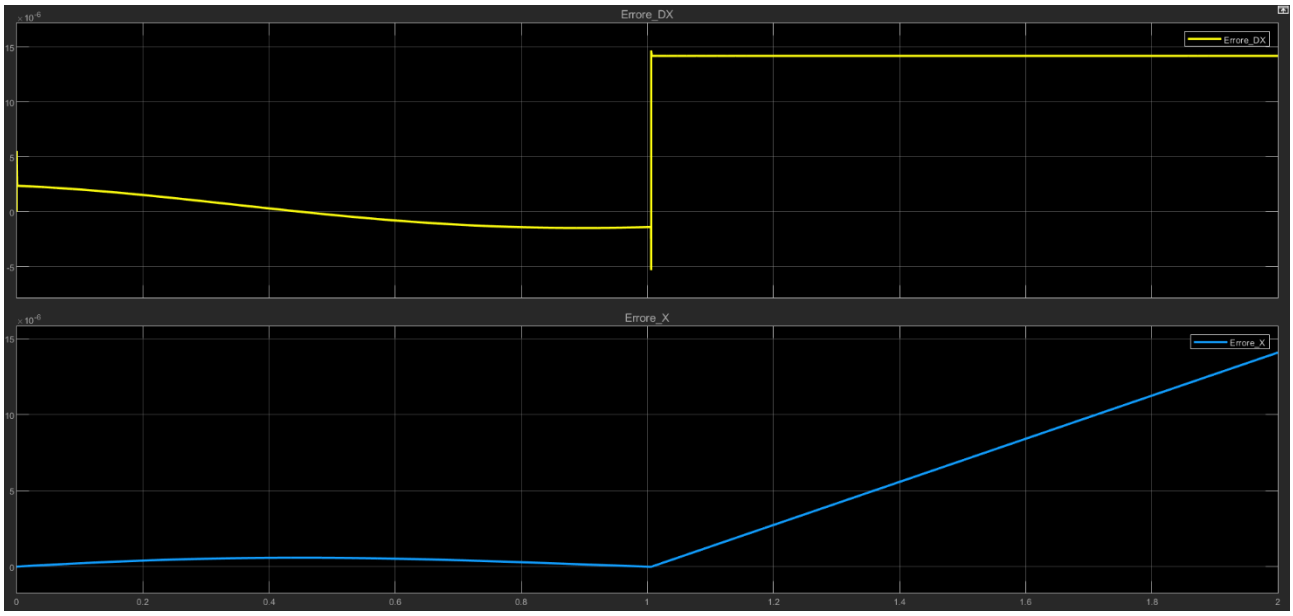

Figure 115: Errors

6.5) Simscape model with EMA 2 D.O.F

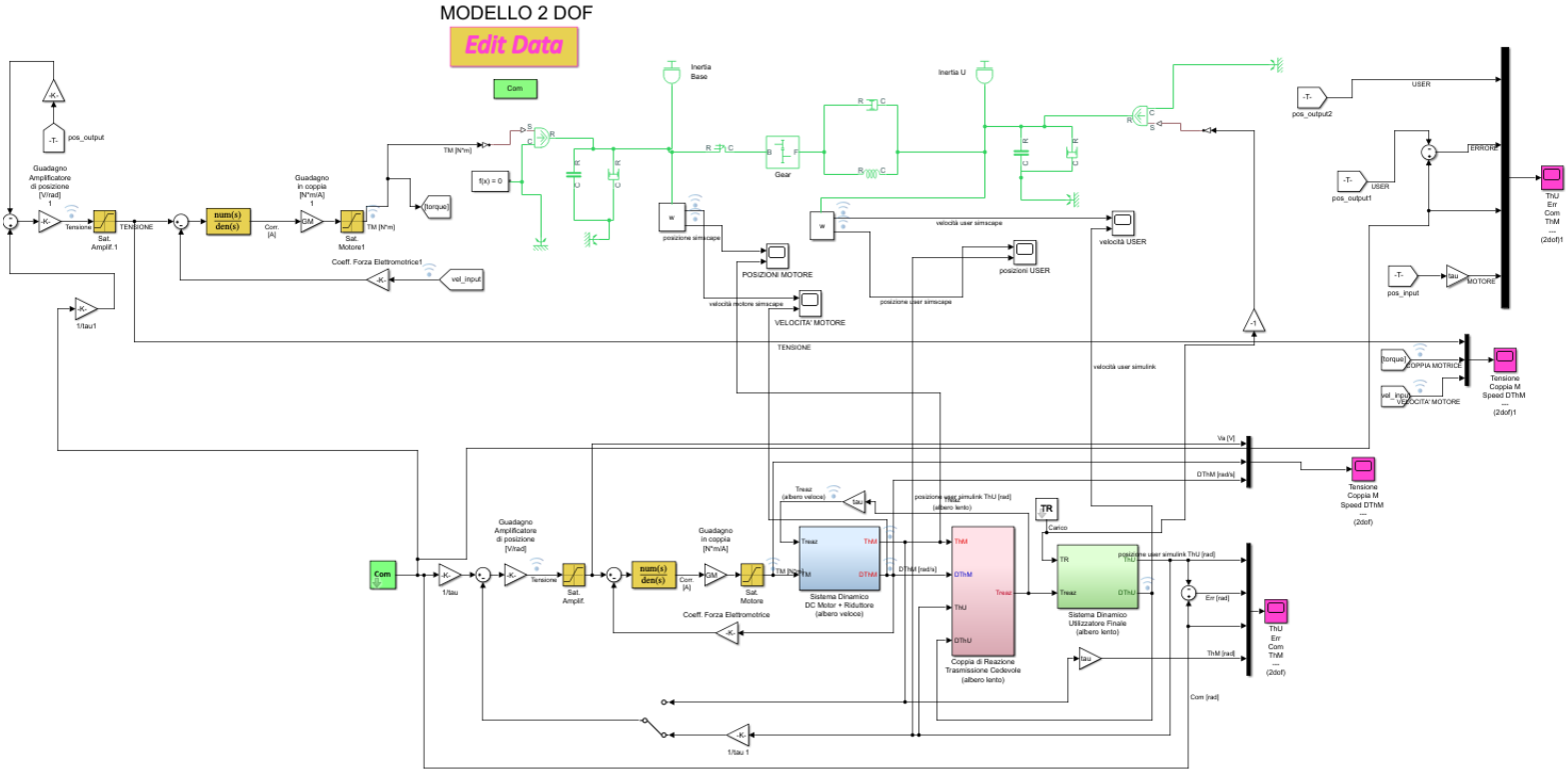

Figure 116: EMA 2 D.O.F. Simscape

The previous figure shows the model which is discussed in this paragraph.

Inside blue and green Simulink blocks (paragraph 4.1) the Saturated Hyper viscous Friction Model is implemented: so it is used, for the Simscape Friction Model, the same value of the *Breakaway friction velocity* used in paragraph 6.4.

The Simscape Model faithfully (and more intuitively than the Simulink model) replicates the physics of the "motor + user" system. The external force is given as input on the right and the drive torque, obtained from the same closed speed control loop of

the Simulink, is given as input on the left (to ensure that the driven torque is the same in both models).

The study of the models is done through the following steps:

- Simulink and Simscape models are compared without backlash;
- Only Simscape model is analysed with backlash;
- Simulink and Simscape are both analysed with backlash.

6.5.1) Models without backlash

Commenting out the backlash block on Simscape, the simulation starts for t=6 s, with an external load like in paragraph 4.1.1 and an input command consisting of a combination of step + ramp like in Figure 117.

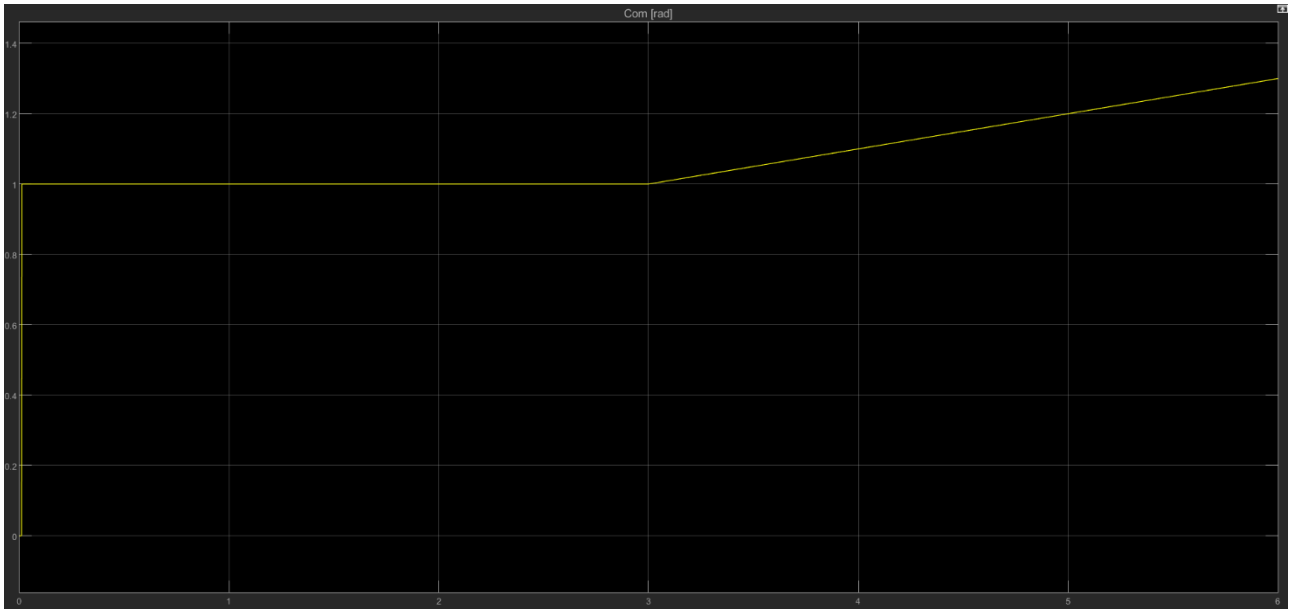

Figure 117: Input command trend

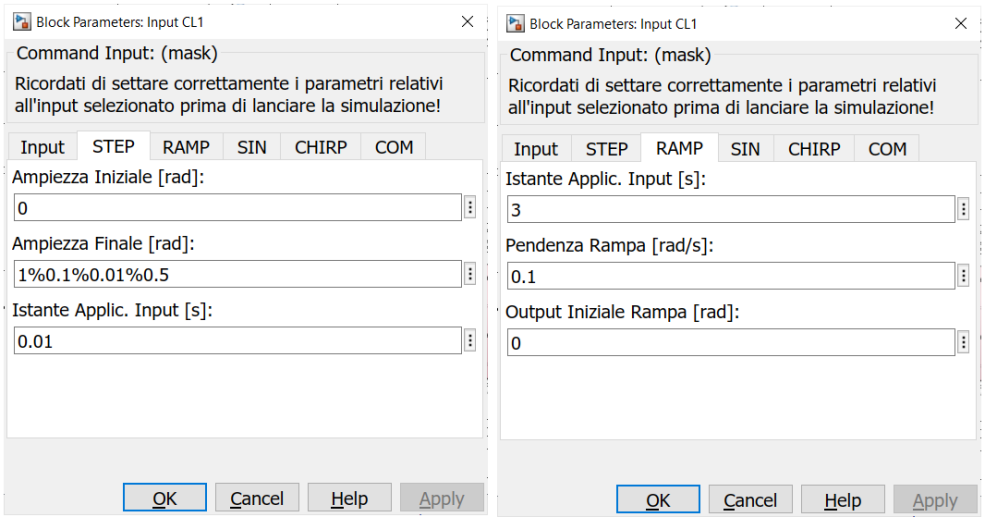

Window 4: Input command parameters

It's possible to examine now the position trends of motor and user, like in the following figures:

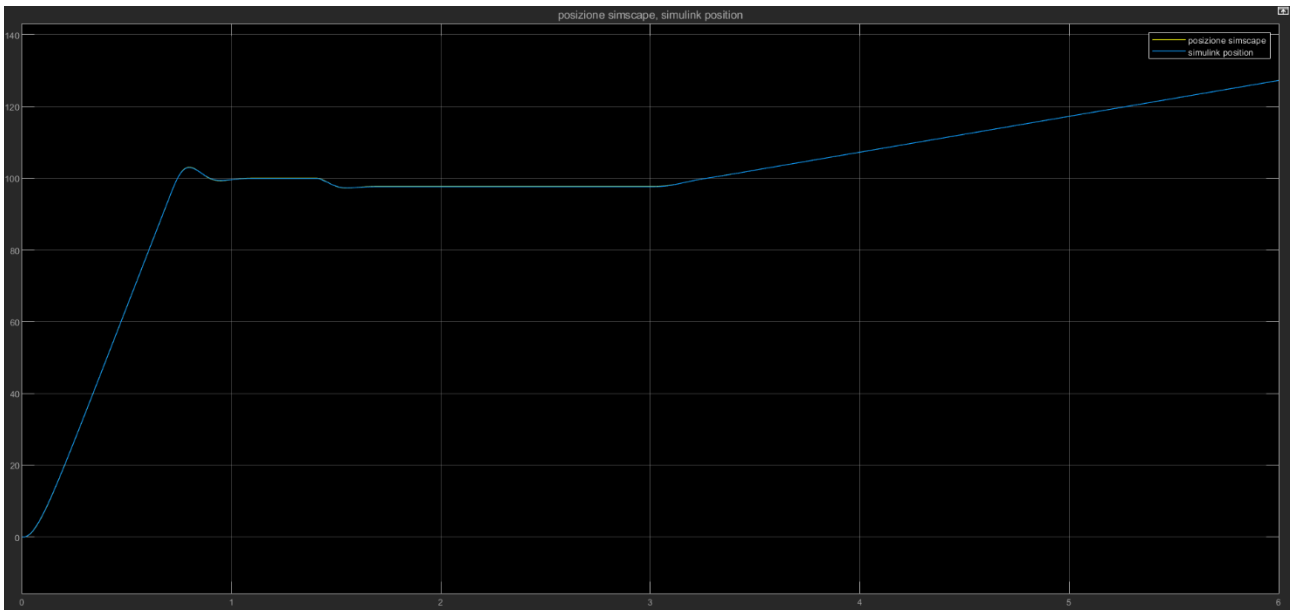

Figure 118: Motor position trends

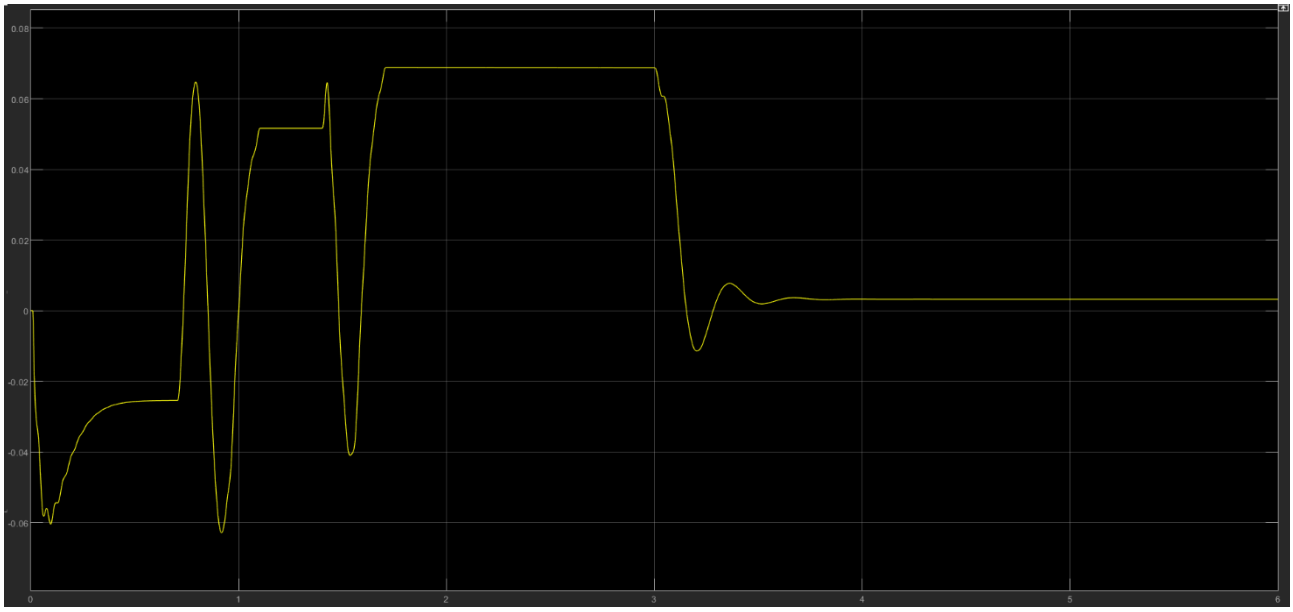

Figure 119: Error motor position trend

The implementation of the Simulink model with Simscape involves an error of 10^{-2} for the motor position between the two models.

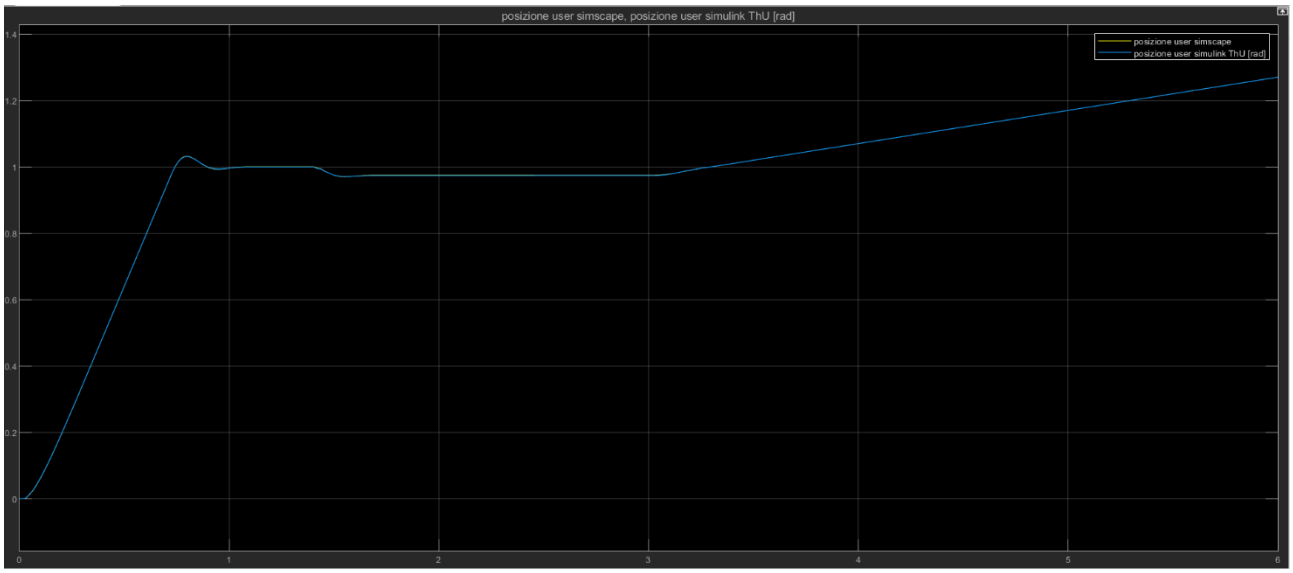

Figure 120: User position trends

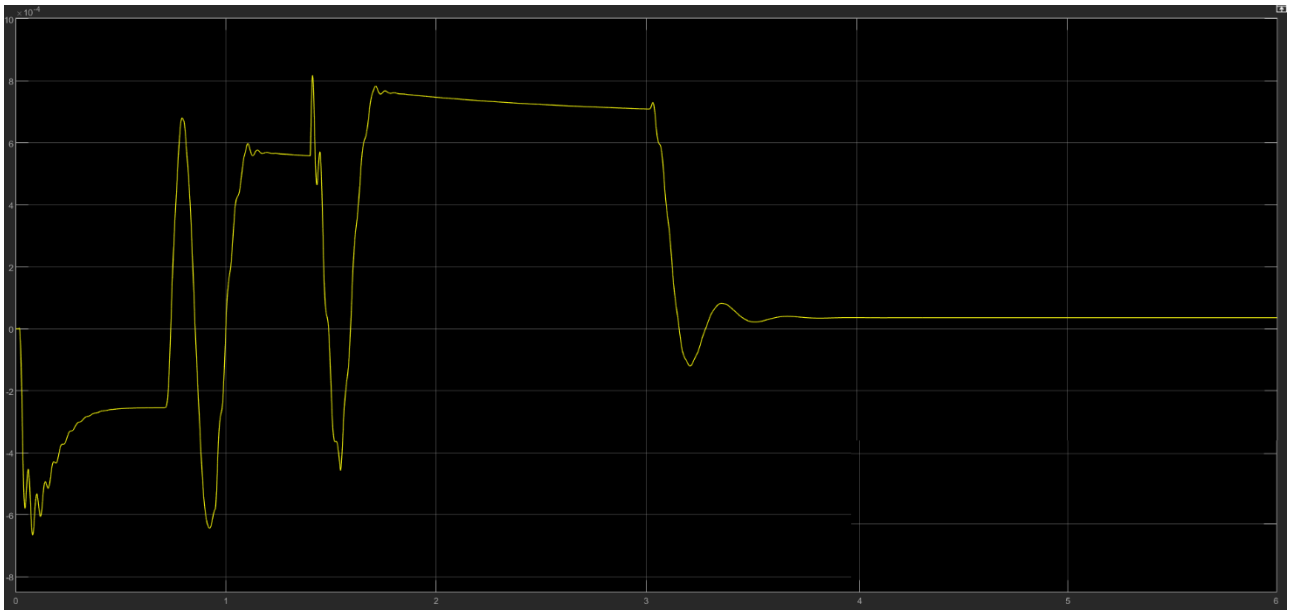

Figure 121: Error user position trend

The implementation of the Simulink model with Simscape involves an error of 10^{-4} for the user position between the two models.

It's possible to examine the speed trends of motor and user, like in the following figures:

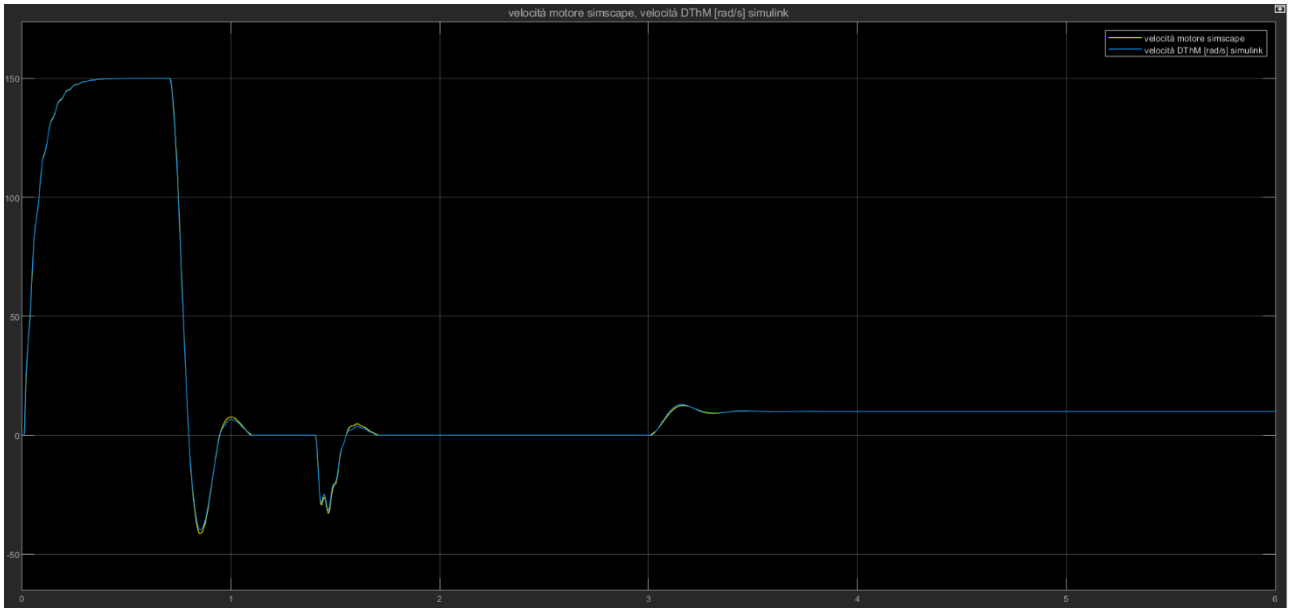

Figure 122: Motor speed trends

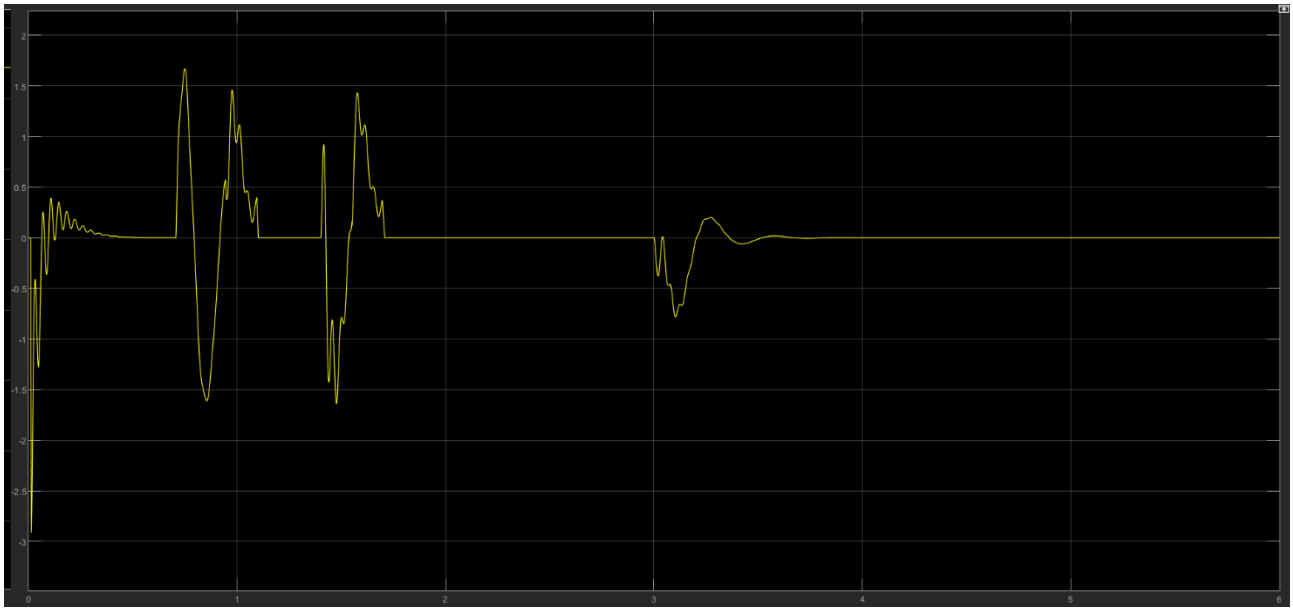

Figure 123: Error motor speed trend

The implementation of the Simulink model with Simscape involves a fair error for the motor speed trend between the two models.

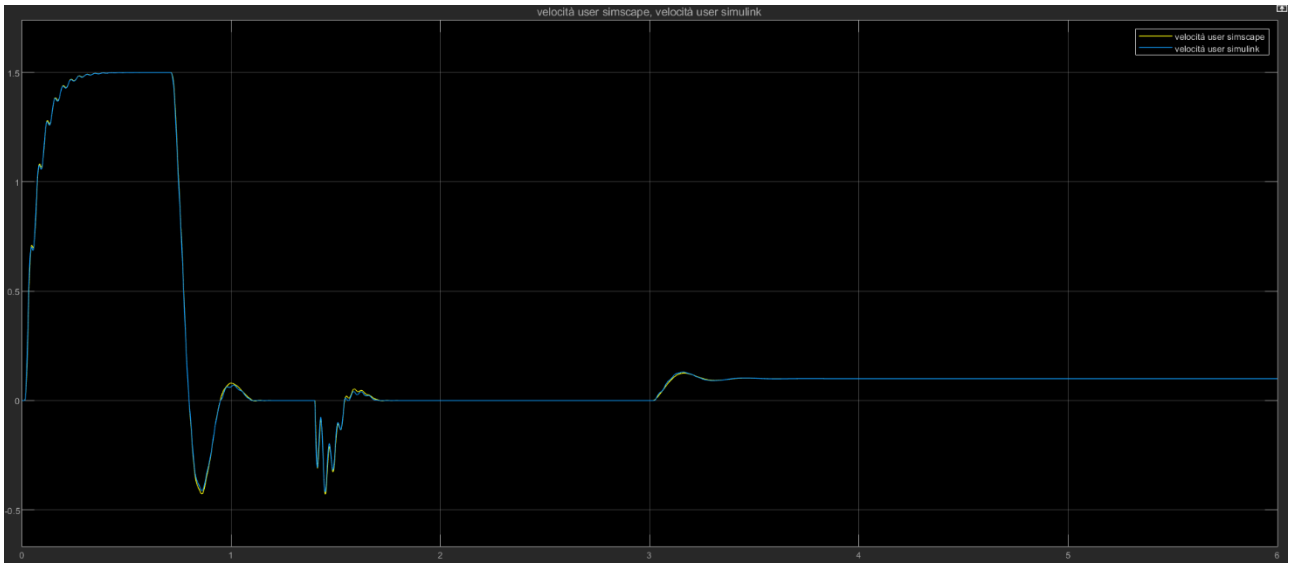

Figure 124: User speed trends

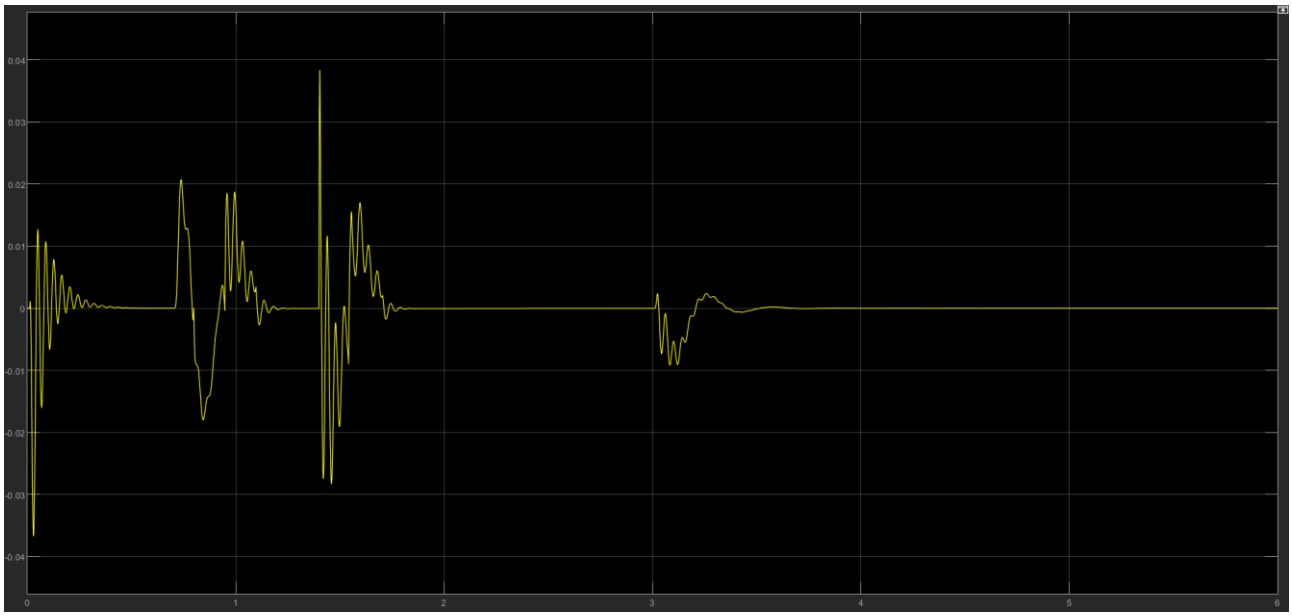

Figure 125: Error user speed trend

The implementation of the Simulink model with Simscape involves an error of 10^{-2} for the user speed between the two models.

6.5.2) Simscape model with backlash

Uncommenting the backlash block on the Simscape model it's possible to see its mechanical effect analysing the user speed trends:

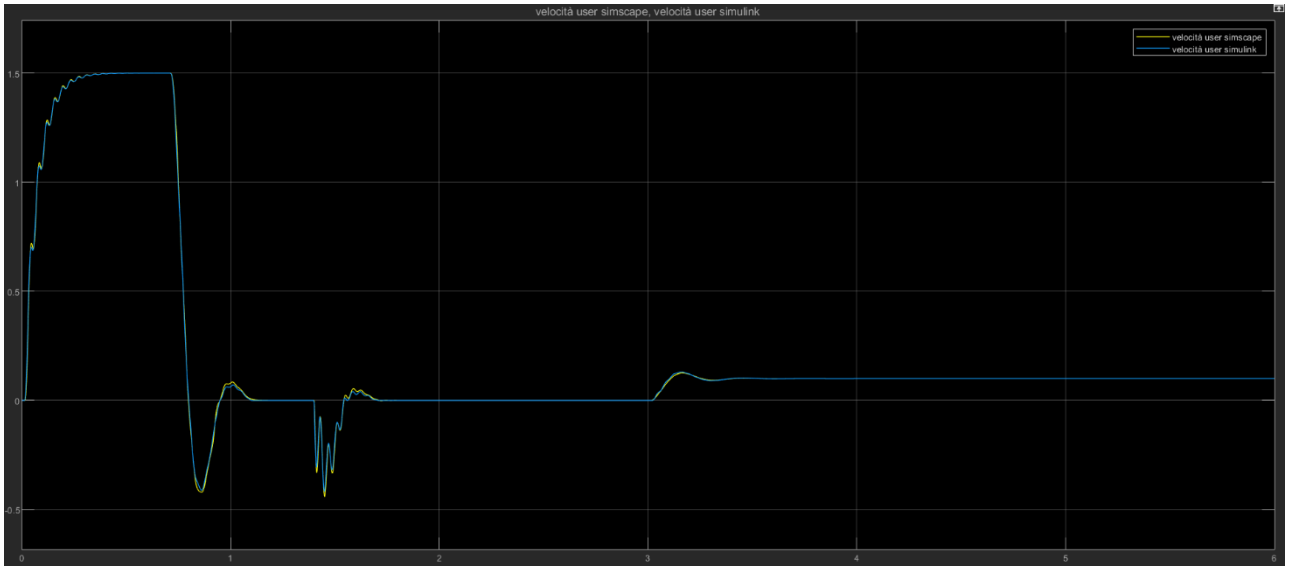

Figure 126: User speed trends

It can see at $t = 0.01426\ s$ a non-linearity on the second order Simscape curve caused by the backlash phenomenon.

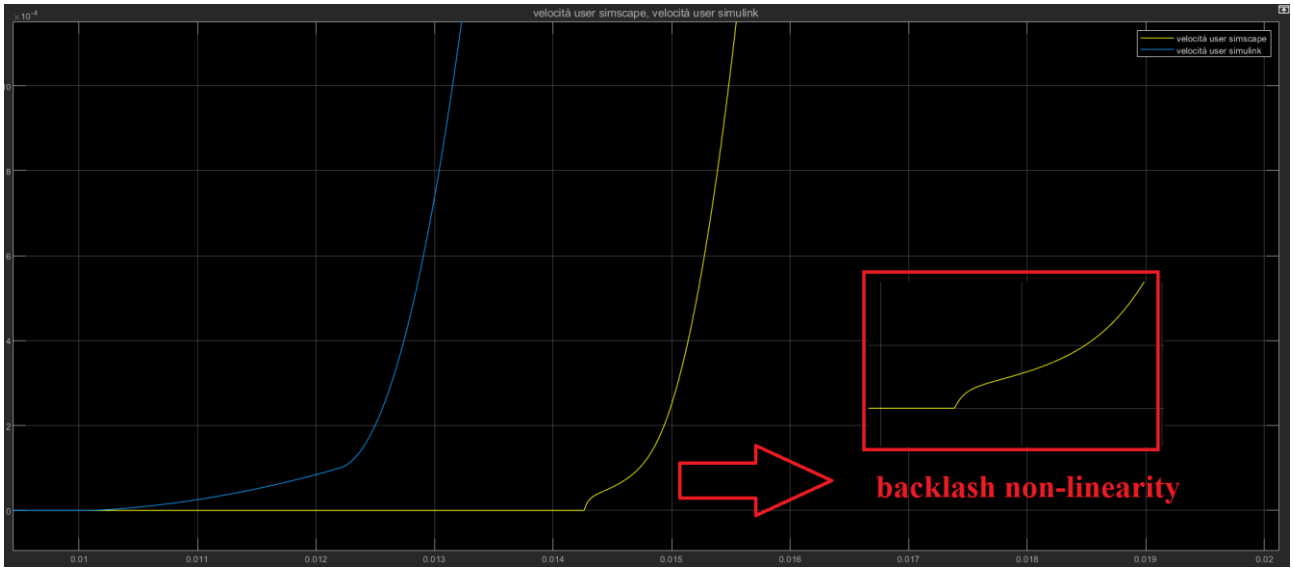

Figure 127: Backlash effect

Moreover, it can see:

- The backlash introduces a "dead zone velocity" and therefore a delay in the dynamics when the user reaches zero speed like in Figure 128 *a)*;
- The delay in the dynamics produces oscillations of an order greater than second order like in Figure 128 *b)*;
- A non-linearity at t = 1.096 s before to reach again the zero speed condition.

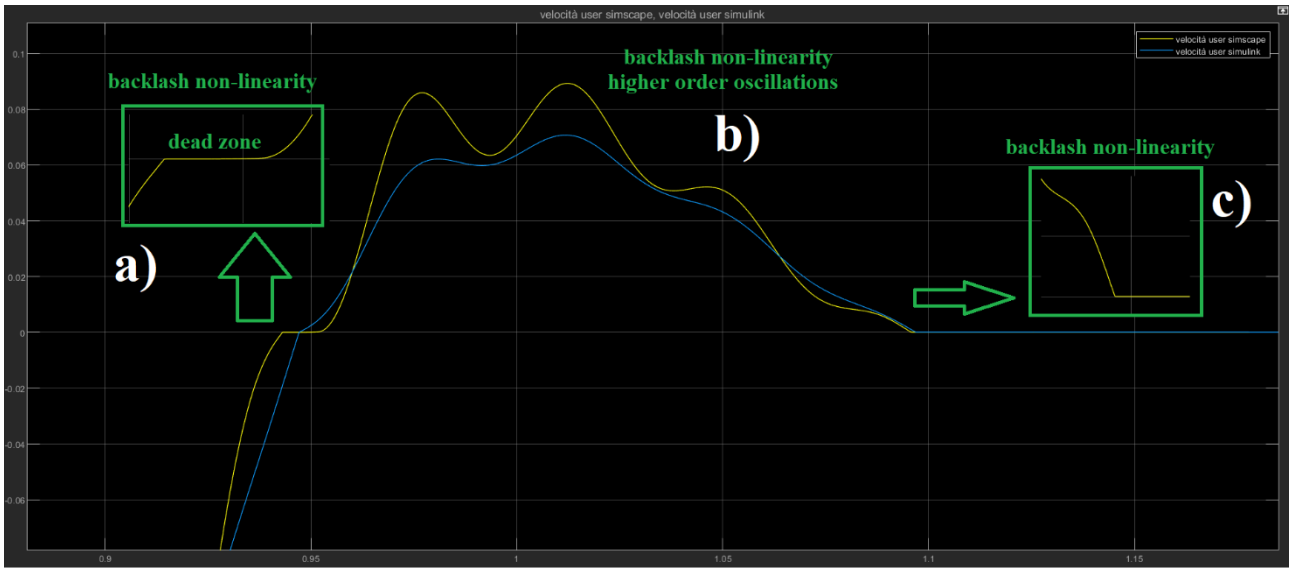

Figure 128: Backlash effects

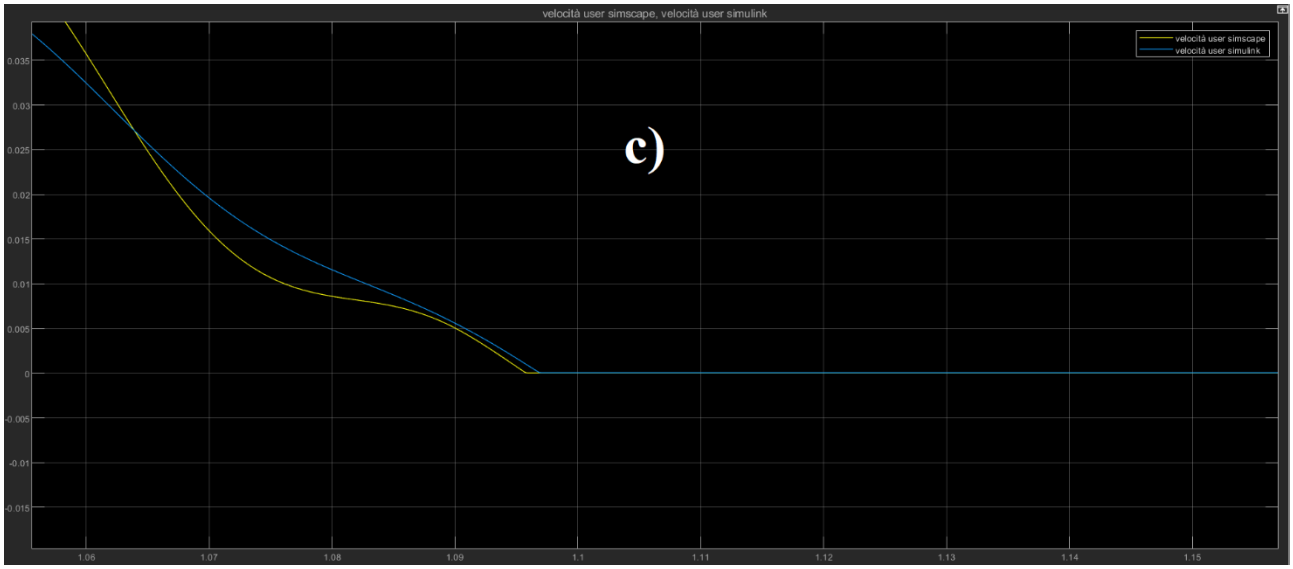

Figure 129: Zoom of the Backlash effect c)

6.5.3) Both models with backlash

Including the backlash phenomenon inside the Simulink it is possible to compare completely the two models.

Backlash block is inserted inside the blue block "Dynamic System DC Motor + Reducer (fast tree)"

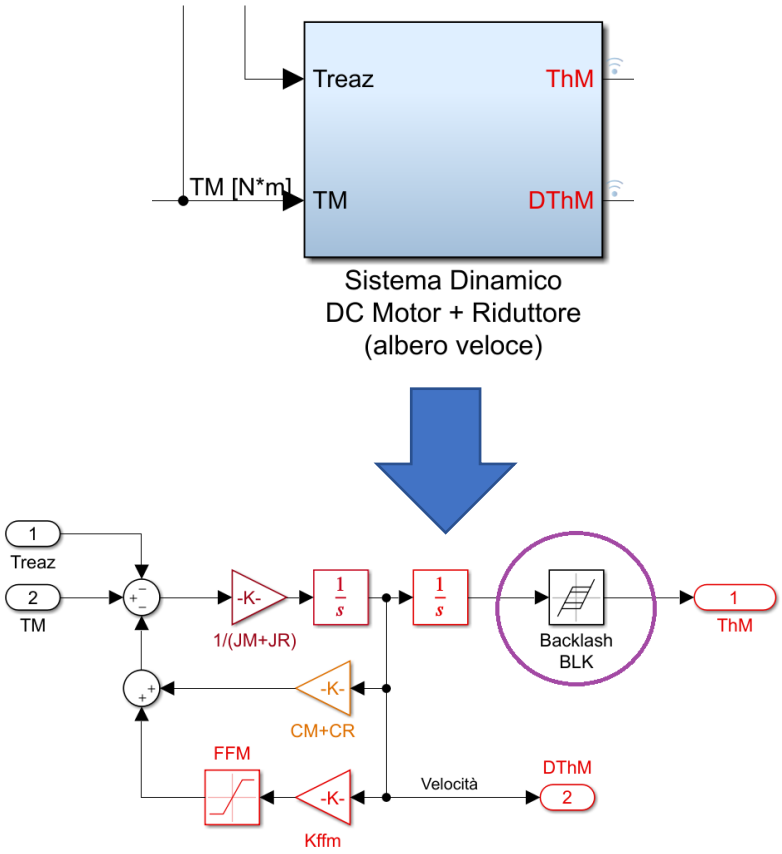

Figure 130: Simulink Backlash position

The appropriate conversion (by **deg** to **rad**) regarding the ***dead band width*** is applied.

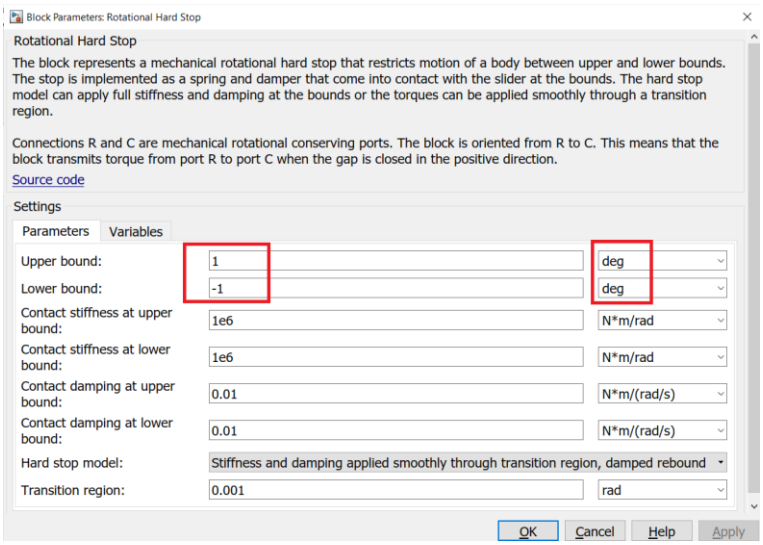

Figure 131: Simscape Backlash

The conversion used is the following:

$$r^{rad} = \frac{g^{\circ} \cdot \pi^{rad}}{180^{\circ}}$$

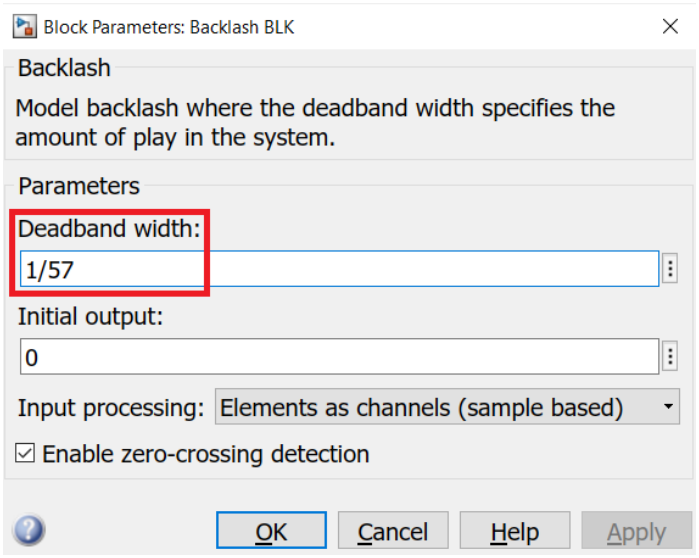

Figure 132: Simulink Backlash conversion

The backlash block in the Simulink model is located in order to act on the motor position and not on the motor speed.

In fact it is possible to see the effect of the backlash in the Simulink model through the motor position graph (and the effect of the backlash in the Simscape model always in the user speed graph).

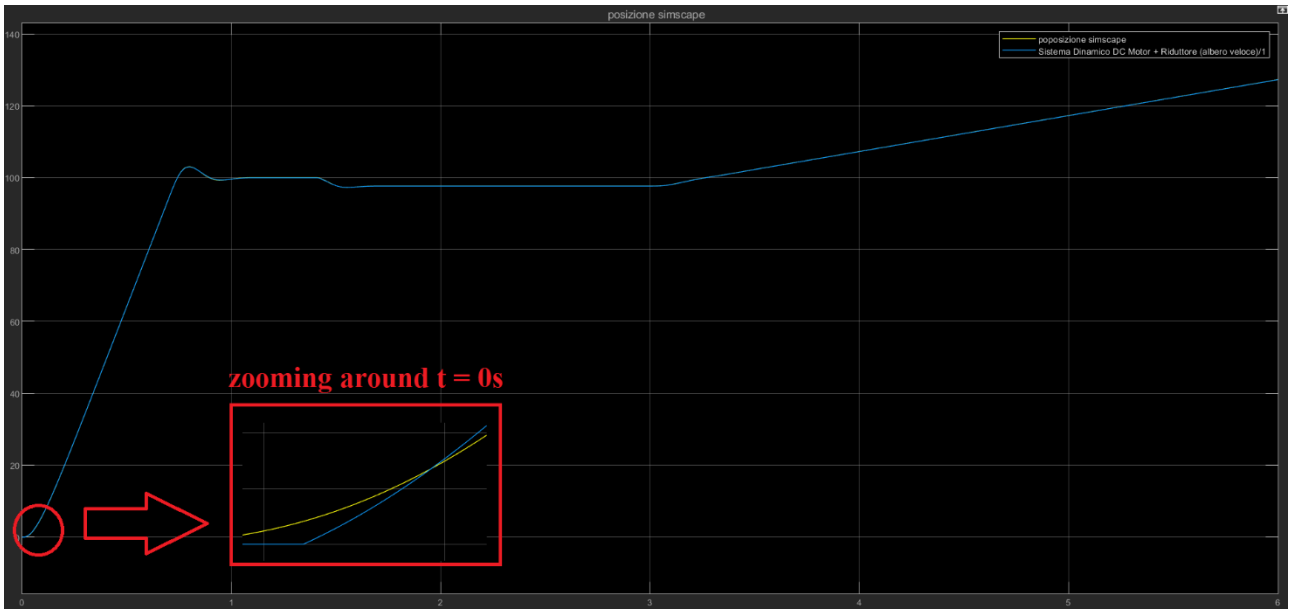

Figure 133: Zoom to see Simulink backlash

Considering a backlash which act on the Simulink motor position, there is a late compared to the Simscape motor position.

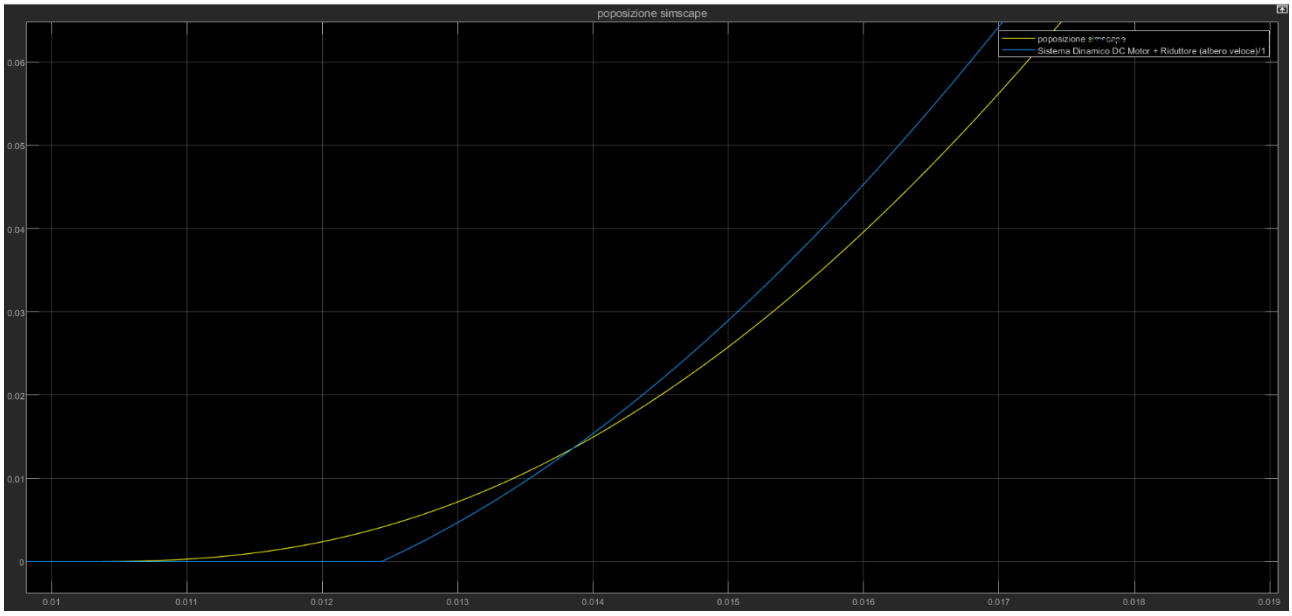

Figure 134: Simulink backlash

Instead if the backlash block is used in order to act on the user's position there are some problems of numerical instability.

6.6) Simscape model with F-16 EMA Low Fidelity

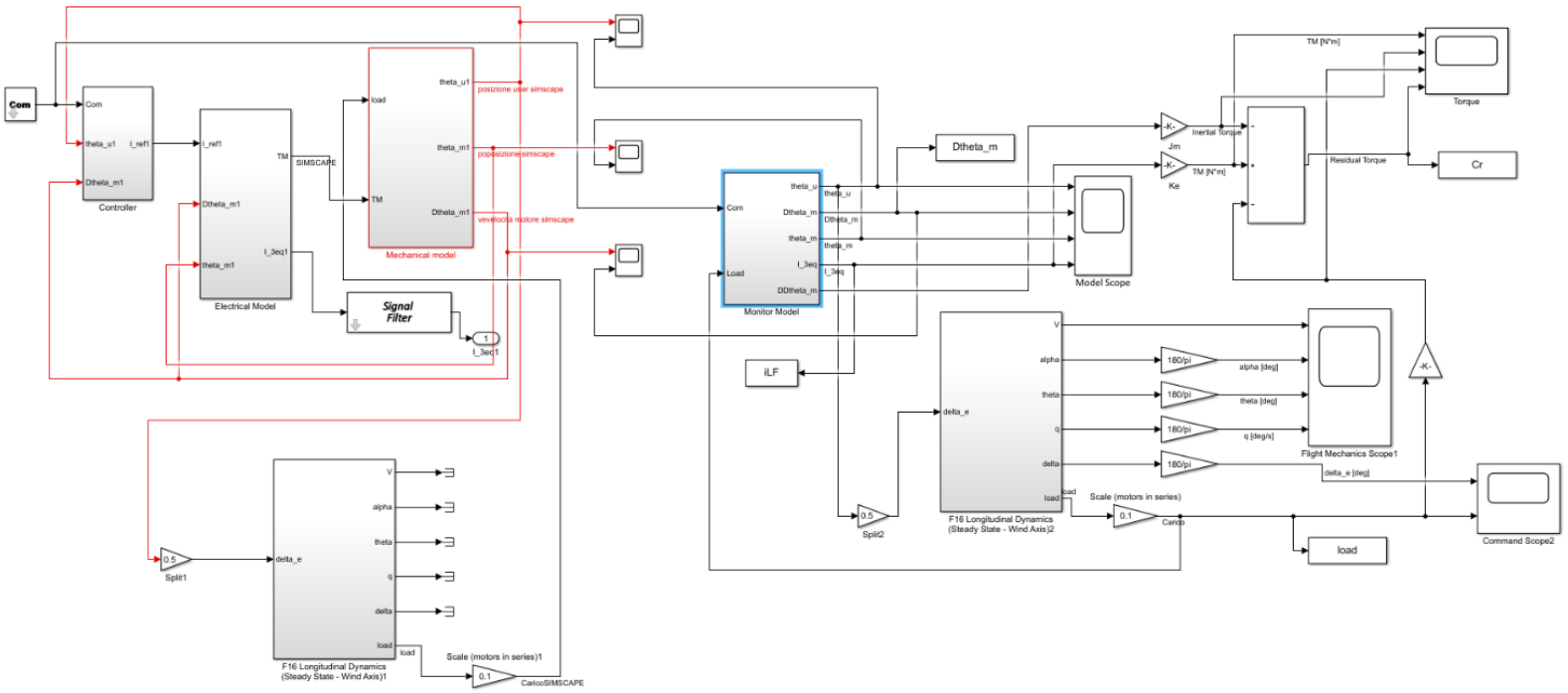

Figure 135: Final model

First of all, inside the F-16 EMA Low Fidelity Simulink model it is necessary substitute the Friction Borello Model of the paragraph 4.2.5) with the more simple Friction

Borello Model of the paragraph 6.4.) and it's necessary to copy a second Simulink F-16 EMA Low Fidelity.

To model correctly the mechanical transmission system in Simscape it is necessary to work inside the new Simulink Monitor model which has only the "command" block in common with the original Simulink Monitor model. Then the Simscape Mechanical model is built inside the new Simulink Mechanical Model.

The amount of theta_m, Dtheta_m, theta_u measured by the Simscape's sensors are used in the copied Simulink model to produce the drive torque and the external load (like hinge moment).

In this way it is possible compare Simscape and Simulink dynamics verifying that they are the same.

To also examine the user's speed affected by backlash in the Simulink model it is important to add a derivative block as in the following figure:

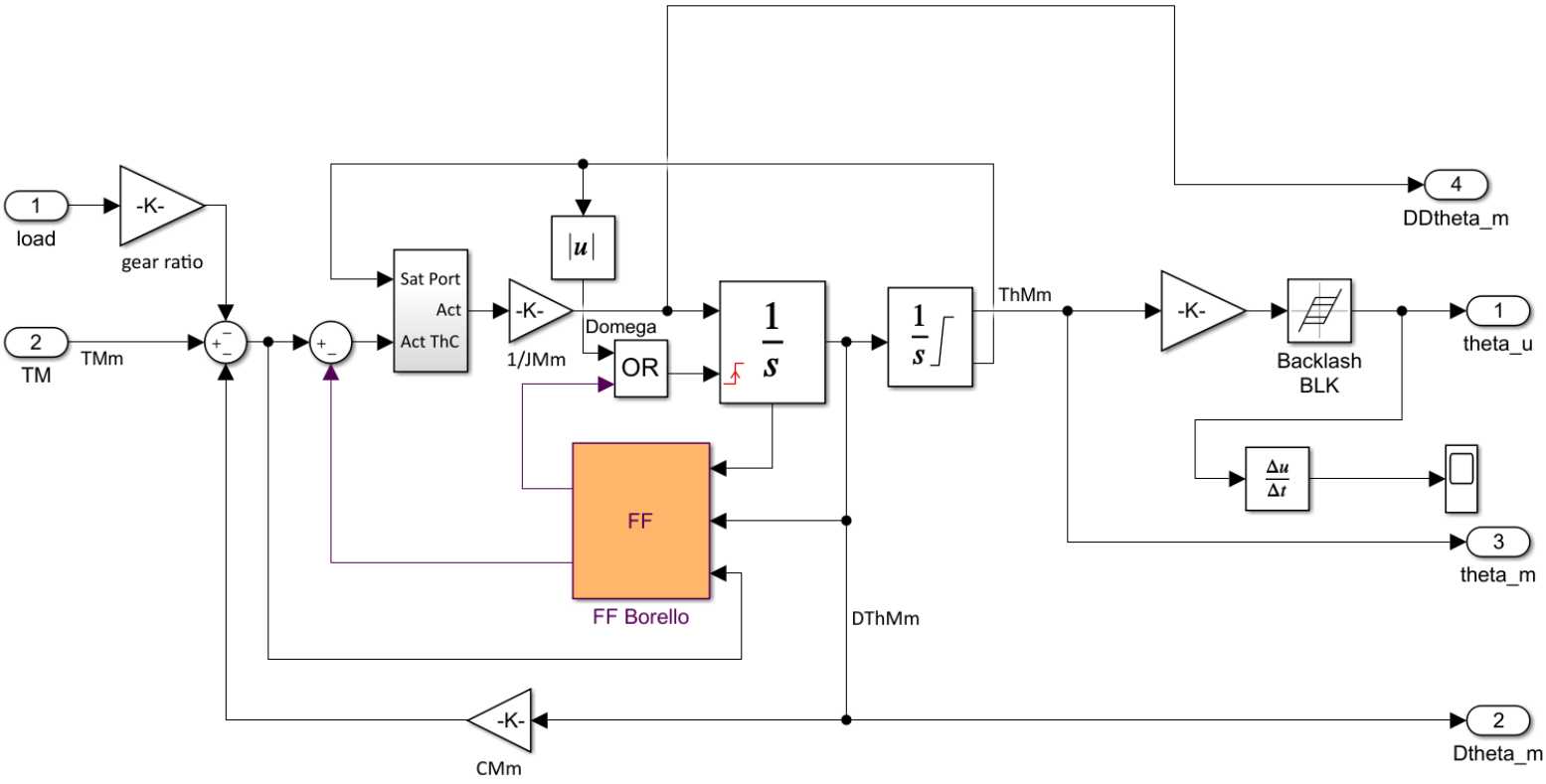

Figure 136: Simulink backlash model

Instead, it is not possible to simulate the backlash in the Simscape model through the classic "Rotational Hard Stop" as it is not inserted in this model between two inertias. Therefore a shortcut is used to study the phenomenon using the Simulink backlash block as shown in the figure.

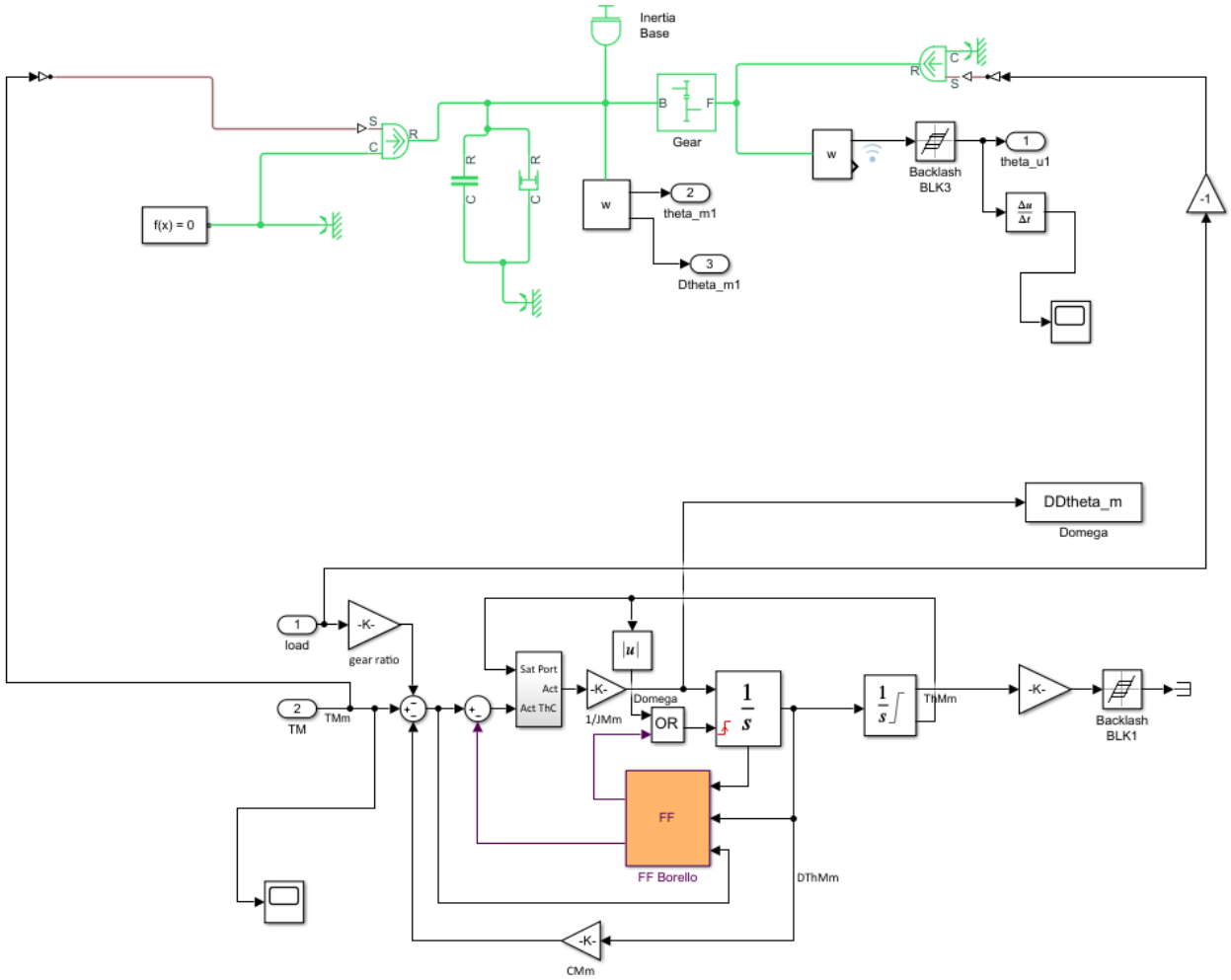

Figure 137: Simscape backlash model

The simulation is carried out with a sinusoidal command with an ***input half-width****: 0.1 rad* and a ***frequency****: 1 rad/s.*

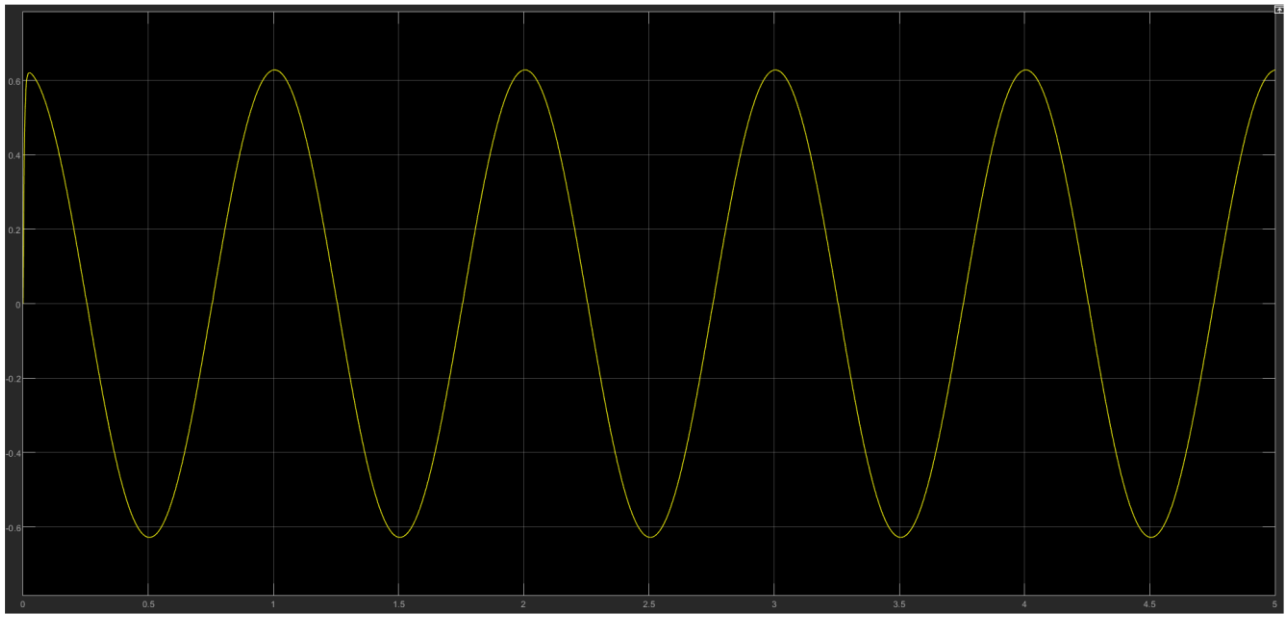

Figure 138: Simulink speed without backlash

About Simulink user's speed it's possible to see the backlash effects:

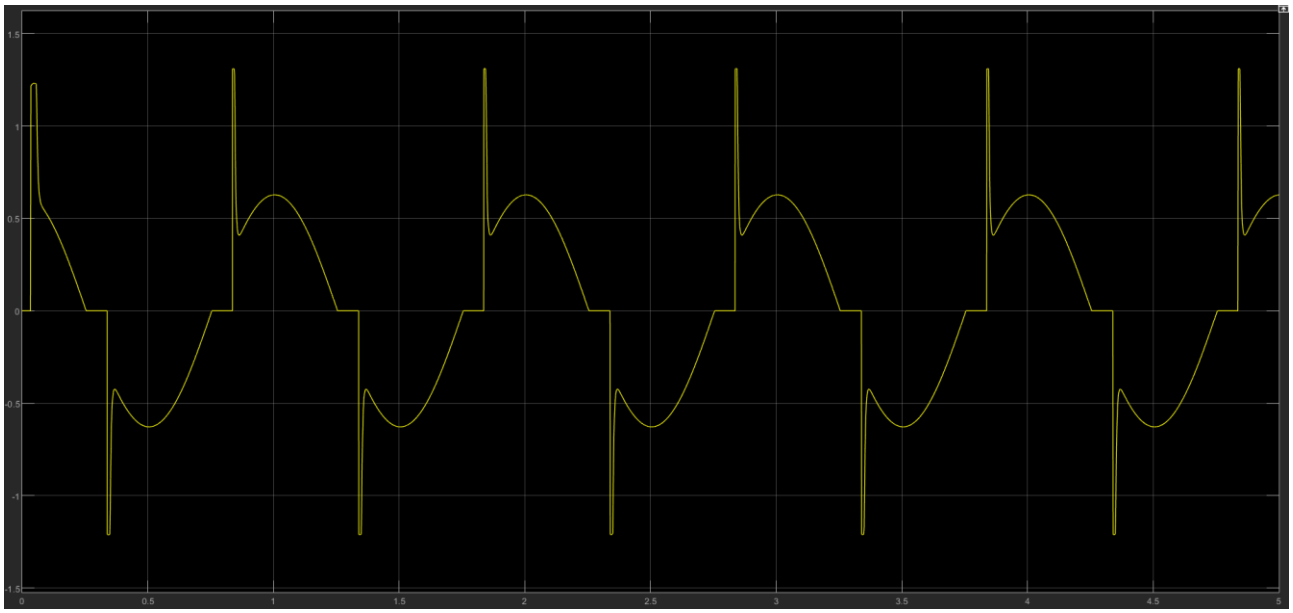

Figure 139: Simulink speed with backlash

It keeps attention, at the zero inversion point, on the dead-band and on the following bumps established between the two mechanical transmission elements.

The following graph represents Simscape user's speed with the backlash effects:

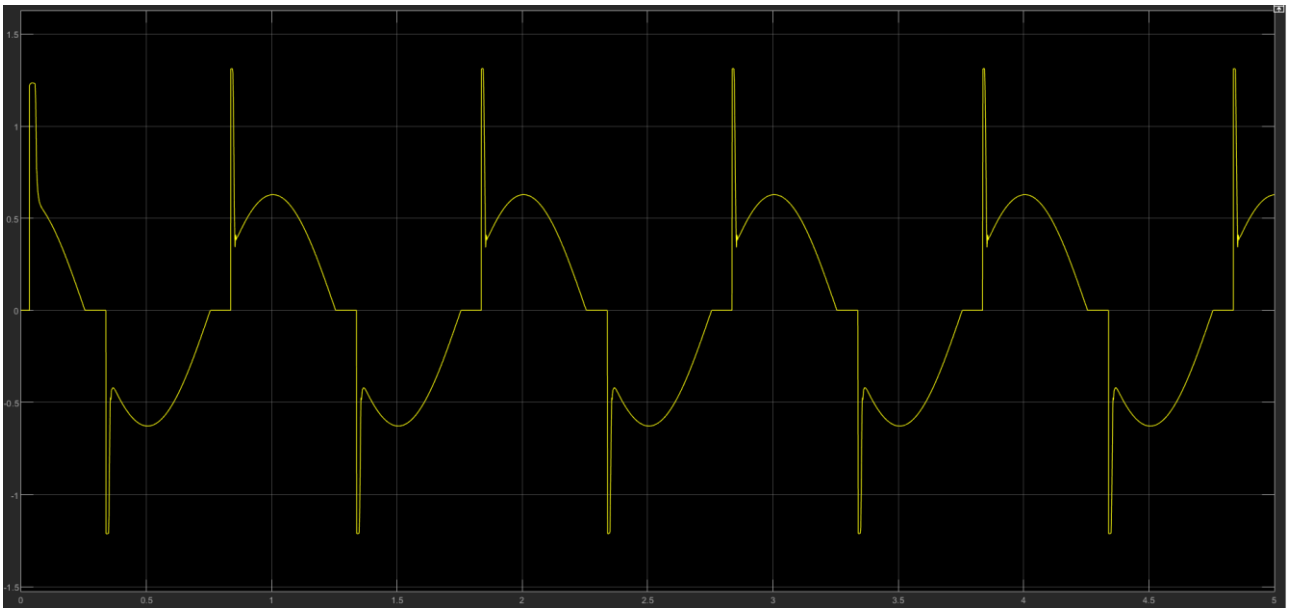

Figure 140: Simscape speed with backlash

At the end of this discussion it's possible to observe the measurement error between Simscape and Simulink regarding theta _ m, Dtheta _ m, theta_ u.

It notes how the curves are quite overlapping and the error is low

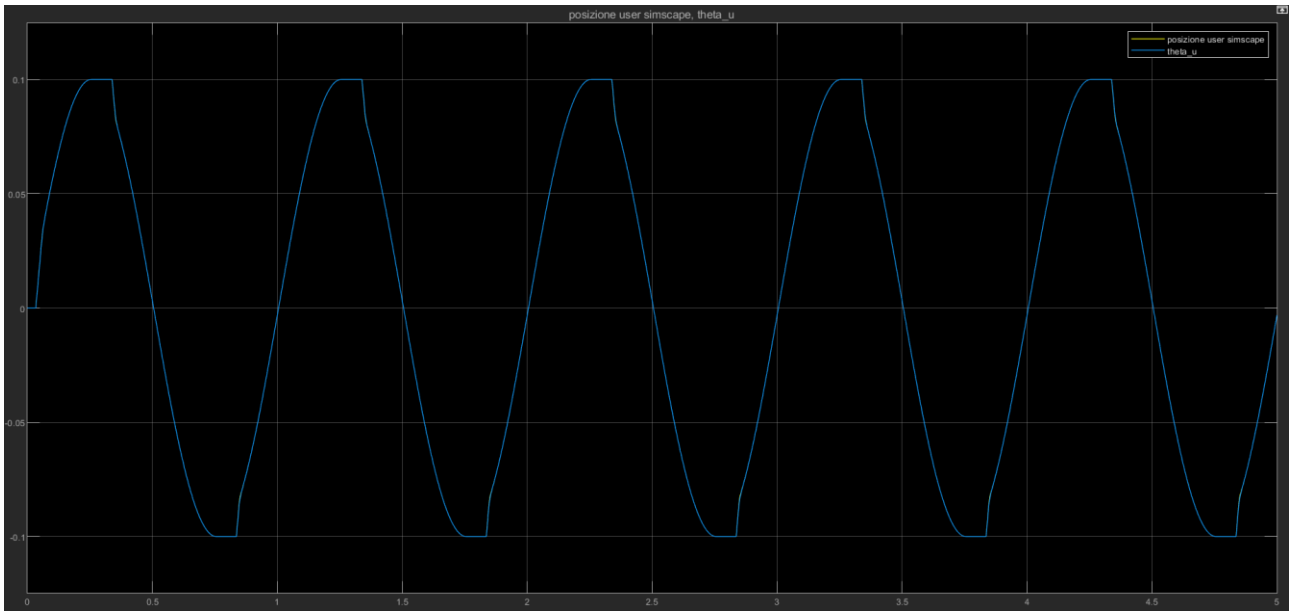

Figure 141: Position user

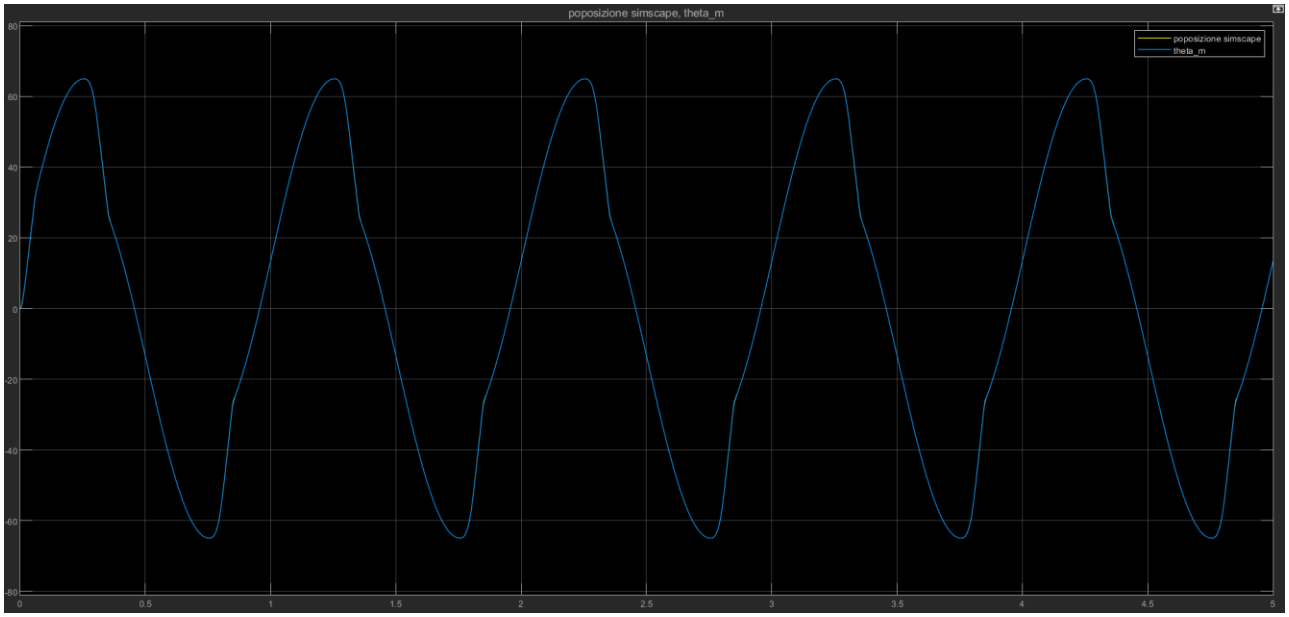

Figure 142: Position motor

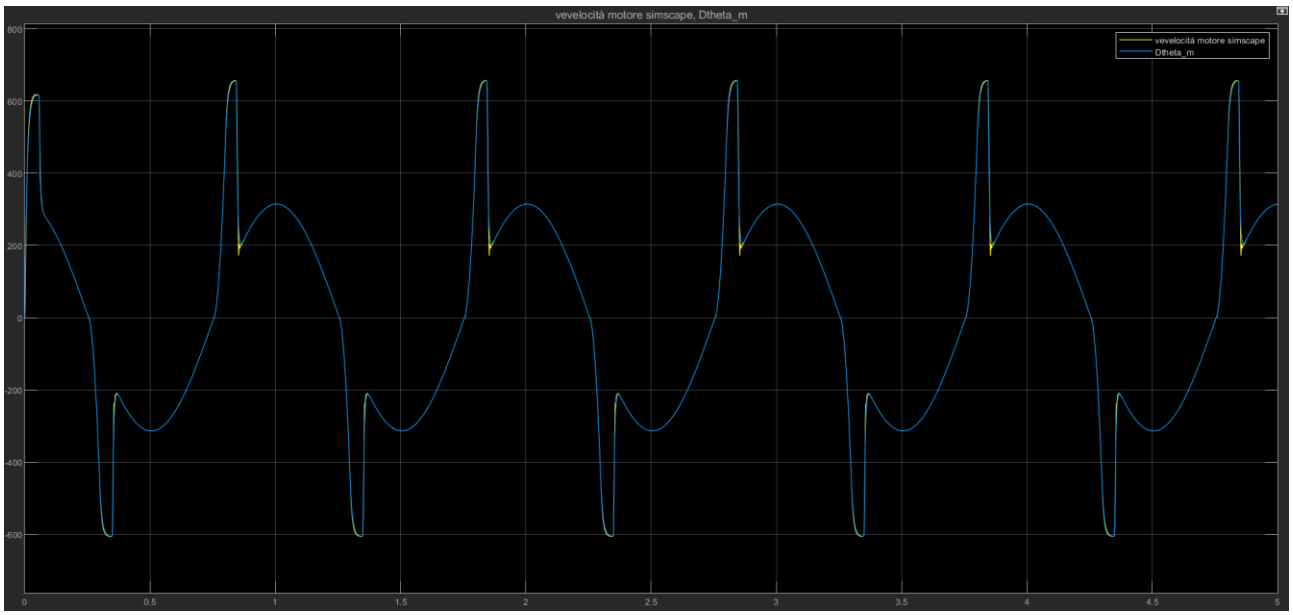

Figure 143: Speed motor

7) Results & final consideration

From the results obtained, it is evident that both models are valid for a correct implementation of the linear dynamic system but there are some problems with the implementation of non-linear phenomena like backlash and friction models.

In fact, the Simscape friction model is not sensitive to external loads compared to Friction Borello model.

Although Simulink and Simscape are not separable simulation environments (as the second one is actually an internal expansion of the first library), there are substantial differences in the methodology to be used. Both are based on a graphic approach, but use different logics:

- The Simulink environment is based on the construction of a block diagram of which the useful parameters must be previously defined.
  The input signals are defined through specific blocks and travel along the branches of the diagram in a single direction.
  The signal flow in Simulink is therefore unidirectional and for this reason the control systems need one or more feedback branches.
  To derive the block diagram it is mandatory to first carry out the mathematical study of the system which is not always easy to analyse.

- The Simscape environment, on the other hand, uses a physical modeling approach. The blocks allow a bidirectional signal flow, therefore they do not require feedback branches.
  The graphs obtained with Simscape are visually more intuitive and are easier to understand even for the less experienced.
  The Simscape environment also has multiple sub-libraries (Fluids, Electric, Multibody, etc.) that can be combined with each other, allowing the analysis of multi-domain models.

The modeling phase has been about understanding and trying to model the systems behaviour graphically. It has been carried out incrementally with a lot of trial and error.

Each component has therefore been tested separately to verify it worked the way it was expected to do analytically, before moving on to the next component. Each component has therefore been tested separately to verify it worked the way it was expected to do analytically, before moving on to the next component.

Each component has also been tested together with one another, starting with two components, and then adding one after another. The process has been iterative in which both forward and backward steps have been taken.

This incremental stepwise time consuming approach made the troubleshooting process a whole lot easier when it was time to simulate the whole model configuration (Simscape mechanical model of F-16 EMA Low Fidelity).

With this background a stepwise approach been conducted which has led to the final model.

About backlash block it is possible to notice how:

- In paragraph 6.5 it is possible using the hard stop block to model the phenomenon because of it can be positioned between two inertias to replicate the mechanical model Simulink
- In paragraph 6.6 it's physically impossible using the hard stop block to model the phenomenon because there is only an inertia as mechanical parameter. In fact, to simulate backlash, it the shortcut of blocking Simulink backlash in the compute branch of Simscape theta_u was used

Nevertheless, this initial model, developed in section 6.6, can serve as good base for further development and gives a good indication that it is possible to build and simulate realistic mechanical models with the Simscape software using the hard stop block for the backlash. The aim of the next works could be finding the way to overcome the problem of only one inertia presence.